Bettina Ottersböck

DISSERTATION

NATURAL AND ARTIFICIAL WEATHERING TESTS OF POLYMER FILMS USED IN SOLAR APPLICATIONS

Dissertation

Natural and artificial weathering tests of polymer films used in solar applications

Authored by

DI Bettina Ottersböck, BSc

Submitted to

Chair of Materials Science and Testing of Polymers

Department Polymer Engineering and Science
University of Leoben
Leoben, Austria

Conducted at

Polymer Competence Center Leoben GmbH

Leoben, Austria

Academic Supervisor

Univ.-Prof. DI Dr. mont. Gerald Pinter

Institute of Materials Science and Testing of Polymers
University of Leoben

Supervisor

DI Dr. mont. Gernot Oreški

Polymer Competence Center Leoben GmbH

Parts of this thesis are already published. Detailed information about that can be found in the respective chapters.

Affidavit

I declare in lieu of oath, that I wrote this thesis and performed the associated research myself, using only the support indicated in the literature cited in this thesis.

DI Bettina Ottersböck, BSc Leoben, April 2017

Acknowledgment

I would like to express my sincere gratitude to Univ.-Prof. Gerald Pinter, Head of the Chair of Materials Science and Testing of Polymers, for providing me the opportunity for this thesis. His cooperative discussions and positive attitude were an encouragement for me.

My gratitude goes to Gernot Oreśki, who guided me through my time as a PhD student. His enthusiasm for polymer science kept me constantly engaged with my research. The trust in me and my scientific skills and his encouragement of self-independent working was a great support. He created a research environment that stimulated original thinking and initiative in which I truly enjoyed working.

My appreciation also extents to my colleagues and friends. I want to thank Marlene Knausz, Antonia Mihaljevic, Marko Omazic, Sandra Pötz and Astrid Rauschenbach for our lively discussions and the enjoyable leisure times. It is a great pleasure working with them and I appreciate not only our work related discussions, their ideas but also their good humour.

I want to thank Jutta Geier, Simone Viola Radl and Florian Wagner for their support and discussions about the scientific work in this thesis. Moreover, I would like to express my gratitude to all colleagues not mentioned who also supported me.

Above ground, I am indebted to my family, who are important persons in my life. My deepest appreciation belongs to my parents Christa and Max Hirschmann for always supporting and believing in me. Without them it would have not been possible for me to study. And finally, I acknowledge my dear husband Markus to whom I owe much. Without his support, love and patience the successful finalisation of this thesis would not have been possible.

Funding

This research work was performed at the Polymer Competence Center Leoben GmbH (PCCL) within the framework of the COMET-program and the project “Weathering of polymers” (FFG Numbers 843276 and 854178) of the Federal Ministry for Transport, Innovation and Technology and Federal Ministry of Economy, Family and Youth in cooperation with the Institute of Materials Science and Testing of Polymers at the University of Leoben. The PCCL is funded by the Austrian Government and the State Governments of Styria and Upper Austria.

Leoben, April 2017

Abstract

Weathering stability is the key factor for the reliability of polymers in outdoor applications like building materials, materials for vehicles and aeronautical applications, but also solar energy. For some applications, such as photovoltaics (PV), polymers have to guarantee lifetimes of 20 years and more with a limited loss in functionality of the component. The weathering performance of polymers is most accurately assessed by outdoor exposure to natural weathering at different locations and the examination of their performance characteristics by following changes in physical and chemical properties. Although natural weathering is the most reliable method to examine long-term performance, its major drawback is the extremely long exposure time required to determine the service lifetime of the components. This long time-scale places a very severe limitation on this method. In order to significantly decrease the testing time for the purpose of more rapid prediction of the long-term weathering performance of polymers, it is necessary to use harsher artificially accelerated weathering tests followed by measurements of physical and chemical changes or changes in performance. To assess the long-term performance and durability of materials, it is essential not only to measure the deterioration of macroscopic physical properties, but also to gain information about degradation processes taking place at the molecular level. In order to gain additional knowledge of the degradation behaviour of polymers and to further establish suitable lifetime models, the influence of the relevant load parameters like ultraviolet radiation, temperature and humidity on the degradation behaviour of the polymer materials as well as the functionality of the components has to be determined.

Therefore this thesis deals with the influence of ageing methods and the influence of the microclimate on the properties of polymeric materials used in solar application. Components which are in the focus in this thesis are the encapsulant of the solar cells and the back side covering (polymeric multilayer backsheet) of a PV module. The results enhance the knowledge in the field of polymer degradation and give an overview of suitable characterisation methods useful to identify different ageing processes and the correlated changes in properties of polymeric films.

After an introduction to ageing of polymers in chapter 1, chapter 2 covers the ageing behaviour of different artificially aged polyethylene terephthalate films. Polyesters are commonly used polymers as a component in a backsheet for PV modules. Therefore, it is an advantage to collect additional knowledge on the degradation behaviour of this material class. The results can help to enhance the existing knowledge of the ageing behaviour of PET films dependent on temperature and humidity level. Furthermore the results might help to draw additional conclusions about the complex ageing

behaviour of PET-based multilayer backsheets. The experimental part includes ageing of different films at various levels of temperature and humidity. Subsequent analysis of material properties shows no significant optical changes. In contrast, changes in mechanical and thermal properties, dependent on the temperature and humidity level, are detected and can be attributed to chemical degradation processes via hydrolysis. A significant correlation of the crystallisation temperature gained by thermal analysis and molar mass characterised by gel permeation chromatography can be found. Thus, the verification of chain scission for polyester films can be done easily via thermal analysis instead of the complex and expensive, wet-chemical process.

In chapter 3 the influence of natural and artificial weathering on polymeric multilayer films is characterised and correlated. The weathering performance of polymeric backsheets is most accurately assessed by outdoor exposure to natural weathering and examination of their performance characteristics by observing changes in properties. The main drawback of natural weathering is the long exposure time. Therefore, a feasibility study of the correlation between natural and standardised artificial weathering of backsheets is conducted, where different effects on the properties of the materials are detected for all materials. The changes in properties after natural weathering for 30 months cannot be correlated with up to 3000 hours of accelerated ageing. The degradation mechanism of the polymeric part during natural weathering has to be considered when trying to simulate natural ageing conditions in order to choose the right parameters for artificial ageing. Thus, the use of the standard ageing test or an adaption of the standard need to be reconsidered.

In the PV industry the standard test to verify backsheet quality in a short time period is a hot and humid test procedure called damp heat test (85°C 85% relative humidity). Usually tests of 2000 hours are conducted. This equals approximately 3 months, which is too long for a fast material pre-selection. For ultra-acceleration of the damp heat test a so called pressure cooker test can be utilised. A decrease in the development time of backsheets can be achieved by an increase of temperature, humidity and pressure. This test is already in use in various industries. However, it has not been clarified if the ageing mechanisms and effects on the material properties are equal to the standard damp heat exposure. Therefore, Chapter 4 deals with the verification of the correlation of the standard accelerated and the ultra-accelerated ageing of polyester-based multilayer backsheets. Thermal and mechanical properties show a very close order of magnitude between pressure cooker tests at 120°C and damp heat tests, with the constraint of presumable differences in the failure mechanism. Nevertheless, it should be acceptable to use the pressure cooker test at 120°C for up to 96 hours for fast quality testing to support fast material development

for polyester-based backsheets instead of 2000 hours of damp heat testing. This would lead to an acceleration of the speed of testing by a factor of 21. Pressure cooker testing is proposed to significantly reduce the ageing time to four days when testing for material quality and infant failures.

Investigations concerning the impact on the microclimate on the ageing behaviour of polymeric encapsulation materials have not been conducted so far with regard to physical and chemical ageing processes due to the sample set-up (single film and laminated module samples). Therefore, chapter 5 focuses on the investigation of the impact of microclimates on polyolefin-based encapsulation materials. It is shown that there is a strong influence of the microclimate on the ageing behaviour of polymeric films. Differences are even detectable in the unaged state between film and module samples after the production process of a PV module. Not only does the sample set-up (film or laminated module sample) highly influence the degradation of the encapsulants, but also the type of ageing. Therefore it is not acceptable to test polyolefin-based encapsulation films as a single film in order to examine long-term performance of films incorporated in a PV module. The application-relevant microclimate has to be taken into account when conducting reliable exposure testing methods.

Kurzfassung

Die Witterungsstabilität von Polymeren in der Außenanwendung wie in der Gebäudetechnik, Verkehrsmittel oder auch bei solaren Anwendungen, stellt einen Schlüsselfaktor für die Zuverlässigkeit dar. Für zahlreiche Einsatzbereiche wie die Photovoltaik (PV) müssen Kunststoffe eine Lebensdauer von 20 Jahren und mehr aufweisen. Die Voraussetzung dafür ist eine begrenzte Abnahme der vorgegebenen Funktionalität während dieser Zeitspanne. Die anwendungsnaheste Beurteilung der Witterungsbeständigkeit von Polymeren stellt die natürliche Bewitterung an verschiedenen Standorten dar. Die möglichen Änderungen der Leistungsmerkmale können nachfolgend anhand von Änderungen der physikalischen und chemischen Eigenschaften untersucht werden. Die natürliche Bewitterung ist dabei die zuverlässigste Alterungsmethode für die Darstellung des Langzeitverhaltens von Kunststoffen. Der größte Nachteil liegt allerdings in der extrem langen erforderlichen Auslagerungszeit, um die entsprechende Lebensdauer der Komponenten abzubilden. Dies stellt in der Industrie jedoch eine starke Einschränkung dar, da vom Markt schnelle Materialentwicklungen gefordert werden. Um die Testzeit für eine Vorhersage der Langzeitwitterungsstabilität von Polymeren signifikant zu verringern, ist die Durchführung beschleunigter Bewitterungstests notwendig. Die Beurteilung der Langzeitstabilität von Polymeren macht es erforderlich, zusätzlich zu Informationen über die Veränderungen der makroskopischen physikalischen Eigenschaften, auch Informationen über auf molekularer Ebene stattfindende Abbauprozesse zu erhalten. Um zusätzliche Erkenntnisse über das Alterungsverhalten von Polymeren zu gewinnen, ist die Bestimmung des Einflusses der relevanten Belastungen wie Ultraviolettstrahlung, Temperatur und Feuchtigkeit, sowie die Funktionalität der Komponenten, eine Voraussetzung. Deswegen beschäftigt sich diese Arbeit mit dem Einfluss von verschiedenen Alterungsmethoden und dem Einfluss des Mikroklimas auf die Eigenschaften von polymeren Materialien, die in Solaranwendungen verwendet werden.

Im Rahmen dieser Arbeit werden die Einkapselungen und Rückseitenabdeckungen (polymere Mehrschichtfolien, Backsheets genannt) eines PV Moduls untersucht. Die daraus gewonnen Erkenntnisse fördern das Wissen auf dem Gebiet des Alterungsverhaltens von Kunststoffen und geben einen Überblick über geeignete Charakterisierungsmethoden zur Identifizierung unterschiedlicher Alterungsprozesse und der korrelierten Veränderungen der Eigenschaften von Polymerfolien.

Nachdem in Kapitel 1 eine allgemeine Einführung zum Alterungsverhalten von Polymeren und Aspekte zur Durchführung von Alterungstests beschrieben werden, behandelt Kapitel 2 das

Alterungsverhalten verschiedener künstlich gealterter Polyethylenterephthalatfolien. Polyester sind häufig eingesetzte Komponenten in Backsheets, wodurch eine detailliertere Kenntnis über das Alterungsverhalten Vorteile bringt. Das kann bei der Charakterisierung des komplexeren Alterungsverhaltens von Polyester-basierten Mehrschichtfolien zusätzlich aufschlussreich sein. Der experimentelle Teil dieses Kapitels umfasst die Auslagerung von verschiedenen Folienproben bei unterschiedlichen Bewitterungsparametern. Dabei sind keine Veränderungen der optischen Eigenschaften feststellbar. Jedoch sind bei mechanischen und thermischen Eigenschaften Änderungen abhängig von der Temperatur und dem Feuchtigkeitsgehalt erkennbar, die auf chemische Abbauprozesse wie Hydrolyse zurückgeführt werden können. Zusätzlich ist eine signifikante Abhängigkeit der Kristallisationstemperatur von der durch Gelpermeations-chromatographie charakterisierten Molmasse feststellbar. Somit kann zum Nachweis von chemischer Degradation an Polyesterfolien, anstatt des aufwändigen nasschemischen Verfahrens, eine deutlich einfachere thermische Analyse verwendet werden.

In Kapitel 3 wird der Einfluss der natürlichen und künstlichen Bewitterung auf polymere Mehrschichtfolien (Backsheets) charakterisiert. Die Witterungsbeständigkeit von Backsheets wird am realitätsnahesten durch die Freibewitterung und der anschließenden Prüfung von Eigenschaftsveränderungen bewertet. Allerdings führt die natürliche Bewitterung zu einer sehr langen Prüfdauer. Daher wird in einer Machbarkeitsstudie die Korrelation zwischen natürlicher und standardisierter, künstlicher Bewitterung von Backsheets durchgeführt. Dabei können die Eigenschaftsveränderungen nach 30 monatiger natürlicher Bewitterung nicht mit bis zu 3000 Stunden künstlicher Alterung korreliert werden. Es ist bei der beschleunigten Simulation von natürlichen Alterungsvorgänge essentiell, die Abbaumechanismen während der natürlichen Bewitterung möglichst genau zu kennen, um diese nachstellen zu können. Daher sind künstliche Auslagerungen streng nach Norm bzw. eine Anpassung der Normen zu überdenken.

In der PV Industrie wird zur Überprüfung der Backsheet-Qualität standardmäßig ein 2000 Stunden dauernder heißer und feuchter Test, genannt „Damp heat test“ (85°C 85% relative Luftfeuchtigkeit) verwendet. Dieser etwa drei Monate dauernde Versuch ist somit für eine schnelle Materialvorauswahl nicht geeignet. Hierfür kann stattdessen ein sogenannter Druckkochtest verwendet werden, der durch eine Erhöhung von Temperatur, Feuchtigkeit und Druck eine Verringerung der Testdauer bewirkt. Dieser Test wird bereits in verschiedenen Branchen eingesetzt. Durch diese Änderung der Auslagerungsparameter ist abzuklären, ob die Alterungsmechanismen und Wirkungen auf die Materialeigenschaften gleich jener sind, die während der üblichen feuchten Wärmebelastung auftreten. Daher befasst sich Kapitel 4 mit der

Überprüfung der Korrelation der standardbeschleunigten mit der ultrabeschleunigten Alterung von mehrschichtigen Backsheets auf Polyesterbasis. Die gemessenen Veränderungen in thermischen und mechanischen Eigenschaften bei beiden Auslagerungsverfahren zeigen vergleichbare Werte. Allerdings muss davon ausgegangen werden, dass es Unterschiede im Alterungsmechanismus gibt. Für eine schnelle Qualitätsprüfung zur Ermöglichung einer raschen Materialentwicklung an Polyester-basierten Backsheets ist der Druckkochtest bei 120°C mit 96 Stunden Auslagerungszeit dennoch geeignet. Dies führt zu einer 21-fachen Beschleunigung der Prüfdauer auf etwa vier Tage.

Der schichtartige Aufbau des PV Moduls aus unterschiedlichen Materialien führt gegenüber der Einzelfolie zu einer Veränderung der lokalen Alterungsbedingungen. Daher konzentriert sich Kapitel 5 auf die Untersuchung der Auswirkungen dieses Mikroklimas auf Polyolefin-basierte Einkapselungsmaterialien. Der verschiedenartige Probenaufbau (Einzelfilm- und laminierte Modulproben) verursacht während der künstlichen Auslagerung unterschiedliche Ausprägungen an physikalischen und chemischen Alterungsprozessen. Bereits im ungealterten Zustand nach dem Herstellungsprozess eines PV Moduls sind zwischen Folien- und Modulproben Unterschiede nachweisbar. Demnach ist das Testen von Polyolefin-basierten Einkapselungsfolien als Einzelfolien für die Charakterisierung der Langzeitstabilität eines PV Moduls nicht aussagekräftig. Bei der Durchführung von zuverlässigen Alterungsmethoden ist daher das anwendungsrelevante Mikroklima zu berücksichtigen.

Table of content

1. Introduction and objectives

The following chapter deals with the state of the art of photovoltaic modules and of polymer degradation. It gives an overview of different ageing types and their influence on the degradation behaviour of polymers.

1.1. Renewable energy

With an increasing world population, a growing energy demand has also been observed. Statistics of the world's energy supply are shown in Figure 1.1 from 1971 to 2014 [1]. Renewable energies like solar, wind, geothermal and photovoltaics are categorised under other. Compared to the main energy sources, such as coal the part of renewable energies is barely visible. However, the importance of renewable energy is increasing [2].

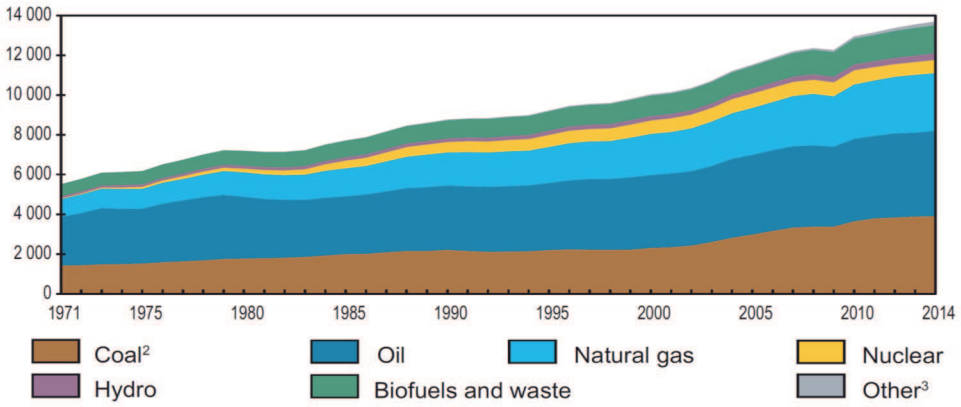

Figure 1.1. Energy supply from 1971 to 2014 by fuel (Mtoe) [1].
[2] peat and oil shale are aggregated with coal
[3] includes geothermal, solar, wind, heat, etc.

Finiteness of our resources is linked to high prices for oil and gas which was already noticeable in the last decades [1]. Simultaneously, we can notice the first influences of burning fossil fuels by the melting of the ice at the poles, the increase of the sea level and an increase of extreme weather events [3–6]. The last catastrophe of Fukushima showed that nuclear energy might not be the type of energy for the future. Additionally, the question of nuclear waste repositories has not been answered yet and fewer people are willing to take the risk of radioactive contamination [7]. These are reasons why renewable energy sources are now established around the world and a rapid growth, especially in the year 2015 with an increase of 147 GW could be observed [2]. Figure 1.2 shows the average annual growth rates of renewable energy capacity, where an increase of 28% in

solar photovoltaic (PV) was registered in 2015 [2]. In general the world now adds more renewable power capacity annually than it adds capacity from all fossil fuels combined [2].

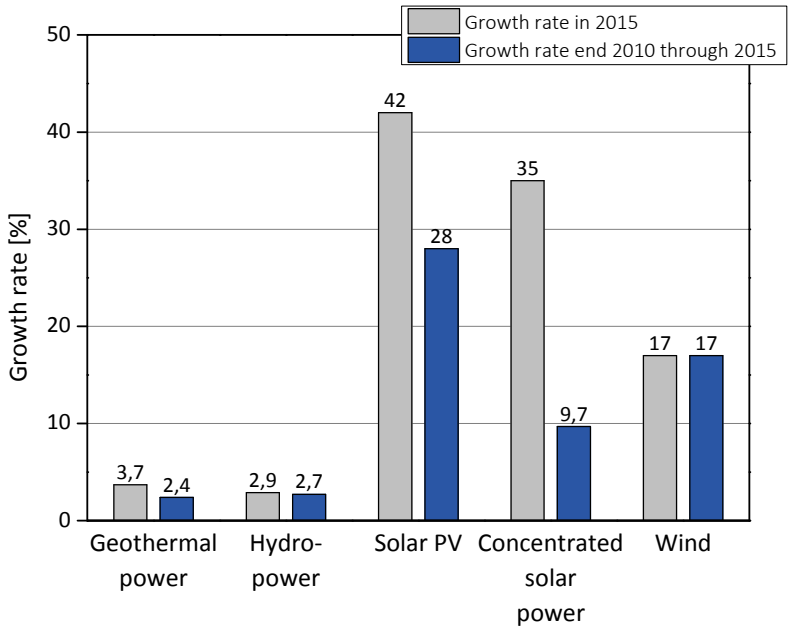

Figure 1.2. Average annual growth rates of renewable energy capacity, End 2010 to End 2015 [2].

If one looks at the estimated global electricity production, the share of renewable energy sources is much higher compared to the share of energy supply (see Figure 1.3) [2]. Reasons for the positive trend in renewables are technological advances and improved financing conditions, which have reduced costs [2]. Nevertheless, a far higher part (76.3%) of the electricity was produced using fossil and nuclear fuels compared to 23.7% from renewable resources in 2015.

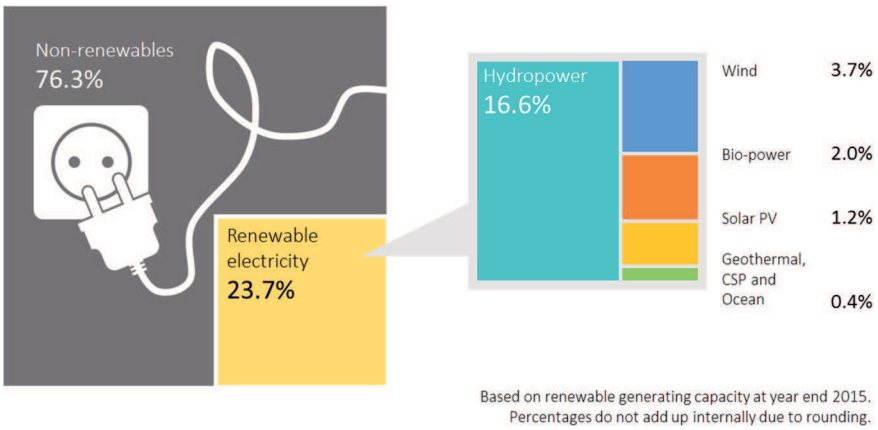

Figure 1.3. Estimated renewable energy share of global electricity production, End-2015 [2].

As each technology of renewable energy has its advantages and drawbacks it is necessary to promote different kinds and use them in dependence on their strengths. Not only political

regulations can help, but also further investments in research have to be made in order to improve the efficiency and reliability of renewable energy technologies.

1.2. Photovoltaic

The following chapter discusses the state of the art and the typical setup of PV modules. Furthermore it focuses on the influence of weathering on the quality and reliability of standard PV modules.

1.2.1. State of the art

As crystalline silicon (c-Si) still dominates the PV market with more than 90% of the annual module production in 2015, this chapter addresses this module type (see Figure 1.4) [8]. Even though c-Si is not the leading technology with efficiencies of around 15 to 20%, the reason for the big market share is an easier and therefore less costly production process [9]. During the last 10 years the material usage for silicon cells has been reduced significantly by around 63% due to increased efficiencies and thinner wafers [8].

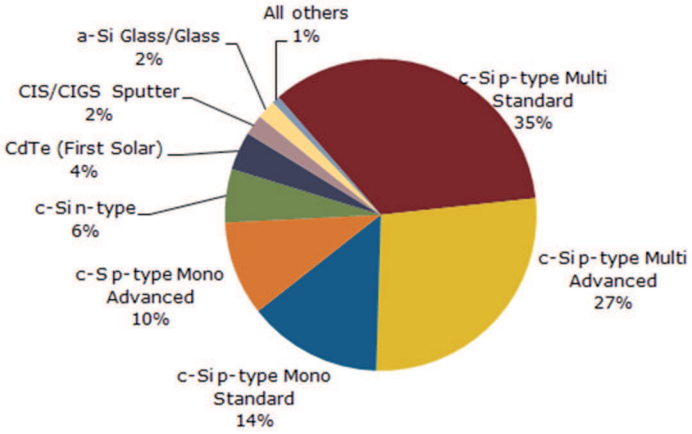

Figure 1.4. Solar PV module production by technology [8, 10].

The principle of the function of the conversion of sunlight via photovoltaic effect is outside the scope of this work, but can be found in the standard literature [7]. Figure 1.5 shows the general setup of a c-Si PV module. The most commonly used material for front protection is glass. For PV modules typically tempered glass with low iron content is used, which results in a higher solar transmittance. The glass cover provides mechanical rigidity, optical transparency, electrical insulation, impact resistance and outdoor weatherability [11, 12]. In some cases the front cover can be a transparent polymer layer, here mainly fluoropolymers are used. The application field for these materials is thin film modules, where an enhanced flexibility and reduced weight is necessary [13].

In order to protect and insulate the brittle solar cells, a low modulus polymeric material is used as encapsulant. This is necessary to compensate for the different thermal expansion coefficients of the materials used. Additionally the purpose of the encapsulant is to bond all components of a module and to ensure the optical coupling with high optical transmittance in the useable wavelength region for c-Si [12, 14]. Furthermore electrical insulation, physical isolation and protection and thermal conduction for the module are required [12]. The most common encapsulant is ethylene vinyl acetate (EVA).

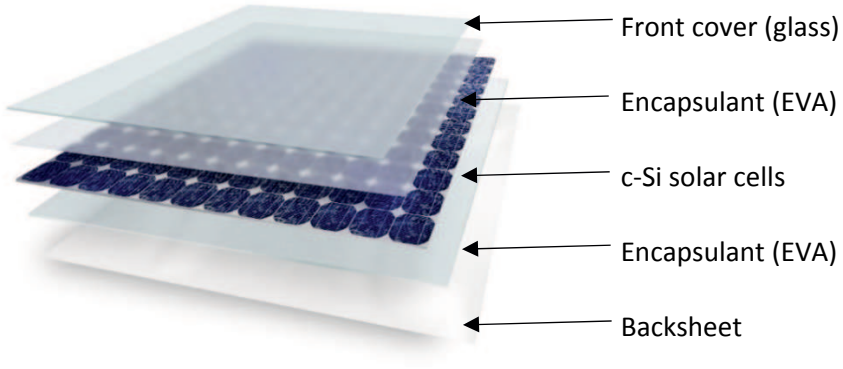

Figure 1.5. Schematic setup of a standard c-Si PV module.

Backsheets function as back cover and have to provide mechanical stability and electrical insulation. Furthermore they should act as a protection against weathering and as a selective barrier for atmospheric gases (water vapour, oxygen, acetic acid, etc.) [15]. Generally multilayer laminates are used as backsheets. In many standard backsheets polyethylene terephthalate (PET) is used as the core layer to offer mechanical stability and sufficient electrical insulation [16, 17]. The core layer is combined with protective outer layers (e.g. fluoropolymers, polyamides (PA), highly stabilised PET or other polymeric materials). The reason for polymeric backsheets are low costs and good processability. As an alternative to polymeric films glass can be used. The disadvantage beside the weight factor of the glass/glass construction is often that it can trap harmful compounds which can catalyse moisture-driven corrosion and may induce additional stresses inside the module [18]. This can enhance delamination and furthermore glass breakage [18].

1.2.2. Quality and reliability of PV modules

PV modules have to withstand various stress influences during their lifetime of more than 20 years. These factors, such as irradiance, temperature, etc. will influence the performance and reliability of a PV module. A lot of research effort has been invested to optimise the solar cells, but the module

is as efficient as all components together [8, 9]. As a result of the variety of components different types of failure can occur. The failure categories of PV modules have been already intensely discussed in former papers, especially those concerning polymeric materials [19–25]. Hence this work will not go into detail on the different types of failures of PV module, but gives a short overview. Most failures occur at the beginning of the use of the module, such as optical losses, delamination, glass breakage and thus, power loss. Most of these infant failures can be attributed to errors in the production, the transportation and handling or the installation of the module [26–28]. Midlife failures due to external impacts, e. g. hail-storms or animals can occur and are defined by the robustness of the PV module. The rate of these failures is comparably low [26, 28]. Most of the PV modules go through the wear out scenario (end of working lifetime), where degradation causes failures. This is highly dependent on the materials used and on the overall design of the module [19, 21, 26, 28]. However, the crucial parts in a PV module are polymeric materials [26]. Their properties have to be the same from the start to the end of lifetime. Therefore a high resistance against weathering is of great importance. The type and therefore the different degradation behaviour of a polymeric component highly affects the long-term stability of the whole PV module [15–17, 23, 28–32]. The loss of functionality can result in delamination of the module, decreased or insufficient electrical insulation properties or critical changes in permeation properties and subsequently can lead to the breakdown of the whole module. Consequently the ageing behaviour of the polymeric layers is critical for the whole PV module during its intended life of more than 20 years [17, 28, 29, 33, 34]. Weathering stability is the key factor for the reliability of polymers in all outdoor applications like solar energy, building materials but also mobility. That is the reason why the following chapters will discuss the influence and furthermore the effect of weathering on polymers.

1.3. Weathering of polymers

All polymeric materials age over their application time. There are many interactions between a material and external stress factors. Additionally, synergies between these stress factors can occur. That is the reason why different complex degradation mechanisms occur, regarding the polymer type and operation site. No universally valid lifetime evaluation method is applicable due to the fact that different chemical structures show different sensitivities to external stress factors and their interactions and therefore react differently. This complex ageing behaviour makes it necessary to implement customised tests regarding different polymer types and their application. The aim of those tests is mostly a classification of materials according to their stability, identification of

degradation mechanisms, correlation, and prediction of service life [35]. In the following chapters natural weathering and its stress factors are described.

1.3.1. Natural weathering

Natural weathering of polymers is their exposure to natural outdoor conditions where stress factors such as temperature, radiation, etc., vary depending on the location. Natural weathering provides an immediate statement of the weatherability of a polymer, but mostly it needs quite a long exposure time. Depending on the location it is possible to accelerate the ageing process. However it has to be taken into account that results and conclusions of natural weathering experiments are only valid for each particular location [36, 37]. But the framework conditions for natural weathering are standardised [38].

1.3.1.1. Weathering stress factors

The primary stress factors concerning weathering are light, temperature and natural conditions, like humidity with the additional influence of oxygen. Secondary stress factors consist of chemical interaction of the polymer part with, for example oil, surfactants, and solvents. Furthermore biological activities and mechanical stress, which have external causes also affect the ageing behaviour of polymers during weathering, see Figure 1.6.

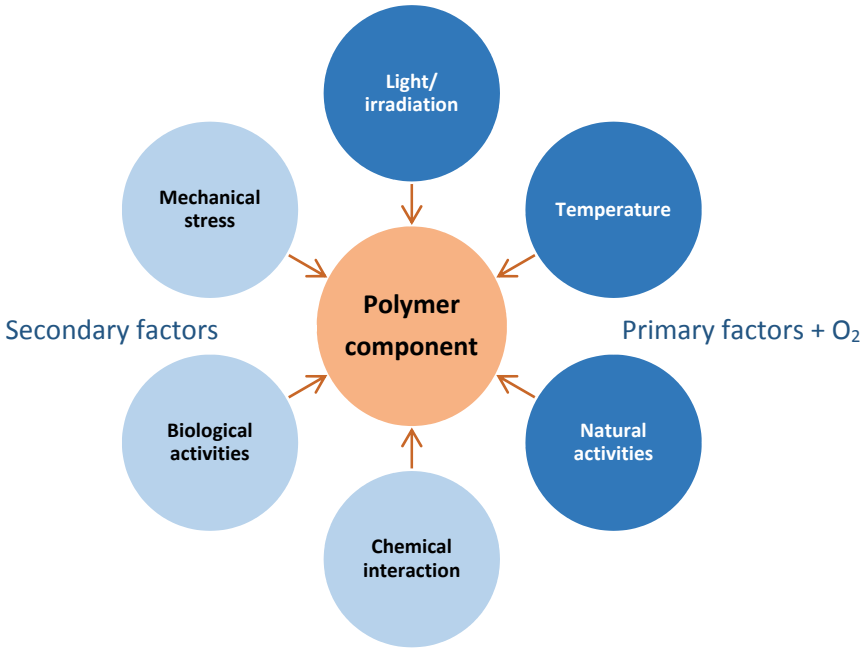

Figure 1.6. Weathering stress factors [39]

Light and irradiation

The sun shows extreme stability of its output and its energy resources are expected to last for four billion years [40]. The relevant irradiation with regard to weathering is the solar global irradiation. It is strongly influenced by the atmosphere, due to absorption loss and scattering. Depending on the location (angle and direction), season, global atmospheric conditions, local climate conditions and the angle of incidence, variations in intensity are possible. This affects the spectral distribution of the global irradiation [35]. AM 1.5 spectrum takes these factors into account, where AM stands for Air Mass and 1.5 is a factor for the distance of the irradiation through the atmosphere depending on the minimal distance, see Figure 1.7. The extra-terrestrial spectrum is characterised by AM 0. For locations at the equator AM 1 is valid.

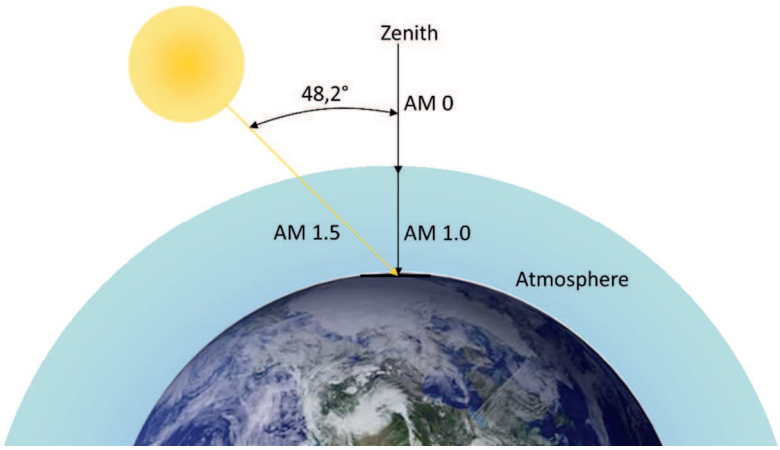

Figure 1.7. Air mass effect of the atmosphere.

As mentioned before, the atmosphere filters and scatters the sunlight, see Figure 1.8. Two theories exist concerning the light scattering by particles in the atmosphere: the Rayleigh law defines the conditions of scattering for particles much smaller in diameter than the wavelength and Mie scattering which covers the scattering of particles about the same diameter as the wavelength. The Rayleigh law implies that light of a shorter wavelength is scattered more than with a longer wavelength. This law is applicable for gas molecules in the atmosphere which are much smaller than the wavelength of the sun's irradiation. Therefore Rayleigh scattering is responsible for the blue sky, due to the fact that blue light is scattered about 10 times more than red light [40]. Mie scattering, caused by bigger particles, such as clouds, water droplets etc. is less wavelength-dependent than the Rayleigh scattering. As a matter of fact radiation with a longer wavelength is preferably scattered. That is the explanation why moisture is mostly responsible for the absorption in the infrared range of the AM 1.5 spectrum [40].

Due to the scattering, global solar irradiation consists of directional and diffuse sky radiation, see Figure 1.8 [7, 35]. A part of the incident light is reflected or scattered in dependence of the albedo. The earth's albedo is highly variable and dependent on the wavelength. As an example, grass reflects almost 60% of infrared but only a few percent of UV and visible light. In contrast to that, snow reflects 63 to 79% of all wavelengths. Sand or concrete reflect only around half the amount of UV compared to visible and infrared [40]. That is the reason why the UV conditions in cities are lower than in rural areas [40].

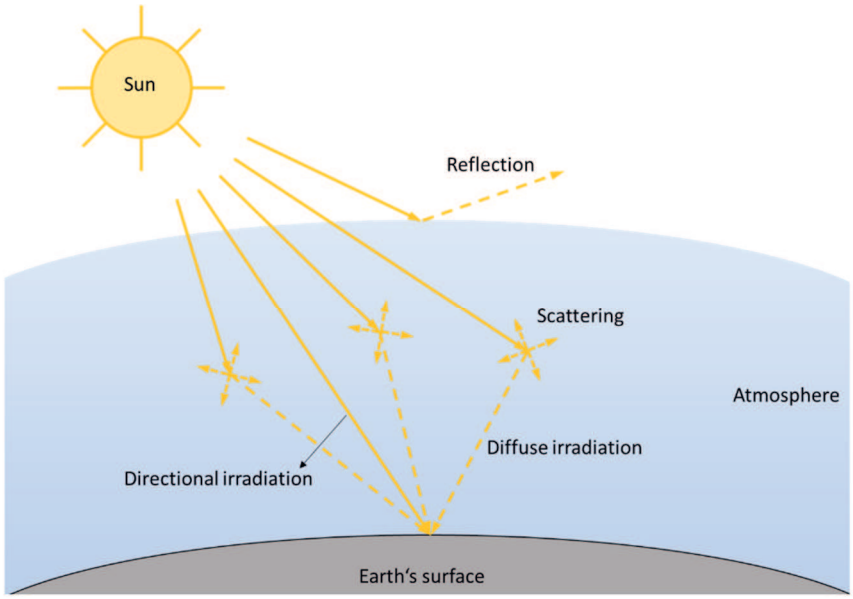

Figure 1.8. Directional and diffuse irradiation [7, 35].

The spectral energy distribution AM 1.5 is shown in Figure 1.9. The wavelength range is between 300 and 2800 nm. Around 5% of the spectral energy is caused by UV light with wavelengths below 380 nm, 54% by visual light with wavelengths between 380 and 780 nm and 41% by IR radiation. Compared to AM 1, around 2% of UV light is absorbed by the atmosphere [35]. UV radiation (wavelengths below 380 nm) of the sunlight is the mainly harmful part. According to the quantum theory, electromagnetic waves carry discrete amounts of energy. The energy depends on the frequency and, as a further consequence, on the wavelength, see Equation 1.1, as stated by Planck's Law. The outcome is the fact that with decreasing wavelength the energy of a photon increases. The whole energy of AM 1.5 arriving on the earth's surface is 994.35 W m^{-2}. However, the radiation varies dependent on the season, location, atmospheric conditions and angle of incidence [7, 41].

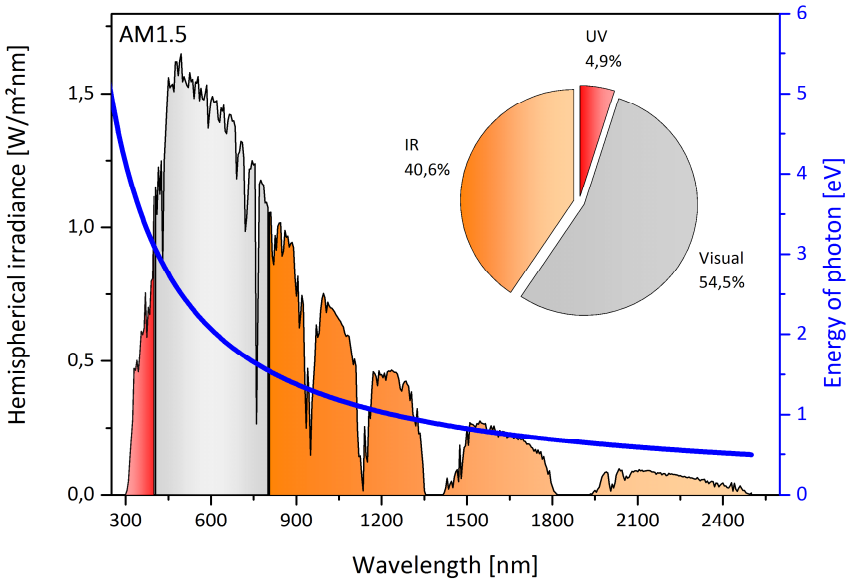

Figure 1.9. AM 1.5 spectral energy distribution according to ASTM 173-03 (2012).

$$E_\nu = h \cdot \nu = \frac{h \cdot c}{\lambda} \qquad \textit{Equation 1.1}$$

with:

- E_ν *energy of radiation of a given frequency*
- h *Planck's constant*
- ν *frequency of radiation*
- c *velocity of light*
- λ *wavelength of radiation*

As stated above UV radiation determines the useful lifetime of even adequately photo-stabilised polymeric products in outdoor applications [42–44]. UV content in sunlight is well known to affect adversely not only the mechanical properties of polymers, but also the optical and chemical properties. This is caused by the fact, that polymers absorb the high energy solar ultraviolet radiation. The material undergoes photolytic and photo-oxidative reactions that result in the degradation of the polymer. The rate of effectiveness of polymer degradation processes at these wavelengths is generally high due to the high energy content at lower wavelengths. A marginal increase in UV quantity can decrease the service life of a polymeric product noticeably [44]. Especially for PV modules a failure of the encapsulation material can be linked to significant power and therefore economic losses, due to discolouration and delamination. The decrease in service life of a polymeric product due to UV radiation is determined by the spectral irradiance distribution, the spectral sensitivity, dose-response characteristics of the material and the efficacy of the available light stabilisers [36, 44].

Temperature

Temperature can cause different effects on polymers. Higher temperatures can cause higher reaction and diffusion rates (internal, like additives or external, like pollutants). Heat can cause expansion or contraction and therefore mechanical tensile or pressure stresses. Additionally, it can promote migration and loss of additives and also humidity. The surface temperature is most important and it is defined by the microclimate [35]. It is essential that the temperature of the sample is considered rather than the ambient temperature, due to the fact that the temperature of the sample depends on the surrounding air temperature, the infrared radiation, the air movement (wind on sample surface) and the properties of the material, like its colour and the thermal coefficients. Infrared radiation affects samples differently depending on their colour. As an example more than 15°C difference was measured between white and black coloured polyvinylchloride (PVC)-coated aluminium plates [45]. But not only has the colour an influence, also whether the samples are mounted with or without a backing. In addition to the temperature influence, the amount of radiant energy received is important for a transparent sample. Radiation can be transmitted through the sample and reflected by the backing. This causes a higher radiant stress for the samples. Temperature differences of more than 10°C are possible [40]. Temperature extremes should be considered as well, as these may cause stress formation and cracking of polymeric materials, especially in the aerospace industry. In combination with a high water content of the material, extreme temperature changes can cause additional stresses due to freeze and thaw cycling (volume changes) [40].

Natural activities: air and precipitation

Degradation of materials usually occurs in the presence of oxygen. As the oxygen concentration is around 21% in the air, it highly influences the degradation mechanism of polymers. Other components of our atmosphere are nitrogen with around 79% and inert gases with below 1%. Furthermore the air contains a highly variable content of water, carbon compounds, ozone and nitrogen compounds in the parts per million (ppm) range. These pollutants can be distributed to the earth's surface either dissolved in water (rain) or by wind. Depending on the type of pollutant, the ageing mechanism of polymers can be influenced differently.

Water's molecular weight is with 18 g mol^{-1} around 40% lower than the average molecular weight of atmospheric components, like oxygen with 32 g mol^{-1}. Thus, water molecules are very mobile, which causes an average "lifetime" from evaporation to condensation of about 9 days [40]. This is sufficient time for a water molecule to be carried around the globe before being precipitated. However, humidity and the amount of precipitation are more local than global climatic phenomena.

Concerning the weathering of polymers, it is an important factor. Analysis of typical weather conditions showed that 10 to 16% of the average day time it is raining in Central Europe [40]. Of course the amount of rain varies dependent on the type of climate. At any rate this parameter is essential due to the fact that many additives in polymers operate on the surface, e. g. plasticizers. Excessive rain or condensation can wash them away which would lead to the deterioration of the material's properties. Additional possible interactions are absorption and desorption processes of water and humidity due to changing concentration. Those cycles are typically observed during daytime and season (spring, summer, autumn and winter). This can cause mechanical stresses and, in combination with extreme temperature changes, even a thermo-shock. Consequently, cracks can be formed. Literature showed that irradiation and constant temperature and humidity conditions for 1000 h caused only discolouration in acrylic melamine coatings. In contrast to that, 24 h of wet-dry cycles caused the formation of a significant number of cracks in the same material [35, 40, 46]. The ageing behaviour of polymers which are sensitive to hydrolysis, e. g. polycarbonate (PC), polyester and polyamide (PA) can be affected by a variation of the amount of humidity in the surrounding air. Hydrolysis is dependent on time and water concentration. Therefore excessive condensation and rain in artificial ageing tests can change the degradation mechanisms of laboratory studies in comparison to the natural performance of the material [40].

Chemical interaction: oils, surfactants, solvents, corrosive gases

The resistance to the influence of chemicals is dependent on the chemical structure and the morphology (degree of crystallinity, etc.) of a polymer, the composition of the chemical reagent and the environmental conditions, such as temperature. Similar effects can be observed as for chemical degradation: hydrolysis and oxidation processes [36]. Additionally stress cracking can occur if the polymer is under stress during the chemical exposure. Physical degradation mechanisms due to interaction of chemicals can be monitored as well: interactions between a chemical medium diffused in the material and the molecular chain. This is in general a reversible process as long as no damage occurs [36, 41].

Biological effects: microorganisms, plants, animals

One has to distinguish between intended and unintended biological attack of a polymer. Even though some polymers are more attractive for living organisms due to the similarity of their chemical structure to food, the unintended attack is very rare [36]. However, especially in tropical countries it has to be considered. The requirement for the degradation of polymers via bacteria or other microorganisms are splitable chemical bonds like esters and amides. Low molecular weight, a soft material and hydrophilic materials support the degradation process [36, 46]. In recent years

a variety of biodegradable polymers have become available on the market and intensive research activities have been conducted [47–50].

Mechanical stress: static stress, dynamic stress, shear stress during processing

A variety of causes including crystallisation, condensation, solvent evaporation, loads imposed during manufacturing, difference in thermal expansion of components – as it is the case for PV modules – can develop internal stresses in a polymeric part. As polymers are considered viscoelastic, they combine properties of liquids and solids. The elastic and viscoelastic part allows stress relaxation. External forces are dissipated with limited changes to the material structure. Plastic deformation leads as well to stress relaxation [40]. Of course temperature distribution in the sample can be another source of stress formation as can external forces [40, 51]. Two mechanisms for surface stress formation are suggested: one by De Bruijn, who concluded that molecular fragments are released by surface degradation. This changes the crystallinity, which causes densification and shrinkage and subsequently internal stress formation [40]. The second mechanism suggests stress formation due to a temperature gradient caused by the exposed side of the sample being substantially warmer than the back side [51].

Microclimate

Determinant for the ageing of polymers is the microclimate and not only the surrounding temperature and humidity conditions as already mentioned. There is an air boundary layer above the polymeric part which can exhibit different conditions compared to the surrounding climate. Therefore the microclimate describes the environment around the sample. It arises from the combination of the surrounding climate conditions and the application specifics (e. g. single polymeric film vs. polymeric film incorporated in a PV module) [36, 52].

Certainly, all these stress factors can't be considered in isolation. Synergistic effects play an essential role in the ageing behaviour of polymeric materials. This is illustrated among other things in a study on desert exposure of polyethylene (PE) films. Two sets of samples were used under the same exposure conditions. The only difference was the exposure temperature. Samples exposed at lower temperature deteriorated more slowly than those at higher temperatures although exposed to the same dose of solar UV radiation [44]. Additionally, the polymer composition impacts the ageing behaviour. Exposure in general to an outdoor or indoor environment not only affects the polymeric material itself, but also the additives, such as dyes, pigments, absorbers, stabilisers etc., see Figure 1.10. Each of these components can react individually or in combination with the other components. Thus, the overall degradation mechanism can be extremely complex [36, 53].

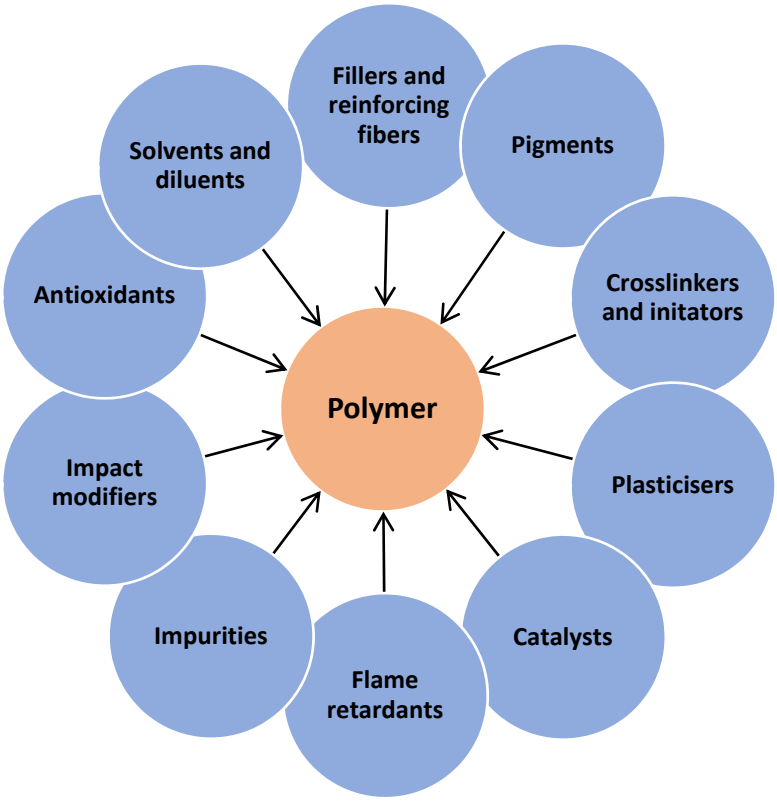

Figure 1.10. Components of a polymer.

1.3.2. Artificial weathering

In general there is a need for faster evaluations of the weatherability of polymers than can be obtained by natural exposure tests. Therefore, devices with artificial light sources are used to accelerate the degradation. Different types of light sources can be distinguished, such as xenon arc, fluorescent, metal halide or carbon arc lamps. These laboratory weathering tests are referred to as artificial weathering or ageing. The aim is to simulate the realistic ageing mechanism of a product in an accelerated and precise way. The big advantage is the relative short exposure time compared to natural weathering, due to the fact that these tests can run continuously without day and night cycles, seasonal variations and weather conditions [37]. Temperature, thermal cycles, humidity and water exposure may also be controlled. Samples can be exposed to the same natural amount of stress as when naturally weathered or beyond the limits of the intended service exposures. Additionally, artificial weathering tests have the advantages of reproducibility and repeatability by controlling weathering stress factors independently [54]. Compromises between correlation, acceleration and precision are necessary, see Figure 1.11, only two of them can be realised at the same time [35]. For example, if a test is fast and precise it might be not realistic. However, caution must be taken not to enable unnatural degradation mechanisms, see Figure 1.12. When choosing artificial experimental parameters it is necessary to consider the real-life behaviour in advance. If

one wants to set up artificially henhouse ageing in order to get a chick, than cooking at 100°C for 7 mins will only lead to an overcooked egg and not to a chick. The reason is that the ageing mechanism is not the same as in natural henhouse ageing. Therefore tailor-made weathering tests are necessary, especially for applications like PV modules [39, 40, 55].

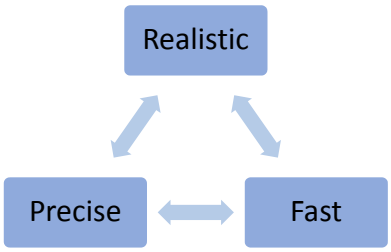

Figure 1.11. Aspects of artificial weathering tests.

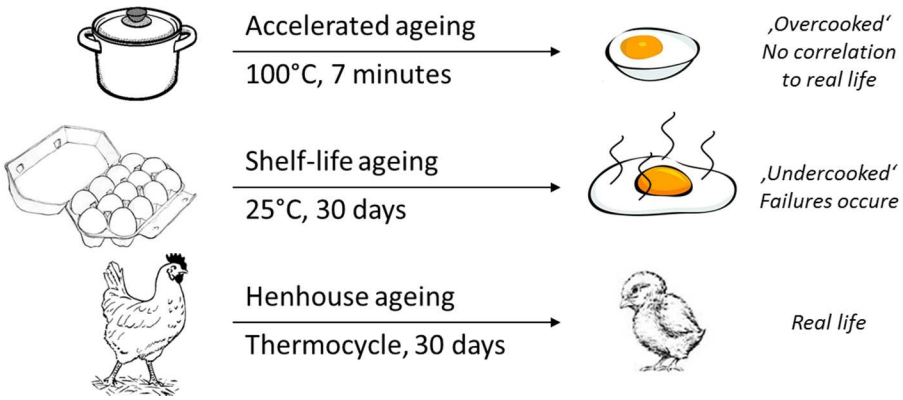

Figure 1.12. Choosing artificial experimental parameters [55].

The quality of radiation used in weathering studies is one of the most important stress parameters to control [40, 54]. When conducting an artificial weathering experiment the benefits and pitfalls of each light source has to be taken into account. Therefore, the following section focuses on the different artificial weathering devises classified by the type of light source.

Xenon arc lamp device

The xenon arc lamp spectrum represents the closest fit to natural sunlight in UV and visible solar radiation when properly filtered, see Figure 1.13 [40, 54]. It is the preferred light source when the material will be exposed to natural sunlight during application. A xenon arc lamp is a precision gas discharge lamp in a sealed quartz tube. Two types can be differentiated: water-cooled and air-cooled xenon lamp devices. The spectral output of the lamp is unaffected by the type of cooling, although it has influence on the overall design of the optical filtering system. Additionally, the

spectrum contains a considerable amount of infrared radiation below the cut-on of solar radiation. Therefore proper optical filter systems need to be used, helping to obtain the desired spectral distribution. Typical filters include quartz, borosilicate glass, soda lime glass, etc. [40, 54].

Xenon weathering devices provide precise control over spectral distribution of energy and the irradiance. It is possible to increase the radiation output by selecting the appropriate filters and by increasing the energy supplied to the xenon lamp in order to accelerate the testing time. Additionally, these instruments provide for adjustment and control of temperature and humidity by using heating and/ or cooling systems, different blower speeds and an ultrasonic fogging system. The devices can also provide for water spray, formation of condensate on the sample's surface, for immersion of test samples in water. Cycles with light and dark phases and dry and spray phases can be programmed [40].

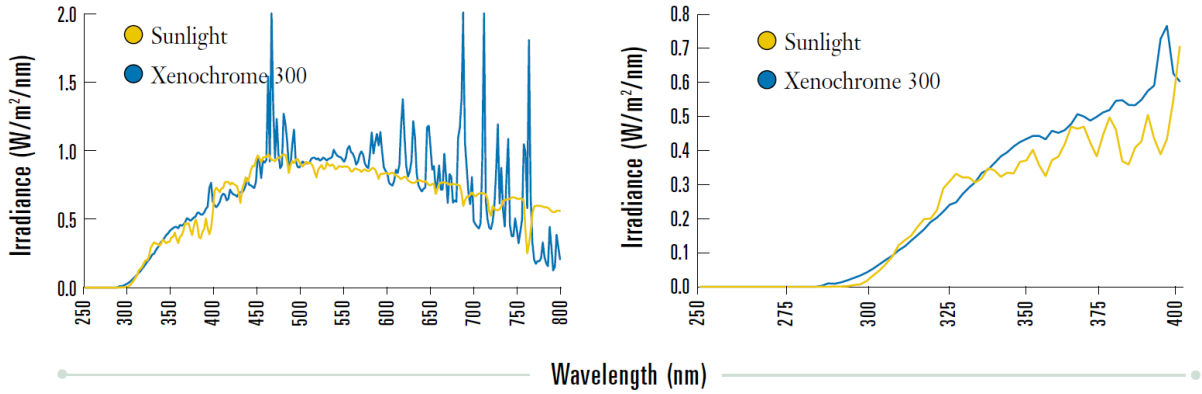

Figure 1.13. Sunlight compared to xenon arc lamp with filter system [54].

Fluorescent lamp device

Fluorescent lamps are utilised in fluorescent UV condensation devices. The lamps have been developed with specific spectral distributions and can be classified in UV-A and UV-B lamps. UV-A lamps are available with peak emissions of 340 to 370 nm, see Figure 1.14. Due to the fact that UV-A lamps do not emit below the cut-on of natural sunlight, these lamps are useful for a fast UV screening. However, the comparison to service lifetime performance or correlation to outdoor exposures may not be valid [40].

UV-B lamps have a peak around 313 nm. Nearly all of their energy is concentrated between 280 and 360 nm. Below 360 nm little radiation is emitted because the majority is at wavelengths shorter than what is present in natural sunlight making the spectrum of UV-B lamps a very high-energy radiation. The degradation mechanisms and kinetics may be significantly different to natural weathering on the earth's surface and also the stability ranking of materials may differ [40].

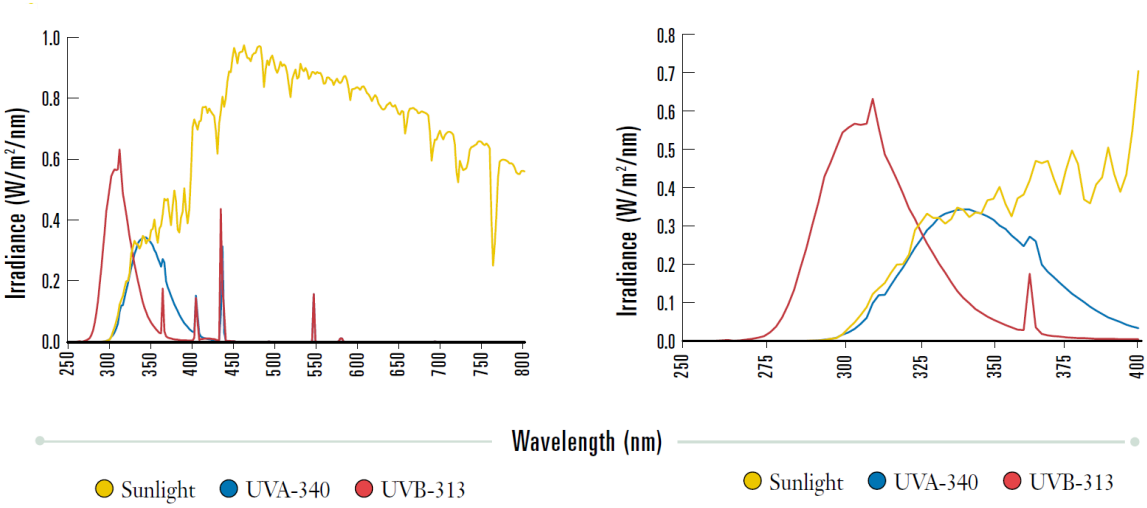

Figure 1.14. Sunlight compared to fluorescent UV lamp with filter system [54].

Fluorescent UV devices offer the control of temperature and spray function. During a dark cycle a condensation process can be started. Throughout this cycle the test surface is exposed to a heated and saturated mixture of air and water vapour with a level of relative humidity of around 100%. The back side of the panel is at room temperature, which causes condensation onto the exposed sample surface. The advantage and simultaneously drawback of the UV lamps are no output in the visible and infrared region. Thus, it is only possible to expose materials of different colours to the same surface temperature in contrast to what they would have during natural or xenon weathering, see Figure 1.15.

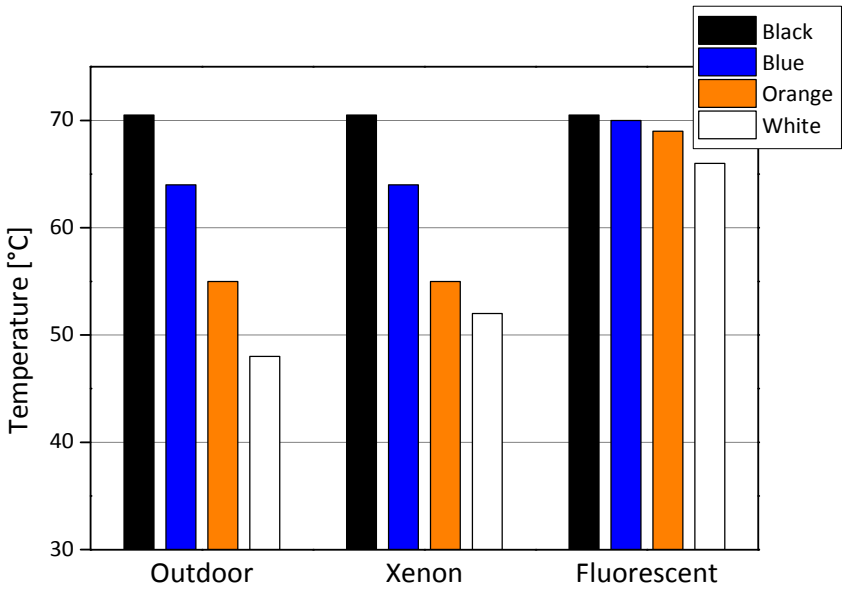

Figure 1.15 Temperature of exposed coloured panels [54].

Metal halide lamp device

Metal halide lamps have outputs similar to xenon arc lamps and therefore represent a close fit to natural sunlight. The main purpose of this type of lamp is to enable studies where degradation is accelerated by increased temperature. Various types of these discharged lamps are produced, which is why it is necessary to define the version. Even though they have a high quality they are not enough to be used as an acceptable source for solar simulation. For solar simulation a full-spectrum match and a uniform, stabilised irradiance is required. They are used primarily in the automotive industry, due to the fact that they are ideally suited for use in large-scale chambers [54].

Carbon arc lamp device

This type of device, using carbon arc lamps, are the oldest source of artificial radiation. Carbon rods are burned continuously as the light source. The spectrum of carbon arc lamps is very unlike that of the natural sunlight. Two strong peaks can be observed at 358 and 386 nm. At other parts of the UV spectrum the intensity is lower than in daylight [40]. But, due to the strong emission peaks the exposure with carbon arc lamps will have a stronger effect on samples which are absorbing long wavelength UV and visible light [54].

The big issue of artificial radiation sources is their stability. Xenon arc lamps are very stable compared to carbon arc lamps, which need to be replaced every day. In order to fulfil the aim of reproducibility and repeatability it is important to replace the source according to the manufacturer's recommendation. During its use the output is automatically controlled and by this is kept constant [40].

In addition to artificial weathering it can be useful to apply ageing methods without irradiation, such as climate chamber or oven ageing. This is helpful in order to validate the single influence of the different stress factors on polymer materials.

1.3.3. Natural versus artificial weathering – correlation and acceleration

As already mentioned several stress factors determine the outcome of weathering studies under natural and accelerated conditions. The probability is high that the results of the different ageing tests will correlate if the degradation mechanisms and kinetics are well understood and the conditions of the experiments are well defined.

When using natural weathering in order to validate ageing mechanisms no repetitions under the exact same conditions are possible. Results are only valid if the climate of exposure corresponds to the climate of application (real-life conditions). It is easily possible to test large samples and

structural components via natural weathering. Test durations are operating lifetimes of the parts and considering lifetimes of 20 years it is not reasonable for many reasons to test that long. An acceleration can be achieved by extreme climates: humid and hot (Florida) or dry and hot (Arizona) depending on the ageing mechanisms of the polymer. In the 1960s the development of equatorial mount with mirror for acceleration (EMMA) devices increased the acceleration further. These devices follow the sun and concentrate the radiation on the sample with a Fresnel reflector system. In doing so the solar spectrum distribution is still the same, but with an up to 8 times higher intensity than the natural sunlight (8 suns) [36]. For example it is possible to increase the radiation from 7900 to 61000 MJ m^{-2} in Arizona [36].

Artificial weathering is feasible when it offers acceleration and control over ageing conditions. The aim of artificial weathering is to perform tests in the minimum possible time and under well controlled, repeatable conditions. However, it is not reasonable to expect that accelerated ageing will exactly simulate natural ageing. Additionally, accelerating a test by intensifying stress parameters, like temperature, etc. requires a good knowledge of the material to ensure good correlation. It must always be a compromise between correlation and acceleration because the faster a test is the more likely it will not correlate [54].

One approach to accelerate and subsequently correlate is to increase the temperature with the assumption that the ageing reaction is a linear process. Almost every model which describes ageing is based on the Arrhenius equation, see Equation 1.2. It defines the temperature dependency of simple reactions and physical processes. The rate constant increase exponentially with the temperature [36].

$$k(T) = A \cdot e^{\frac{-E}{RT}} \qquad \textit{Equation 1.2}$$

with:

- *k* *speed of reaction*
- *T* *temperature*
- *A* *constant*
- *E* *activation energy*
- *R* *universal gas constant*

The requirements for the validity of this equation are that only one (dominating) ageing process is responsible for the ageing of a polymer in dependence of the temperature and the activation energy is independent on the temperature. The difficulty is that not just one reaction is responsible for the degradation of a polymer but a variety of simultaneous reactions. Additionally, the temperature-time extrapolation is also limited [36].

Another approach to correlate different weathering tests is the equivalence of radiation. It means that the same dose of radiation causes the same effect on polymers. A constant relation between absorption and irradiation is required over the whole exposure time, which is hardly possible. Another drawback of this method is that the influence of the temperature is completely neglected, even though higher temperatures cause a speed-up of reactions. Therefore, it only makes sense to use this approach if the ageing tests are conducted under the same temperatures und spectral distribution of light [36].

In order to conduct and correlate weathering tests the diversity of polymers and with this the main degradation mechanisms have to be taken into account for the test design. Therefore the next chapter concerns the main ageing processes of polymers during weathering.

1.3.4. Influence of weathering on polymers

Organic polymers are much more prone to ageing than most other materials. Due to the more frequent use of polymeric materials, the research of polymer durability in industrial laboratories and at universities has increased [53, 56–62]. As already described, polymers can be influenced by a variety of environmental agents which cause ageing. An overview of these factors is provided by Figure 1.16.

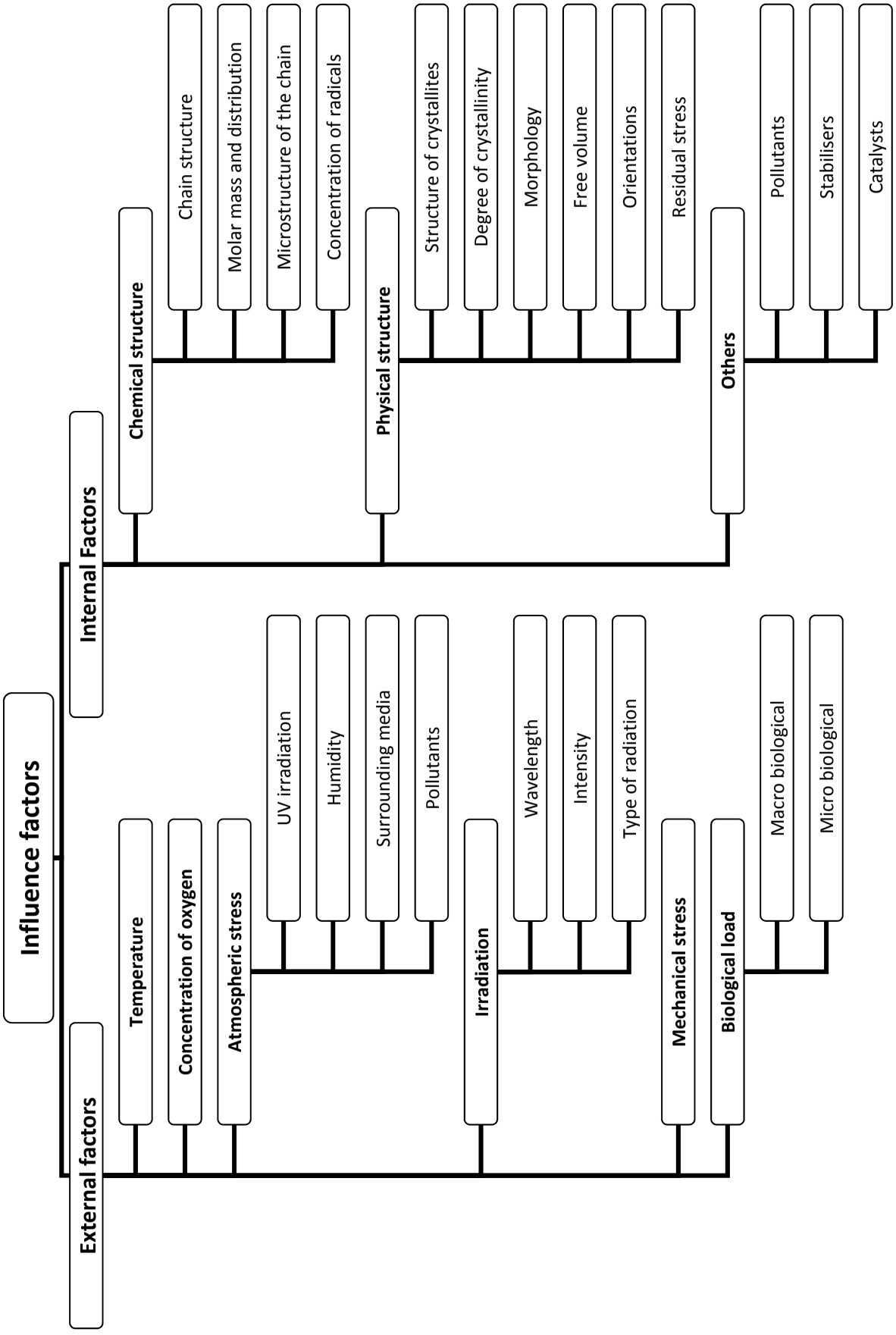

Figure 1.16.Influence factors concerning ageing of polymers [36].

1.3.5. Ageing processes of polymers

All prevailing processes in a polymer part are caused by ageing. The term ageing is per definition the sum of all chemical and physical changes of a material during the application time, and these changes can reduce the lifetime of any polymer part. DIN 50035 is more precise and defines all positive and negative irreversible chemical and physical changes of properties during the application time. However, also reversible processes can highly influence the lifetime of a polymeric part. In general all ageing processes can be divided in physical and chemical ageing processes. The distinction between the effects of physical and chemical processes is not trivial, as the processes act together and in synergy. Figure 1.17 gives an overview of chemical and physical ageing effects of a polymer [36]. These effects are caused by ageing processes which are described in the following chapters.

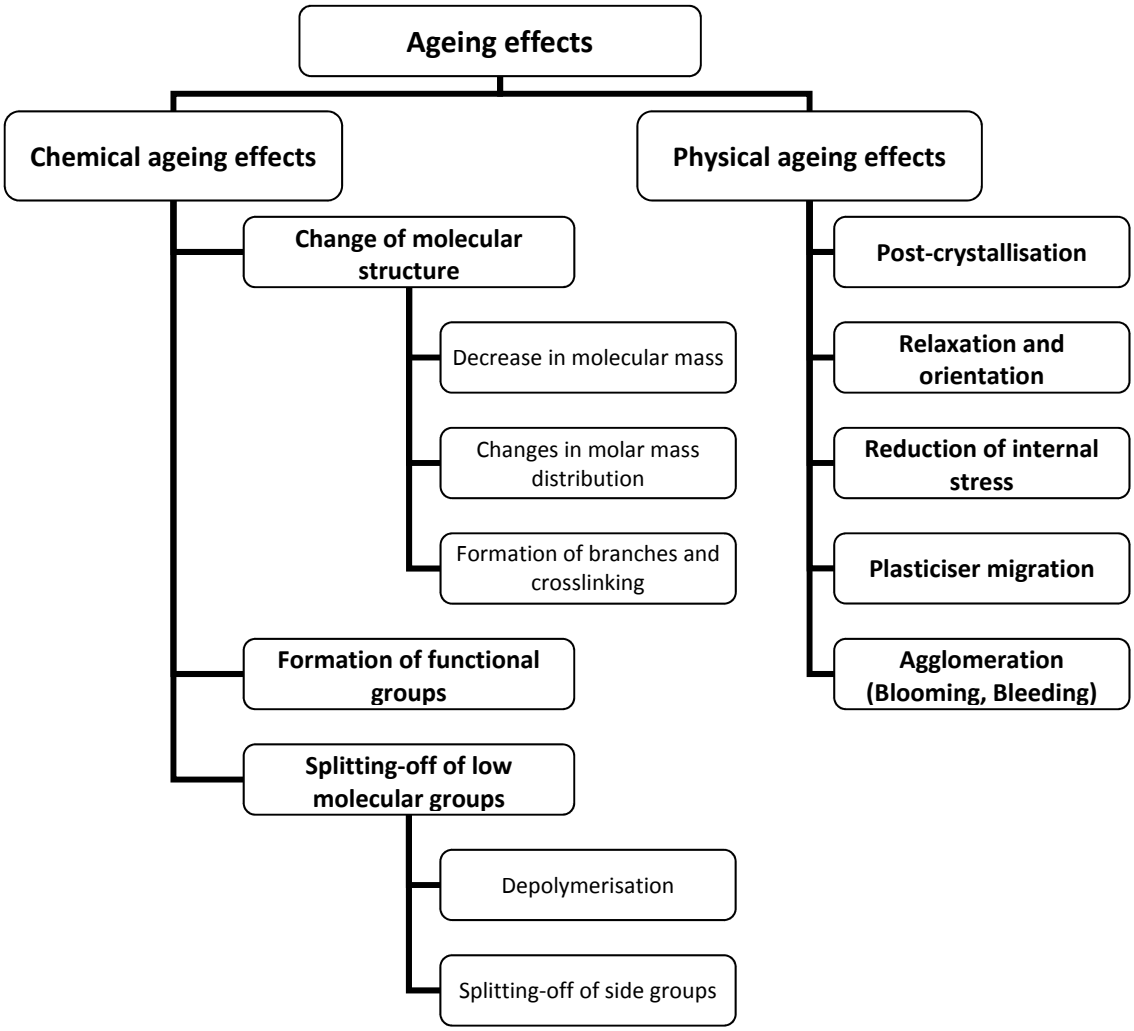

Figure 1.17. Overview of ageing effects [36].

Even though one can differentiate between physical and chemical ageing processes in theory, the two must not be seen separately from each other. In general it is always the case that the ageing

of polymers is a complex process composed of a number of parallel and sequential reactions and interactions. The degradation process is influenced not only by outer stress, the known state and components of a polymer but also by contamination and degradation products induced by processing. Moreover, unknown interactions can take place.

1.3.5.1. Chemical ageing processes

Chemical ageing processes affect all changes in the chemical composition, molecular structure and/or molecular size. These processes are irreversible and the main phenomena are changes in the molecular structure (e. g. molar mass), the forming of functional groups and separation of low-molecular products [36].

The weak link in polymers is the macro-molecular structure with its relatively low bonding forces compared to other materials. For example, the aliphatic C-C bond exhibits a bonding energy of 335 kJ mol^{-1} [36]. Compared to that ceramic materials can show bonding energies of more than 1000 kJ mol^{-1} [63]. The bonding energy is dependent on the bonding distance in general and the direction in space for a polymeric anisotropic material. With an increase of the number of bonding the bonding energy will as well increase (single < double < triple bonding) [36].

Changes in the molecular structure can influence the mechanical properties such as the strain or stress at break. The formation of functional groups can cause changes in colour which affect the transmittance and therefore the optical quality. This is, for example, of significance for PV modules. Additionally it is possible that the electrical properties are changed and olfactory impairments occur.

Thermal degradation

The reason for thermal degradation is the over-stressing of the intramolecular bonds. With increasing temperature the oscillation of the atoms increase until the bonding energy is overcome. This results in the decrease of the molecular mass, due to chain scission in the backbone of the polymer. But formation of low molecular mass products and crosslinking reactions are also possible. The latter leads to an increase of the molecular mass. The purely thermal degradation takes place without the participation of other components, which means in an oxygen-free environment. It is also called pyrolysis. Different kinds of purely thermal degradation can be distinguished:

- *Statistic chain scission*

  This type strongly depends on the bonding energy. Weak links are preferred, which is the reason why mostly the polymeric backbone is affected and not the side groups. Almost no splitting-off of low molecular groups can be detected. A decrease in mechanical properties is the output.

- *Depolymerisation*

  This type of degradation starts at the end of a polymeric chain and no significant changes in molar mass can be detected at the start of the process. The ultimate product may be the monomer, as for polymethyl methacrylate (PMMA) or volatile chain fragments such as the range of short chain alkanes and alkenes for PE [53]. A resulting strong odour is possible as well as the influence of optical and electrical properties.

- *Splitting-off of side groups and formation of low molecular groups*

  In this case the bonding energy of the side groups is lower compared to the main chain, enabling side groups to split-off. Discolouration and changes in the electrical properties are typical results of this process.

As an example, Figure 1.18 shows the depolymerisation reaction for PMMA. It is a radical chain reaction in the region of 300 to 400°C. The initiation is by scission of the polymer randomly along its length. Radicals are formed initiating a reaction exactly reverse of the propagation process in polymerisation reactions. As in polymerisation the termination can occur by interaction of pairs of radicals or by disproportionation, see Figure 1.19 [53].

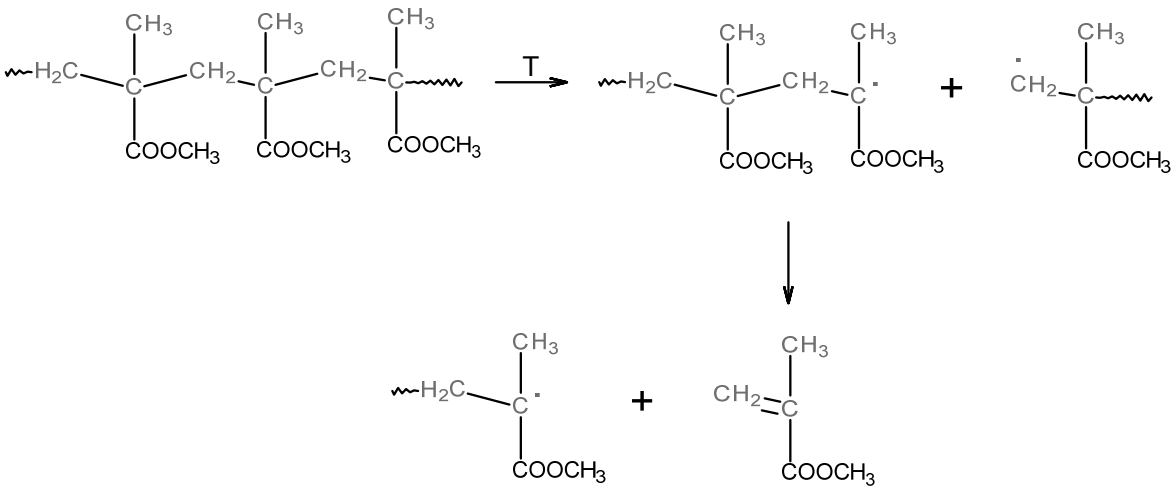

Figure 1.18. Depolymerisation process of PMMA.

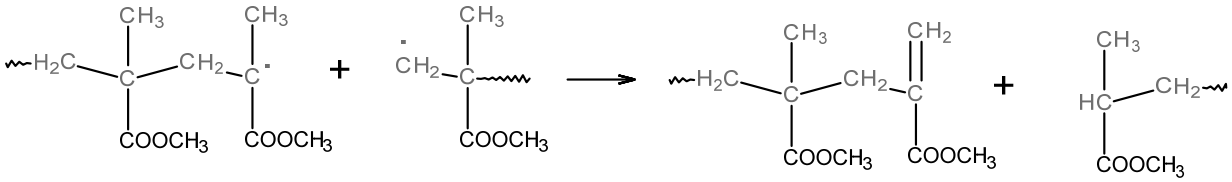

Figure 1.19. Termination of depolymerisation process of PMMA.

In dependence on the polymer type and the temperature, the reactions can be superimposed. J. Hepperle showed that if the hydrogen atom at the α-carbon atom is replaced in polystyrol (PS) by another atom or molecule group, the depolymerisation is significantly increased [36, 53, 64]. However, temperatures of 250 to 300°C are not very likely to cause thermal degradation due to high enough bonding energy values [36]. A purely thermal chain scission of PE needs 264 kJ mol^{-1}, whereas the oxidative degradation needs only 59 kJ mol^{-1} [36, 64]. However, thermal degradation as a single ageing process is not very common, as it means an exclusion of air and therefore oxygen. That is the reason why primarily thermo-oxidation takes place.

Oxidative degradation

Degradation of polymers is almost always faster in the presence of oxygen. Oxidation of hydrocarbons is normally auto accelerating. In the presence of oxygen radical chain reactions can take place. This can lead to chain scission, crosslinking and branching in dependence on the reaction partner, outer stress and the chemical and physical state of the material. The initial step is caused by free radicals, see Figure 1.20. The formation of these radicals can be initiated by thermal energy, radiation, mechanical stress or the influence of metal ions. Reaction (II) has a low activation energy and occurs with high frequency, whereas step (III) involves the breaking of a carbon-hydrogen bond and exhibits a higher activation energy. At normal oxygen pressures, the rate of this reaction determines the overall rate of oxidation in most polymers. The exception is when the radical R• is strongly resonance-stabilised. Due to a low stability of the O-O bond, step (IV) is initiated and alkoxy radicals are formed. These cause an increase in radicals and branching. The alkoxy radicals can attack the main chain (VI) and propagate this series of reactions or decay while forming carbonylic bonds, like step (VIII). The formed alkyl radicals from step (VI) and (VII) can decay with the formation of double bonds (IX) and affect further reactions (X). This oxidation process can be aborted by recombination, disproportion (VII, VIII), forming of less reactive alcohol or ketone bonds (XIV) or reaction with contamination. Step (V) and (VIII) are responsible for the decrease of the molar mass. The recombination of two macro radicals (XII) can cause crosslinking. The main degradation products are alcohols, esters, carbon acids and chains with carboxyl bonds [36, 53]. As a result, odour is possible as well as the deterioration of optical and mechanical properties.

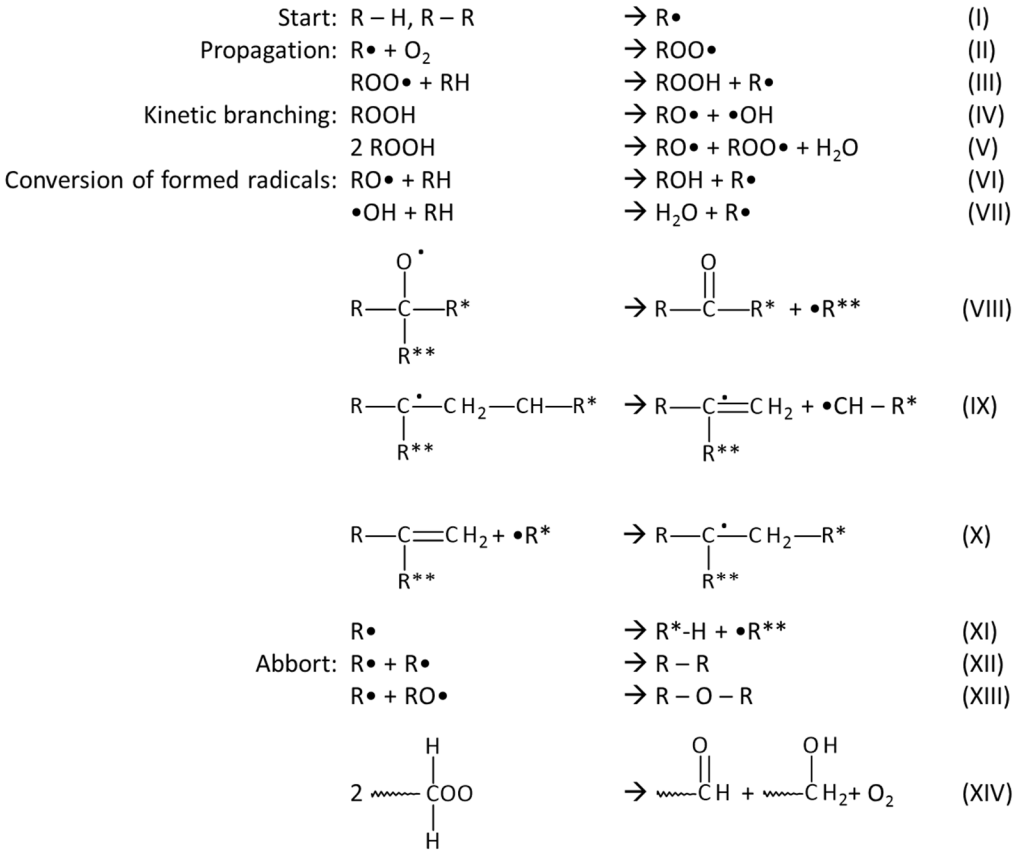

Figure 1.20. Scheme of oxidation via radicals [36, 53].

As already mentioned, the oxidation process is an autocatalytic process. At the start the reaction speed is slow (induction time) and with increasing hydro-peroxides and their breakdown into radicals it increases, see Figure 1.21. The more radicals present the faster the oxidation reaction takes place. As the oxidative degradation is auto accelerated it is also called autoxidation. The origin of the primary radical is still being discussed. The direct reaction of oxygen with polymers is excluded due to kinetic and thermo-dynamic conclusions. However, commercial hydro-carbon polymers are not pure in the chemical sense. They contain chemical modifications due to side reactions which occur during polymerisation. But they may also contain catalyst residues, such as metal ions, crosslinks or oxygen-containing groups introduced by adventitious oxidation which can form the primary radical. Figure 1.21 shows that the kinetic process exhibits four steps. It includes a fast initiating process of oxygen to active centres (I), an induction period depending on stabilisation systems (II), an increase of the speed of oxidation (III) and a decrease of the speed of oxidation due to a decrease of reactive centres (IV). It has to be taken into account that the speed of oxygen absorbed is proportional to the mass and not to the surface of the sample [36, 53].

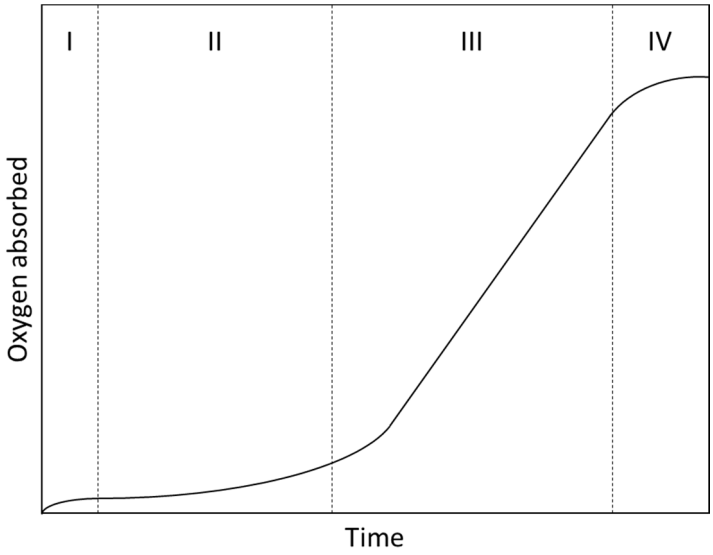

Figure 1.21. Kinetic process of oxidation [36, 53].

In solid polymers the oxidation process takes place heterogeneously. Due to the structure and the morphology of the polymer, contamination, catalyst residues, mini-reaction centres can be formed. In semi-crystalline polymers this heterogeneous behaviour can be caused by the oxidation preferred in the amorphous phase [36].

As inhibitors for autoxidation antioxidants are used, mainly phenolic antioxidants, organic phosphites, as well as sulphur compounds. All stabilisers work only in their molecular surrounding region. That is the reason why it is important that radical catchers have to be homogenously distributed in the polymer. The aim of an inhibitor is to prevent or retard the formation of hydro-peroxides for as long as possible [36, 53]. As shown in Figure 1.21, these additives act in the induction period (II). Usually concentrations of antioxidants are 0.03 to 0.3 wt. %, in special applications more than 1 wt. % are possible. However, due to the high market price an increased stabiliser level is not very usual. The operating principles of the different stabiliser systems are known and therefore won't be described in detail in this thesis. The reader is referred to standard literature concerning this topic [36, 53, 65–69].

Photo-oxidative degradation

Ultraviolet content in sunlight is well known to adversely affect the mechanical properties of polymers. This is caused by the fact, that polymers absorb solar ultraviolet radiation. The energy of the UV light, and possibly also of the visible components of sunlight, is sufficient to break chemical bonds. The energies of 700, 400 and 300 nm photons exhibit approximately 170, 300 and 390 kJ mol^{-1}, respectively. This is enough to split C-C and C-H bonds with bonding energies of approximately 420 and 340 kJ mol^{-1} or less, depending on the environments, e. g. in the

neighbourhood of aromatic or unsaturated structures [53]. However it is not enough that energy at a sufficient level is available in order to split bonds. Chromophoric groups are necessary to absorb the incident radiation [36, 53]. If a molecule absorbs incident light it can transfer the energy to another molecule or emit this energy with a higher wavelength. In some cases a photo-chemical reaction is initiated. An understanding of the spectral sensitivity is necessary in order to assess the effect of solar irradiation exposure on polymeric materials. Table 1.1 shows UV characteristics for common polymers according to Hamid et al. [42]. The absorbed wavelength is partly dependent on the molecular structure. For example, carbonyl groups of ketones and aldehydes absorb incident radiation in the wavelengths at 187 and 280 to 320 nm [36, 44].

Table 1.1. UV characteristics of common polymers.

Polymer	Absorption maximum in nm	Most efficient wavelength in nm	Cut-off in nm	Outdoor lifetime in years
Polyethylene (PE)	<150	300 300-340	<180	0.5-1.0
Polypropylene (PP)	<200	310,370 320-380	<180	0.2
Polyamide (PA)			~240	~8
Polyester		325		
Polystyrene (PS)	<260	318	~270	~0.1

The material undergoes photolytic, photo-oxidative reactions that result in the degradation of the polymer [44]. The essential first step to photo-degradation is the absorption of radiation. The absorbed energy will be attenuated as it passes through the material. Therefore the reaction is concentrated in the surface layers and thus is described as a 'skin effect' in photo-initiated reactions [53]. For transparent and unstabilised materials it is possible that photo-oxidative degradation can also be detected on the back side of the sample. The initial step in photo-oxidation is a homolytic bond scission to form free radicals. These radicals react rapidly with any oxygen present. This makes radiation particularly effective as initiator of oxidation. However it is important to note that light alone is not an important degradative stress in ageing of most polymers. It is the combination with oxygen (photo-oxidation) which makes it a crucial influence [44, 53].

A strongly absorbing group does not necessarily cause degradation. For example acrylic esters are stable against UV light, but their carbonyl group is highly absorbing [36]. The absorbed energy does not necessarily induce a reaction in the same molecule which absorbed the light. But, as already mentioned, the energy can be transferred to a more sensitive molecule. For example, ether groups can be split by that mechanism even though they do not absorb UV light [36].

Figure 1.22 shows the photo-degradation of PET as an example. The initial chain scission can occur in the ester group at one of the points indicated by the dashed lines. Scission at point 1 and 2 may cause the formation of carbon dioxide and carbon monoxide. All of the formed radicals may abstract hydrogen from elsewhere in the system. An alternative process is shown in Figure 1.23. During this reaction vinyl groups are formed in the degrading polymer which is analogous to the thermally induced ester decomposition, also described as Norrish II scission. The basic chemical pathways by which common polymers photo-degrade are fairly well known [36, 42–44, 53]. However, the combination of other outer stress factors, such as temperature and humidity can highly influence the ageing behaviour of polymers under irradiation. As a result the molar mass decreases and this leads to the deterioration of mechanical and optical properties.

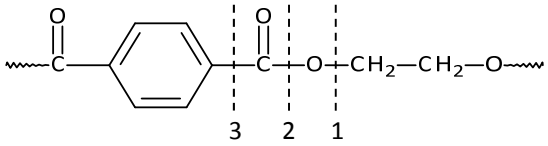

Figure 1.22. Photo-degradation of polyethylene terephthalate [36, 53].

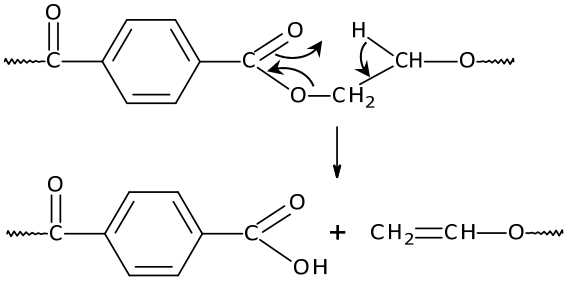

Figure 1.23. Photo-degradation Norrish type II of polyethylene terephthalate [36, 53].

Effective organic light absorbers such as hindered amine light stabilisers (HALS), benzotriazoles, benzophenones and phenyl esters are used in polymeric materials for outdoor use. The typical amount used is 0.05 to 2.0 wt. %. Due to the high market price, an increased stabiliser level in the composition is very unusual. The share of light absorbers in the cost of a product such as a greenhouse film can be as much as 30% [44]. Inorganic opacifiers such as titan dioxides or carbon offer an effective level of protection. However, higher levels will affect processability, power consumption and the lifetime of processing equipment due to the increased melt viscosity. Additionally, these inorganic opacifiers can only be used for applications where colour and transparency is not of primary importance. This is the case for backsheets of a PV module. Protective surface coatings as they are applied in multilayer backsheets will control the light-

induced degradation. In case of PV backsheets typically a fluoro- or higher stabilised polymeric layer is used as an outer protection against UV radiation [36, 44].

Hydrolysis

Hydrolysis is the chemical degradation via the influence of water. Especially polycondensates, which are formed via splitting-off of water are sensitive to hydrolysis. These include polyesters, polycarbonates, polyamides, poly dialkyl siloxanes and polyurethanes (PUs). In each of these groups hydrolysis causes a scission of the main chain which implies a rapid decrease in molar mass and deterioration of mechanical properties [36, 53, 70]. Especially the combination of humidity and catalytic acting acids or alkalis can increase the degradation process. During the hydrolytic process acid groups are formed and lead to an autocatalytic reaction [62, 71, 72]. However, Pickett and Coyle showed that this is not the case for PET [62, 73].

Figure 1.24 shows the general mechanism schemes for the hydrolytic degradation for PET. It includes chain scission at ester linkages where each water molecule breaks down one ester bond. This reverse esterification causes an increase in smaller chain fragments [72]. Depending on the pH value the degradation kinetics are different. Under acidic conditions the process involves protonation of the in-chain oxygen atom. The following reaction with water causes the formation of hydroxyl and carboxyl end groups. Under alkaline conditions the carboxyl oxygen atom reacts with the hydroxide anion, thus forming hydroxyl and carboxyl end groups [70, 74]. The result of these chain scissions is the deterioration of mechanical and optical properties.

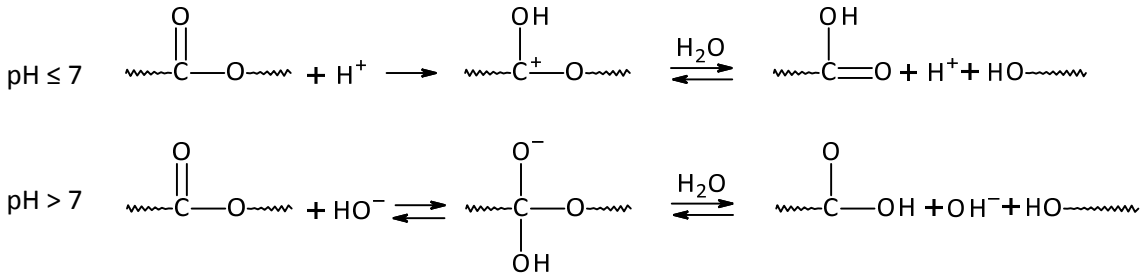

Figure 1.24. Hydrolytic degradation of an ester bond under acidic or neutral conditions and alkaline conditions [70].

In semi-crystalline polymers such as PET the crystalline fraction is nonreactive to hydrolysis due to the fact that it is impermeable to water. Water can diffuse only in the amorphous region and therefore chain scission occurs in this fraction. The formed small chains have a higher mobility and can realign in the polymer media and increase the crystallinity [36, 70]. This process is called chemo-crystallisation. Around five to six monomer units can incorporate into the crystalline phase per

chain [75]. Therefore the polymer morphology highly influences the hydrolytic degradation process. For this reason it is possible to increase the crystallinity of a polymer in order to enhance the resistance to hydrolysis [70]. A reduction of the acid content can also improve the thermal and hydrolytic stability for polyesters [70]. Different types of additives have been introduced, such as carboimides, ketonimides and cyclic acetals [76].

1.3.5.2. Physical ageing processes

Physical ageing processes only cause measurable changes of physical properties, e. g. changes in molecular structure, molecular order, concentration ratio or outer form and structure, provided that no chemical degradation is dominant. In general physical ageing processes are reversible and can be eradicated by melting. The main phenomena are relaxation, post-crystallisation, swelling, segregation, plasticiser migration and agglomeration [36].

Physical ageing processes are always caused by thermo-dynamically instable states, such as residual stress, orientations, imperfect crystalline structure caused by the cooling conditions during the production process. These polymers solidify as an undercooled melt and therefore no state of equilibrium is reached [77, 78]. With increased temperatures physical ageing processes are accelerated. However, physical ageing occurs in broad temperature ranges even below the glass transition temperature (T_G) [77]. Often the dimensions change when the physical structure is changed. If expansion or shrinkage occurs restraint stress can be induced in the material. As a consequence of these stresses cracks and fractures can emerge [78].

Physical ageing – concept of free volume

The term physical ageing describes the change of properties caused by the thermodynamic disequilibrium at temperatures below their glass transition down to the highest secondary transition (T_β). Solidified 'frozen' polymers have a higher volume, entropy, etc., than they would have in their equilibrium state, see Figure 1.25. This phenomenon is also called the free volume concept and is described, inter alia, by Struick [77]. At temperatures above T_G the polymer behaves as a rubber or a fluid and at small strains the segment mobility and the free volume (holes) among molecular chains are large. During cooling the mobility and the free volume decrease. Free volume exists because its generation is accompanied with an increase in entropy. When passing the glass transition of the material, the free volume amount remains constant at a first approximation, only the mobility decreases slightly due to thermal activation. However, the material is not in its equilibrium state, but has the tendency to reach this state, by decreasing its free volume. This behaviour is primarily determined by the amorphous region. It influences at least the small-strain

mechanical properties, but it has to be considered particularly in the prediction of the long-term behaviour of polymeric parts [56, 77, 78].

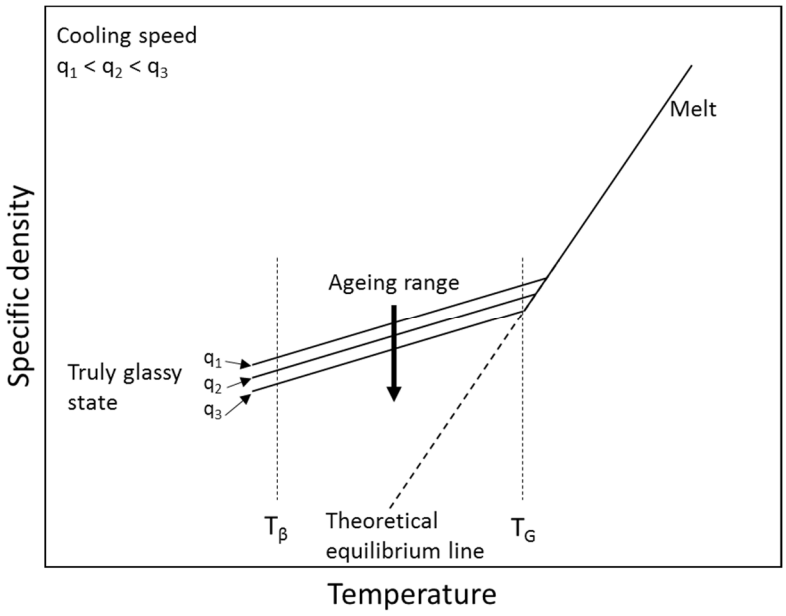

Figure 1.25. Physical ageing of amorphous polymers [36, 77].

Post-crystallisation

For semi-crystalline polymers post-crystallisation occurs especially at elevated temperatures. However, also room temperature can be enough to induce post-crystallisation as is the case with thermoplastic polyurethane (TPU). During post-crystallisation the physical structure changes and the crystallinity increases. This is caused by an increase of the thickness of the lamella and is also due to a perfection of the crystalline structure. Amorphous parts can accumulate at the transition to the crystalline phase. The result is a denser package of the molecules and consequential shrinkage or deformation and a possible crack formation of the polymer part can occur [36, 61, 74, 79–81].

Relaxation of orientations

Orientations of macromolecules are mainly induced by the processing, such as injection moulding or extrusion. The molecular chains are oriented in the flow direction. Simultaneously there are entropy-elastic resetting processes against the orientations. These relaxation processes in the solid polymeric materials are increased at higher temperatures (above transition temperature T_G). As a consequence of this process the polymeric component can deform along with the formation of cracks [36, 78, 81].

Reduction of internal stress

Internal stress is mainly caused by uneven changes in the volume of the polymer, independent on amorphous or semi-crystalline morphology. The reason is the temperature gradient resulting from the cooling from temperatures higher than T_G. However, also plasticiser migration can be the reason for internal stress. Relaxation processes can lead to deformation and formation of cracks in the polymeric part [36, 78].

1.3.5.3. Weathering effects on the properties of polymeric materials

The most critical phenomenon of ageing is the deterioration of mechanical properties which leads to the loss of mechanical integrity. Depending on the degradation mechanism, the changes in mechanical properties are material-specific. For example crosslinking increases the tensile strength and reduces the strain at break [82, 83]. However, the critical process is chain scission, for example due to oxidation which causes a deterioration in mechanical values [84–86]. If such changes are only surface related and there is no crack formation, the tensile strength decreases and elongation stays almost constant. This is due to the fact that the bulk properties are not changed. If there is crack formation on the surface both the tensile strength and elongation decrease rapidly. This is because the cracks act as notches. Of course these changes do not only depend on the outer stress factors, but also on their combination with the geometry of the polymeric part [34, 40, 61, 84, 85, 87–89]. Rheological properties are also influenced by degradation mechanisms. Especially the decrease of the molar mass causes a reduction of the viscosity [83, 85].

Optical changes like discolouration, loss of gloss or transparency can occur. This can happen due to the formation of coloured substances by photo-initiated radicals. It can be the formation of polyenes, as it is the case for PVC, or additional double bonds conjugated with the aromatic ring like it is for aromatic polymers, such as PET, PC or PU. Of course these changes are dependent on the chemical composition of the polymer and the outer stress factors. However, a lack of discolouration is not necessarily a sign of stability. For example PE degrades rapidly without discolouration if it is not stabilised. This is because PE is very unlikely to form conjugated double bonds during photo-chemical reactions [40]. It is also possible that reactions change the optical properties in the other direction, as is the case with the photo-bleaching effect. The combination of oxygen with UV radiation and increased temperature can cause a bleaching effect of the formerly discoloured encapsulant of PV modules [12, 90–94]. Additionally the electrical properties can be changed during degradation processes by forming low molecular and functional groups. By the splitting-off of side groups and formation of low molecular and degradation products a strong odour is possible.

As already mentioned there are two types of changes which are important: the change of the surface and the change of the bulk. The changes on the surface are qualitatively the same for most polymeric materials with regard to photo-oxidation reactions. The formation of hydro-peroxides is the first step of photo-oxidative degradation on the surface of the material. The permeability of the polymer influences the further degradation of the bulk. Especially for the hydrolysis process the changes in the morphology and therefore the permeability is of importance. The reason is that water vapour can only permeate in the amorphous regions of the polymer.

When weathering polymers it is necessary to qualify and quantify the influence. Therefore typical characterisation methods of weathered polymer parts are listed below [39]. The different measurements and their parameters will be discussed in detail in the chapters 2 to 5.

- Visual evaluation
- Microscopy
- Mass or density change
- Colour and/or gloss change
- Spectrophotometry
- Molecular weight change
- Rheological properties
- Thermal analysis
- Mechanical analysis
- Other non-destructive test methods

1.4. Objectives

As already outlined in the introductory part – chapter 1, weathering stability is the key factor for the reliability of polymers in outdoor applications. For some applications, such as photovoltaics (PV), polymers have to guarantee lifetimes of 20 years and more with a limited loss in functionality of the component. All materials age over time, but organic materials, such as polymers are much more prone to do so in a shorter period than inorganic materials. This is especially serious if the properties change critically within the desired life time.

The weathering performance of polymers is assessed most accurately by outdoor exposure to natural weathering at different locations and the examination of their performance characteristics by following changes in chemical and physical properties. Although natural weathering is the most reliable exposure method to examine long-term performance, its major drawback is the extremely

long exposure time required to achieve the corresponding service lifetime of the components. This long time-scale places a very severe limitation on its use. In order to decrease the testing time significantly for the purpose of faster prediction of the long-term weathering performance of polymers, it is necessary to use harsher, artificially accelerated weathering tests followed by measurements of chemical and physical changes or changes in performance.

To assess the long-term performance and durability of materials, it is necessary not only to measure the deterioration of macroscopic physical properties, but also to gain information about degradation processes taking place at molecular level. In order to establish suitable knowledge about the degradation mechanisms, the influence of the relevant load parameters like ultraviolet radiation, temperature and humidity on the degradation behaviour of the polymeric materials has to be taken into account. Additionally, the functionality of the components has to be determined. However, significant for the ageing of polymers is the microclimate and not only the surrounding conditions. It arises by the combination of the surrounding climate conditions and also by the application specifics. This is important when conducting ageing studies and analysing ageing effects of polymers. Therefore the general objectives of this work was to study the influence of different ageing methods and the influence of the microclimate on the properties of polymers used in PV applications in order to gain a detailed knowledge of the degradation behaviour.

Chapter 2 discusses the effects of artificial ageing on different polyethylene terephthalate (PET) films. PET films were chosen, as they are widely used as a component in a backsheet for PV modules. It enhances the existing knowledge of the ageing behaviour of PET films depending on temperature and humidity level and might help to draw further conclusions about the ageing behaviour of PET-based multilayer backsheets.

Chapter 3 deals with the comparison of natural and artificial weathering tests of PV backsheets. As already stated, natural weathering is the method of choice when it comes to application relevant reliability testing of PV module materials. However the PV industry still uses artificial ageing methods in order to verify the ageing behaviour and the reliability of polymer materials, such as encapsulants or backsheets. This is the reason why it is necessary to investigate the different influences of natural and artificial weathering and the comparability of those test types.

Chapter 4 focuses on the influence of weathering types on polymer degradation. Special emphasis was given to the ultra-acceleration of artificial ageing. A feasibility study is conducted in order to verify whether climate chamber ageing can be correlated with ultra-accelerated pressure cooker

ageing for PET-based PV backsheets. These both tests are state of the art in the PV industry and in research work, however, an investigation on the correlation of these tests has not been conducted yet.

Chapter 5 discusses the influence of microclimates on polymer degradation. It deals with the question if it is possible to age encapsulation materials as single film samples and use the results to draw conclusions about the material behaviour when it is incorporated in a PV module.

1.5. References

[1] IEA - International Energy Agency. 2016. *Key World Energy Statistics 2016*. https://www.iea.org/publications/freepublications/publication/key-world-energy-statistics.html.

[2] REN21. 2016. *Renewables 2016*. *Global status report*.

[3] Levermann, A., Clark, P. U., Marzeion, B., Milne, G. A., Pollard, D., Radic, V., and Robinson, A. 2013. The multimillennial sea-level commitment of global warming. *Proceedings of the National Academy of Sciences of the United States of America* 110, 34, 13745–13750.

[4] Lewis, S. C. and King, A. D. 2016. Evolution of mean, variance and extremes in 21st century temperatures. *Weather and Climate Extremes*.

[5] Gillis, J. 2016. Seas Are Rising at Fastest Rate in Last 28 Centuries. *New York Times* 2016, 22.02.2016 (Feb. 2016).

[6] Powell, J. P. and Reinhard, S. 2016. Measuring the effects of extreme weather events on yields. *Weather and Climate Extremes* 12, 69–79.

[7] Mertens, K. 2011. *Photovoltaik*. *Lehrbuch zu Grundlagen, Technologie und Praxis*. Hanser, München.

[8] Philipps, S. 2016. *Photovoltaics Report*, Freiburg.

[9] NREL National Renewable Energy Laboratory. Best Research-Cell Efficiencies 2014. free download: http://www.nrel.gov/ncpv/.

[10] Hill, J. S. 2013. Multicrystalline Silicon Modules To Dominate Solar PV Industry In 2014. *Clean Technica* 2013 (Oct. 2013).

[11] King, D. L., Quintana, M. A., Kratochvil, J. A., Ellibee, D. E., and Hansen, B. R. 2000. Photovoltaic Module Performance and Durability Following Long-term Field Exposure. *Prog. Photovolt: Res. Appl.* 8, 8, 241–256.

[12] Czanderna, A. W. and Pern, F. J. 1996. Encapsulation of PV modules using ethylene vinyl acetate copolymer as a pottant: A critical review. *Solar Energy Materials and Solar Cells* 43, 2, 101–181.

[13] Stollwerck, G., Ehbing, H., Hoffmann, A., and Peerlings, H. 2004. Kunststoff-Verkapselungen für Solarmodule. *Kunststoffe*.

[14] Cuddihy, E., Coulbert, C., Gupta, A., and Liang, R. 1986. Flat-Plate Solar Array Project Final Report. Volume VII: Module Encapsulation. *JPL Publication*.

[15] Oreski, G. and Pinter, G., Eds. 2013. *Aging Characterization of Multi-Layer Films Used as Photovoltaic Module Backsheets*. 28th European Photovoltaic Solar Energy Conference and Exhibition; 3050-3054 4AV.4.13.

[16] Liu, F., Jiang, L., and Yang, S. 2014. Ultra-violet degradation behavior of polymeric backsheets for photovoltaic modules. *Solar Energy* 108, 0, 88–100.

[17] Knausz, M., Oreski, G., Eder, G. C., Voronko, Y., Duscher, B., Koch, T., Pinter, G., and Berger, K. A. 2015. Degradation of photovoltaic backsheets: Comparison of the aging induced changes on module and component level. *J. Appl. Polym. Sci.* 132, 42093, 1–8.

[18] Jorgensen, G. J., K. M. Terwilliger, J. A. DelCueto, S. H. Glick, M. D. Kempe, J. W. Pankow, F. J. Pern, and T. J. McMahon. 2006. Moisture transport, adhesion, and corrosion protection of PV module packaging materials. *Solar Energy Materials & Solar Cells* 90, 2739–2775.

[19] Sample, T. Failure modes observed in real use and long-term exposure. In *PV Module Reliability Workshop, Berlin, Germany, 2011*.

[20] *Accelerated Lab Testing*. *Topic 4*. PV Module Reliability Workshop 2011, Berlin, Berlin.

[21] Tony Sample. 3., 2012. *Field Experiences and Failure Categorization as Basis for FMEA*. PV Module Reliability Workshop 2012 Lugano, Lugano.

[22] *IEA PVPS Task 13 Workshop at 29th PVSEC, Amsterdam, Netherlands, 2014*.

[23] Friesen, T. PV modules failure modes observed in real use and long term exposure. In *PV Module Reliability Workshop, Berlin, Germany, 2011*.

[24] Wang, E., Yang, H. E., Yen, J., Chi, S., and Wang, C. 2013. Failure Modes Evaluation of PV Module via Materials Degradation Approach. *Energy Procedia* 33, 256–264.

[25] Gambogi, W. J., Heta, Y., Hashimoto, K., Kopchick, J. G., Felder, T., MacMaster, S. W., Bradley, A., Hamzavytehrany, B., Garreau-Iles, L., Aoki, T., Stika, K. M., Trout, T. J., and Sample, T. 2014. A Comparison of Key PV Backsheet and Module Performance from Fielded Module Exposures and Accelerated Tests. *IEEE J. Photovoltaics* 4, 3, 935–941.

[26] Weiß, K.-A. Alterung von Materialien für PV Module. In *Workshop Qualität und Zuverlässigkeit in der PV, Leoben, Austria, 2014*.

[27] Winkler, G. Transport von PV-Modulen: Konzepte und Schäden. In *8. Workshop "Photovoltaik-Modultechnik" TÜV Rheinland, Köln, Germany, 2011*.

[28] IEA PVPS Task 13. 2014. *Review on Failures of PV Modules*. *Report IEA-PVPS T13-01:2013*. Performance and Reliability of Photovoltaic Systems. INTERNATIONAL ENERGY AGENCY.

[29] IEA Task 13. 2014. *Degradation Behaviour of PV Modules under Different Accelerated Stress Conditions Based on Stress Conditions Evaluated from Real-time Outdoor Testing*. *Report IEA-PVPS T13-04:2014 Degradation Behaviour of PV Modules under Different Accelerated Stress Conditions Based on Stress Conditions Evaluated from Real-time Outdoor Testing*.

[30] Park, N., Jeong, J., Kang, B., and Kim, D. 2013. The effect of encapsulant discoloration and delamination on the electrical characteristics of photovoltaic module. *Microelectronics Reliability* 53, 9-11, 1818–1822.

[31] Wohlgemuth, J. H. and Kempe, M. D. Equating Damp Heat Testing with Field Failures of PV Modules. In *39th Photovoltaic Specialists Conference IEEE, Tampa Bay, USA, 2013*.

[32] Peike, C., Hülsmann, P., Blüml, M., Schmid, P., Weiß, K.-A., and Köhl, M. 2012. Impact of Permeation Properties and Backsheet-Encapsulant Interactions on the Reliability of PV Modules. *ISRN Renewable Energy* 2012, 1–4, 1–5.

[33] Looney, K. and Brennan, B. Modelling the correlation between DHT and true field lifetimes for PET based backsheets. In *29th European Photovoltaic Solar Energy Conference and Exhibition, Amsterdam, Netherlands, 2014*, 2467–2470.

[34] Oreski, G. and Wallner, G. M. 2005. Delamination behaviour of multi-layer films for PV encapsulation. *Solar Energy Materials and Solar Cells* 89, 2-3, 139–151.

[35] ATLAS Material Testing Technology GmbH, Ed. 2012. *Die Faktoren der Bewitterung*.

[36] Ehrenstein, G. W. and Pongratz, S. 2007. *Beständigkeit von Kunststoffen*. Carl Hanser Verlag, Munich.

[37] Krebs, C., Leu, K. W., and Krebs-Avondet-Leu, Eds. 1999. *Langzeitverhalten von Thermoplasten*. *Alterungsverhalten und Chemikalienbeständigkeit*. Hanser, München.

[38] DIN, Normausschuss Kunststoffe (FNK). 2011. *Kunststoffe - Freibewitterung Teil 1-Allgemeine Anleitung,* 877-1.

[39] ATCAE Solar. 7., 2011. *Weathering testing of polymeric materials for use in PV applications*. ATLAS® Technical Conference on Accelerated Ageing and Evaluation (ATCAE), Berlin.

[40] Wypych, G. 2008. *Handbook of material weathering*. Chem Tec Publ, Toronto.

[41] Ehrenstein, G. W., Ed. 2000. *Thermische Einsatzgrenzen von Kunststoffen in Verarbeitung und Anwendung*. Ingenieur-Werkstoffe Sonderpubl. Springer-VDI-Verl., Düsseldorf.

[42] Hamid, S. H., Ed. 1992. *Handbook of polymer degradation*. Environmental science and pollution control series 2. Dekker, New York u.a.

[43] Valadez-Gonzalez, A., Cervantes-U, J., and Veleva, L. 1999. Mineral fller influence on the photo-oxidation of high density polyethylene: I. Accelerated UV chamber exposure test. *Polymer Degradation and Stability,* 63, 253–260.

[44] A. L. Andrady, S. H. Hamid, X. Hu, and A. Torikai. 1998. Effects of increased solar UV radiation on materials. *Journal of Photochemistry and Photobiology B,* 46, 96–103.

[45] Feil, F., Schönlein, A., and McGreer, M. 2015. Coating Surface Temperature During Artificial Weathering: Significance for Lifetime Prediction. *SunSpots,* 45/97.

[46] ATLAS Material Testing Technology GmbH, Ed. 2012. *Grundlagen der Bewitterung II*.

[47] Holland, T. A., Bodde, E. W. H., Cuijpers, V. M. J. I., Baggett, L. S., Tabata, Y., Mikos, A. G., and Jansen, J. A. 2007. Degradable hydrogel scaffolds for in vivo delivery of single and dual growth factors in cartilage repair. *Osteoarthritis and cartilage* 15, 2, 187–197.

[48] Luef, K. P., Petit, C., Ottersböck, B., Oreski, G., Ehrenfeld, F., Grassl, B., Reynaud, S., and Wiesbrock, F. 2016. UV-Mediated Thiol-Ene Click Reactions for the Synthesis of Drug-Loadable and Degradable Gels Based on Copoly(2-oxazoline)s. *European Polymer Journal*.

[49] Choong, G. Y. and Focatiis, D. S. de. 2016. A method for the determination and correction of the effect of thermal degradation on the viscoelastic properties of degradable polymers. *Polymer Degradation and Stability* 130, 182–188.

[50] Andorko, J. I., Hess, K. L., Pineault, K. G., and Jewell, C. M. 2016. Intrinsic immunogenicity of rapidly-degradable polymers evolves during degradation. *Acta biomaterialia* 32, 24–34.

[51] Qayyum, M. M. and White, J. R. 1993. Effect of stabilizers on residual stresses in weathered polyethylene. *Polymer Degradation and Stability* 39, 2, 199–205.

[52] Phillips, N. H. and Scott, K. P. 2014. Quantifying PV module microclimates and translation into accelerated weathering protocols. In *SPIE Solar Energy + Technology*. SPIE Proceedings. SPIE, 91790L. DOI=10.1117/12.2063122.

[53] Grassie, N. and Scott, G. 1988. *Polymer Degradation & [and] stabilisation*. Cambridge Univ. Press, Cambridge u.a.

[54] ATLAS Material Testing Technology GmbH. 2001. *Weathering Testing Guidebook*, USA.

[55] *Accelerated Aging*. *Challenge, Opportunity and Necessity*. PV Module Reliability Workshop 2011, Berlin, Berlin.

[56] Y. Huang, X. Wang, and D.R. Paul. 2006. Physical aging of thin glassy polymer films: Free volume interpretation. *Journal of Membrane Science* 277, 1-2, 219–229.

[57] Chiao-Chi Lin, Peter J. Krommenhoek, Stephanie S. Watson, and Xiaohong Gu. 2016. Depth profiling of degradation of multilayer photovoltaic backsheets after accelerated laboratory

weathering: Cross-sectional Raman imaging. *Solar Energy Materials and Solar Cells* 144, 289–299.

[58] Jentsch, A., Eichhorn, K.-J., and Voit, B. 2015. Influence of typical stabilizers on the aging behavior of EVA foils for photovoltaic applications during artificial UV-weathering. *Polymer Testing* 44, 242–247.

[59] Grabmayer, K., Wallner, G. M., Beißmann, S., Braun, U., Steffen, R., Nitsche, D., Röder, B., Buchberger, W., and Lang, R. W. 2014. Accelerated aging of polyethylene materials at high oxygen pressure characterized by photoluminescence spectroscopy and established aging characterization methods. *Polymer Degradation and Stability* 109, 40–49.

[60] Hirschmann, B. and Oreski, G. Implementation and evaluation of accelerated weathering tests for the aging characterisation of polymer composite films used in photovoltaic modules. In *Austrian-Slovenian Polymer Meeting, Bled, Slovenia, 2013*.

[61] Oreski, G. and Wallner, G. M. 2005. Aging mechanisms of polymeric films for PV encapsulation. *Solar Energy* 79, 6, 612–617.

[62] Pickett, J. E. and Coyle, D. J. 2013. Hydrolysis kinetics of condensation polymers under humidity aging conditions. *Polymer Degradation and Stability* 98, 7, 1311–1320.

[63] Carter, C. B. and Norton, M. G. 2007. *Ceramic materials*. *Science and engineering*. Springer, New York, NY.

[64] Hepperle, J. Schädigungsmechanismen bei Polymeren. In *Jahrestagung Polymeraufbereitung 2002*.

[65] D. Hummel. 2002. *Atlas of Plastics Additives*. *Analysis of Spectrometric Methods*.

[66] Nadejzda Haider and Sigbritt Karlsson. 2001. Loss of Chimassorb 944 from LDPE and identification of additive degradation products after exposure to water, air and compost. *Polymer Degradation and Stability,* 74, 103–112.

[67] ATLAS Material Testing Technology GmbH, Ed. 2012. *Stabilisierung von Polymeren*.

[68] Aden, M., Roesner, A., and Olowinsky, A. 2010. Optical characterization of polycarbonate: Influence of additives on optical properties. *J. Polym. Sci. B Polym. Phys.* 48, 4, 451–455.

[69] Beinert, A., Peike, C., Dürr, I., Kempe, M., and Weiß, K.-A. The Influence of the Additive Composition on the Photochemical Degradation of EVA. In *29th European Photovoltaic Solar Energy Conference and Exhibition, Amsterdam, Netherlands, 2014*.

[70] Hosseini, S. S., Taheri, S., Zadhoush, A., and Mehrabani-Zeinabad, A. 2007. Hydrolytic degradation of poly(ethylene terephthalate). *J. Appl. Polym. Sci.* 103, 4, 2304–2309.

[71] Allen, N. S., Edge, M., Mohammadian, M., and Jones, K. 1994. Physicochemical aspects of the environmental degradation of poly(ethylene terephthalate). *Polymer Degradation and Stability* 43, 2, 229–237.

[72] Edge, M., Hayes, M., Mohammadian, M., Allen, N. S., Jewitt, T. S., Brems, K., and Jones, K. 1991. Aspects of poly(ethylene terephthalate) degradation for archival life and environmental degradation. *Polymer Degradation and Stability* 32, 2, 131–153.

[73] Launay, A., Thominette, F., and Verdu, J. 1994. Hydrolysis of poly(ethylene terephthalate). A kinetic study. *Polymer Degradation and Stability* 46, 3, 319–324.

[74] Aljoumaa, K. and Abboudi, M. 2016. Physical ageing of polyethylene terephthalate under natural sunlight. Correlation study between crystallinity and mechanical properties. *Appl. Phys. A* 122:6, 6, 1–10.

[75] Sammon, C., Yarwood, J., and Everall, N. 2000. An FT-IR study of the effect of hydrolytic degradation on the structure of thin PET films. *Polymer Degradation and Stability,* 67, 149–158.

[76] Lane, C. A. and Koziar, J. C. 1976. *Process for preventing hydrolytic degradation of linear saturated aromatic polyesters comprising a thermoplastic saturated aromatic polyester and a moisture scavenger polymer,* 4,075,263.

[77] Struick, L. C. E. 1977. Physical Aging in Plastics and Other Glassy Materials. *Polymer Engineering and Science* 17, 3.

[78] John H. Hutchinson. 1995. Physical Aging of polymers. *Progress in Polymer Science*.

[79] Ehrenstein, G. W., Ed. 2011. *Polymer Werkstoffe*. Carl Hanser Verlag GmbH & Co. KG.

[80] Oreski, G. and Wallner, G. M. Damp Heat induced physical ageing of PV encapsulation materials. In *12th Intersociety Conference on Thermal and Thermomechanical Phenomena in Electronic Systems, Las Vegas, USA, 2010*.

[81] Ehrenstein, G. W., Engel, L., Hermann Klingele, and Helmut Schaper, Eds. 2010. *Werkstoff-Führer Kunststoffe*. Carl Hanser Verlag GmbH & Co. KG.

[82] Hirschl, C., Neumaier, L., Puchberger, S., Mühleisen, W., Oreski, G., Eder, G., Frank, R., Tranitz, M., Schoppa, M., Wendt, M., Bogdanski, N., Plösch, A., and Kraft, M. 2015. Determination of the degree of ethylene vinyl acetate crosslinking via Soxhlet extraction: Gold standard or pitfall? *Solar Energy Materials and Solar Cells* 143, 494–502.

[83] Menges, G., Haberstroh, E., Michaeli, W., and Schmachtenberg, E. 2002. *Werkstoffkunde Kunststoffe*. Carl Hanser, Munich.

[84] Namsu Kim, Seoungsoo Lee, Xing Guan Zhao, Dajung Kim, Chulmin Oh, and Hanjun Kang. 2016. Reflection and durability study of different types of backsheets and their impact on c-Si 5PV6 module performance. *Solar Energy Materials and Solar Cells* 146, 91–98.

[85] Grellmann, W. and Seidler, S. 1998. *Deformation und Bruchverhalten von Kunststoffen*. VDI-Buch. Springer.

[86] Oreski, G. Accelerated indoor durability testing of polymeric photovoltaic encapsulation materials. In *SPIE Solar Energy + Technology, San Diego, USA, 2010. DOI*=10.1117/12.860390.

[87] Ottersböck, B., Oreski, G., and Pinter, G. 2016. Correlation study of damp heat and pressure cooker testing on backsheets. *J. Appl. Polym. Sci.*

[88] Oreski, G. and Wallner, G. M. 2009. Evaluation of the aging behavior of ethylene copolymer films for solar applications under accelerated weathering conditions. *Solar Energy* 83, 7, 1040–1047.

[89] Oreski, G., Wallner, G. M., and Lang, R. W. 2009. Ageing characterization of commercial ethylene copolymer greenhouse films by analytical and mechanical methods. *Biosystems Engineering* 103, 4, 489–496.

[90] Oreski, G. Encapsulant materials and degradation effects-Requirements for new materials and research trends. In *IEA PVPS Task 13 Workshop at 29th PVSEC, Amsterdam, Netherlands, 2014*.

[91] F.J. Pern. 1996. Factors that affect the EVA encapsulant discoloration rate upon accelerated exposure. *Solar Energy Materials and Solar Cells,* 41/42, 587–615.

[92] Peike, C., Purschke, L., Weiß, K.-A., Köhl, M., and Kempe, M. D. Towards the origin of photochemical EVA discoloration. In *39th Photovoltaic Specialists Conference IEEE, Tampa Bay, USA, 2013*.

[93] Klemchuk, P., Ezrin, E., Lavigne, G., Holley, W., Galica, J., and Agro, S. 1997. Investigation of the degradation and stabilization of EVA-based encapsulant in field-aged solar energy modules. *Polymer Degradation and Stability,* 55, 347–365.

[94] Oreski, G. and Wallner, G. M. 2006. Structure–infrared optical property-correlations of polar ethylene copolymer films for solar applications. *Solar Energy Materials and Solar Cells* 90, 9, 1208–1219.

2. Artificial ageing effects on properties of polymeric films

The following chapter discusses the effects of different types of artificial ageing on various polyethylene terephthalate (PET) films. PET films were chosen, as they are widely used as a component in a backsheet for photovoltaic (PV) modules. The results can help to enhance the existing knowledge of the ageing behaviour of PET films dependent on temperature and humidity level. Furthermore it might help to draw additional conclusions about the complex ageing behaviour of PET-based multilayer backsheets.

2.1. Introduction to artificial ageing effects on properties of polymeric films

Polymer films are used in many applications and this led to investigations to obtain materials with simultaneously high performance and low cost, respectively [1]. PET is one of the films which are used when mechanical strength, thermal and chemical stability as well as barrier properties to atmospheric gases in combination with a good processability are required, such it is the case for the component in a PV backsheet. After the first synthesis of PET in the 1940s the amount produced grew rapidly [2, 3]. Scheirs and Long gave a detailed review of PET synthesis and processing [3]. Due to its properties PET is a widely used thermoplastic polymer which is applied in the packaging sector, in the PV industry, in the fibre sector and in many others [1, 4–8].

Weathering stability is the key factor for the reliability of PV modules among other outdoor applications. The main critical parts concerning degradation are polymeric materials [9–12]. During the life cycle of a polymeric part it is prone to interact with different stress factors like oxygen, light, mechanical stresses, temperature or water. These factors can cause individual or synergistic degradation and diminish the performance of the polymeric part [11–13]. The loss of functionality can result in critical changes of its required properties and subsequently can lead to the breakdown of the whole part. Because PET is such a common material a large quantity of research on PET, PET blends, recycled PET, reinforced PET and many other topics has already been carried out [1, 14–26]. The reported results are generally loss of mechanical, thermal or rheological properties. The major drawback of PET is that it is prone to degrade under humidity and high temperature (hydrolysis). In general hydrolysis leads to chain scission which results in embrittlement, but also physical ageing processes (e. g. post-crystallisation) can take place, which lead to a loss in mechanical properties [21]. However, the single and combined influences of different stress factors during artificial ageing on the degradation mechanisms of PET have not been investigated sufficiently [27, 28].

Therefore the aim of this work was a systematic investigation of the impact of different ageing temperatures and relative humidity levels on the ageing behaviour of various PET films. The outcomes of this work will help the understanding of the ageing behaviour of PET, as well as benefit a better comprehension of the structure-property correlation concerning ageing and morphology, respectively. Furthermore the results might help to draw additional conclusions about the complex ageing behaviour of PET-based multilayer backsheets.

2.2. Experimental procedure

Three commercially available PET films with different stabilisation characteristics were analysed (see Table 2.1). The unaged and aged materials were characterised in order to verify the influence of stress factors on the ageing behaviour. In Table 2.2 the ageing parameters are listed. The duration for each ageing type were 1000, 2000 and 3000 h. To verify the influence of temperature and humidity, water absorption tests, gel permeation chromatography (GPC), differential scanning calorimetry (DSC), spectroscopic characterisation, dynamic mechanical analysis (DMA) and tensile tests were conducted.

Table 2.1. Information of the datasheets for all materials

Material	**Thickness**	**Characteristics**
PET 1	50 µm	White, 1-layer construction, UV absorber and hydrolysis resistant
PET 2	50 µm	Transparent, 3-layer construction, coextruded, biaxial drawn
PET 3	19 µm	Transparent, 1-layer construction UV absorber

Table 2.2. Ageing parameters

Oven	**Climate chamber**
65°C	65°C 85% relative humidity (r. H.)
85°C	85°C 85% r. H.
95°C	95°C 85% r. H.
125°C	

Water absorption tests were done in accordance with ISO 62. Square samples (60 x 60 mm) were cut and dried in an oven at 50°C. Subsequently the samples were cooled to room temperature in a desiccator. This was done until the mass was constant after this drying routine. A Vötsch climate chamber type VC 7020 (Balingen, DE) at 23°C and 50% r. H. was used and the samples were weighed regularly. For each material three samples were used.

GPC measurements were conducted with the aim to quantify chemical degradation via the molar mass. An Agilent Technologies GPC 50 with two detectors (refractive index and 4-capillar viscosity detector) was used in combination with two PSS SDV analytical linear M (8 x 50 mm and 8 x 300 mm), columns with a particle size of 5 µm were chosen. The calculation of molecular weight and its distribution requires calibration [29]. Therefore a universal calibration with polystyrol (PS) ($K=1.91\ 10^{-4}$ dl g^{-1} and $\alpha=0.693$) and a detector calibration with PS standard 133000 Da was done. The samples were prepared by dissolving them in pure hexafluoroisopropanol (HFIP) and subsequent slow dilution with chloroform ($CHCl_3$) to reach a final concentration of around 2.5 mg ml^{-1} in a $CHCl_3$:HFIP mixture (98:2 vol. %). At the beginning the temperature was kept at 40°C in order to prevent an early precipitation of the samples. The amount of injected sample was 100 µl and the solvent flow 1 ml min^{-1} at 25°C.

The thermal behaviour was analysed via DSC using a Perkin Elmer DSC 4000 (Waltham, US) over the range of 23-270°C with a heating rate of 10 K min^{-1}. Approximately 10 mg of samples were cut and put into 50 µl pans with perforated lids. Nitrogen atmosphere was used in order to prevent further oxidation processes. In order to identify reversible and irreversible processes two heating runs were conducted. Peak temperatures and enthalpies were evaluated according to ISO 11357-3 [30]. Three samples were used to obtain an average.

Fourier transform infrared (FTIR) spectra were collected in attenuated total reflection (ATR) mode using a Spectrum GX spectrometer (Perkin Elmer, Waltham, US). The transmittance spectra were recorded from 4000 to 650 cm^{-1} with a resolution of 4 cm^{-1}. For a better comparison all ATR spectra were normalised to the absorbance peak at 1408 cm^{-1}, which corresponds to the ring in-plan deformation. This band is usually used as an internal standard because it is not sensitive to effects of orientation or conformation. Miyake has reported that even after drawing a PET film, this band did not change [31].

Ultraviolet/ visible light/ near-Infrared (UV/Vis/NIR) spectroscopy was carried out on a Perkin Elmer Lambda 950 (Waltham, US). The wavelength range was between 250 and 2500 nm with a measuring interval of 5 nm. Hemispherical transmission measurements were done with an Ulbricht sphere.

DMA was performed using a Perkin Elmer DMA 8000 (Waltham, US) in tension mode. The sample had the dimensions of 10 x 4 mm. A heating rate of 3 K min^{-1} and a frequency of 1 Hz were used. The tests were conducted from 23 to 200°C. At least two samples were measured to obtain an average.

Tensile tests on rectangular samples (15 x 100 mm) were carried out using a Zwick-Roell Z001 (Ulm, DE) at ambient temperature according to EN ISO 527-3 [32]. A testing speed of 50 mm min^{-1} and a gauge length of 50 mm were used. The Young's modulus, yield stress, strain at break and stress at break were determined for at least seven specimens for each test series.

2.3. Results and discussion

Despite the same sample dimensions (60 x 60 x 0.05 mm) PET 2 is the sample with the higher mass compared to PET 1 (around 265 g). PET 1 exhibits approximately 10 g less. This may be due to the fact that PET 2 is biaxially oriented and therefore be more dense, have more crystalline content or a different molar mass. The results of the water absorption tests revealed no significant ability to absorb water for all PET samples. Lahokallio et al. have already reported that the water absorption measurements were not optimal for thin films [33].

Figure 2.1 shows chromatograms of the GPC measurements for PET 2 aged under 95°C and a relative humidity of 85%. The intensity of the main peak decreased and the run time of the peak maximum increased with ageing time. This is evidence that during ageing at high humidity chain scission via hydrolysis was taking place and the molar mass decreased. This effect was more intense the higher the temperature and humidity level was. A part of small molecular mass was also detected, which could be seen as a smaller peak at about 670 s with around 1% wt. In the case of the unaged material this could be due to additives and lubricants. According to the datasheet, PET 2 should not contain any additives, however lubricants are not rated as additives. This is the case even though they decrease the shear and therefore the mechanical stress on the polymer during processing. Particularly montan waxes and their derivates are used for PET [12]. With increasing ageing time and also ageing temperature this content increased to a value of around 4% wt., which was caused by the splitting-off of low molecular groups.

An interesting effect could be observed only at the dissolving process of PET 2, which is shown in Figure 2.2. Holes in a regular pattern were formed. This effect might be caused by very small differences in thickness due to the biaxial stretching process. Another possibility might be a regular pattern of the amorphous and crystalline regions, which are not as quickly soluble as the amorphous parts. In addition, also regular orientations of the crystalline regions might be a possible reason [34].

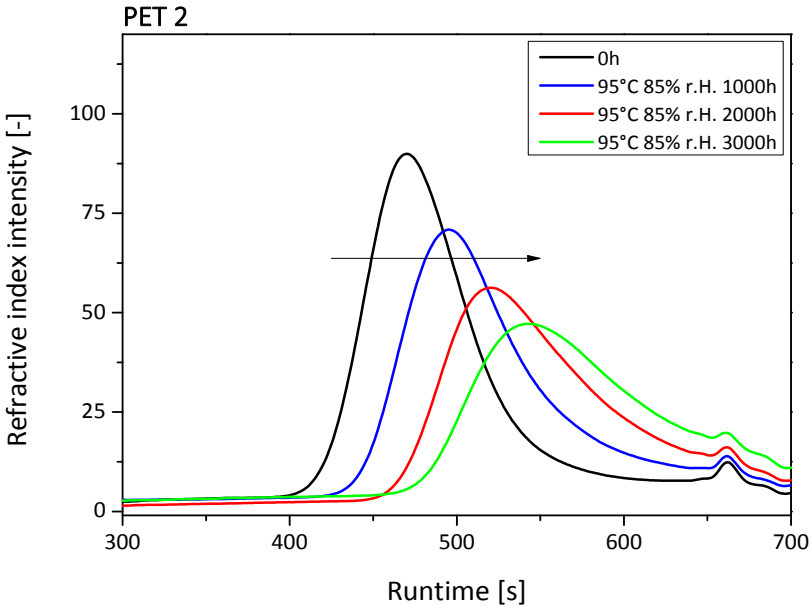

Figure 2.1. Chromatograms of unaged and aged PET 2.

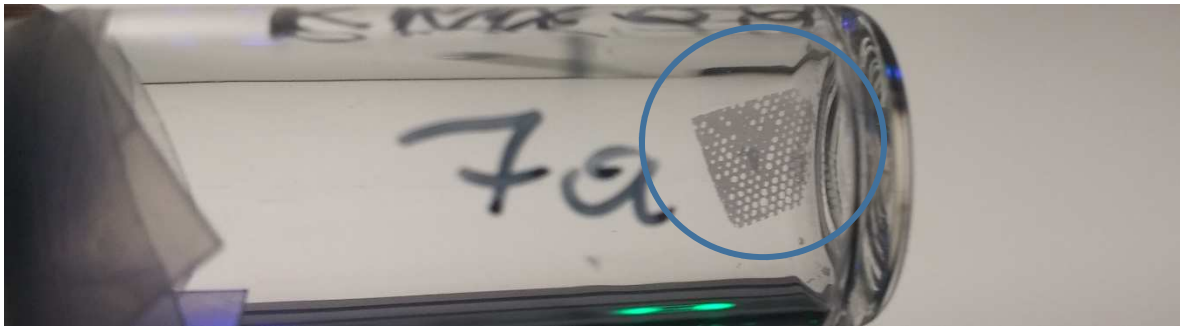

Figure 2.2. Dissolving process of PET 2.

Figure 2.3 shows the development of the molar mass with ageing duration. It can be confirmed that the molar mass is drastically reduced to values below 10000 g mol^{-1} for samples aged at 85°C and 95°C, both at 85% r. H., respectively. Storage at high temperatures (125°C) also caused a decrease in molar mass; however, the degradation was not as severe as it would have been with humidity. This is due to the fact, that humidity in combination with temperature causes chain scission (hydrolysis). Ehrenstein and Pongratz already published the fact that the reaction rate for thermo-oxidation is 5000 times slower than for hydrolysis with an activation energy of around 136 kJ mol^{-1} at 100°C and a relative humidity of 100%. Carboxyl end groups are formed during hydrolysis, which act autocatalytically [12]. Already a content of around 0.01% wt. of water is enough to reduce the molar mass significantly due to hydrolysis [12]. But compared to other aliphatic polyesters, PET is relatively resistant to hydrolysis. The literature described that starting at a temperature of 100°C

hydrolysis of the ester bond sets in [12]. This is due to the aromatic parts, which are hydrophobic and increase the steric hindrance and the dense package of the molecules in PET [12, 35]. That is the reason why high temperatures (125°C) caused more chemical degradation than lower temperatures and high humidity levels (65°C 85% r. H.). The first step in the still not completely clarified mechanism of thermo-oxidation of PET is the formation of carboxyl end groups during chain scission. As in other polymers, a classic radical chain reaction takes place, where the primary radical is formed at the methylene group. The degradation via thermo-oxidation is influenced by catalysts, inhibitors and the content of diethylene glycol (DEG), which is formed during degradation [12].

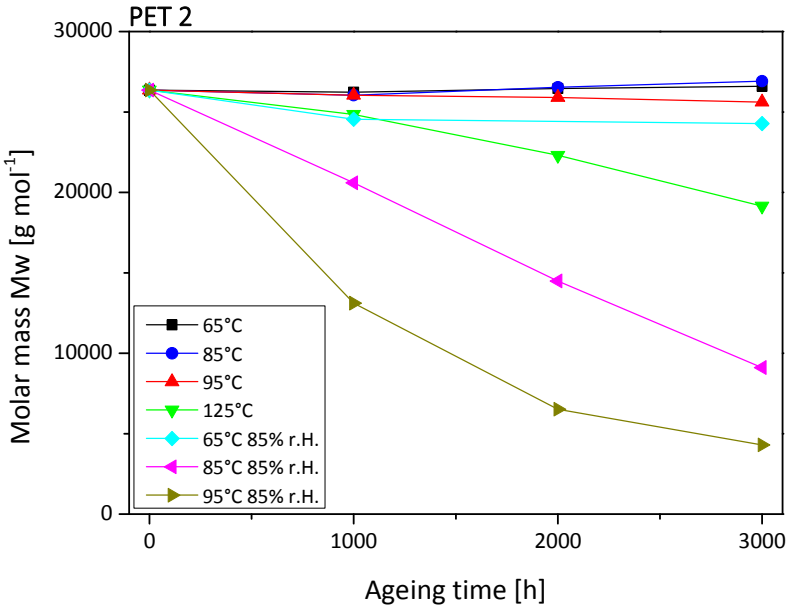

Figure 2.3. Molar mass of PET 2.

Nearly all PET samples behaved as described above. The only exceptions were the samples of PET 1 aged at 125°C. During the oxidation process curing reactions could take place and this led to the formation of gel or bigger networks [12]. The solubility of the samples decreased with increasing duration of ageing, see Figure 2.4. Vinyl ester ends formed during degradation can act as crosslinkers and gelling agents in polyesters [36]. Even though ATR measurements revealed no significant results concerning chemical degradation, GPC tests showed significant changes depending on temperature and humidity level.

Figure 2.4. Solubility of PET 1 after ageing at 125°C, left: 1000 h, middle: 2000 h, right: 3000 h.

In addition to GPC measurements the thermal behaviour was also investigated. Figure 2.5 shows the DSC heating curves for all unaged PET materials. It was not possible to determine the glass transition temperature in the thermograms. At the first heating all samples started to melt at around 225°C where only the thinner crystal lamella were involved. With further increasing temperature the thicker lamella melted. Melting peak temperatures were in a similar range for all PET samples with 254 ± 0°C, 256 ± 0°C and 252± 0°C, respectively. PET 3 exhibited an additional small peak at 230°C indicating a dual lamella thickness distribution [37]. The three layer structure of PET 2 could not be determined from the thermograms. PET 1 and PET 2 exhibited a slightly higher degree of crystallinity with around 45.5 ± 0.4% and 44.9 ± 4.8%, respectively, compared to PET 3 with a value of 43.1 ± 1.0%. For oriented materials the crystal fraction increases upon drawing because the alignment of the polymer chains favours the formation of an ordered crystalline structure which explains a relatively high degree of crystallinity compared to values in the literature [2, 38, 39]. However, the reachable maximum crystallinity is still below the maximum value which can be attained for PET. This indicates that further orientation is still possible [2, 6].

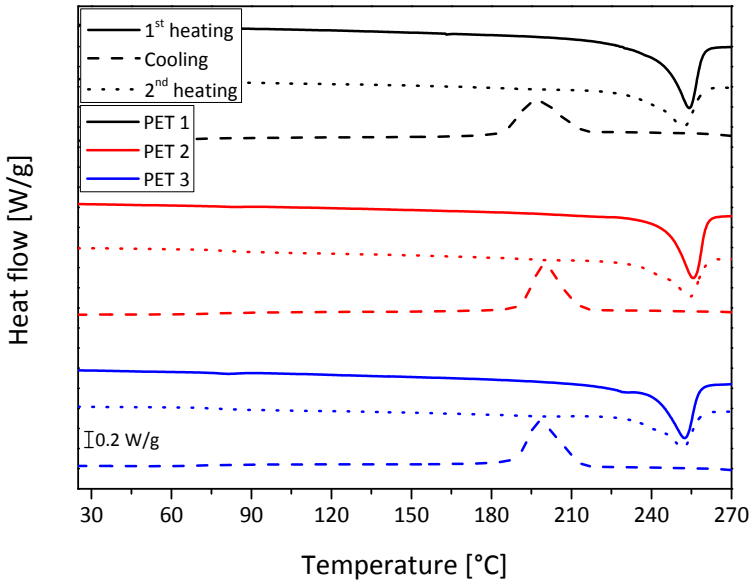

Figure 2.5. Thermograms of all unaged PET samples.

Compared to the thermograms of the first heating run those of the second heating run exhibited a different shape. For all materials a small secondary peak at around 240°C was visible, see Figure 2.6. This second endotherm could be formed due to the presence of a dual lamella thickness distribution produced during crystallisation [37]. The main peak temperature changed only slightly to 252 ± 0°C, 254 ± 0°C and 252 ± 0°C for PET 1, 2 and 3, respectively. Kong and Hay showed that the melting characteristics of PET are very complex, depending on the experimental and processing conditions [37].

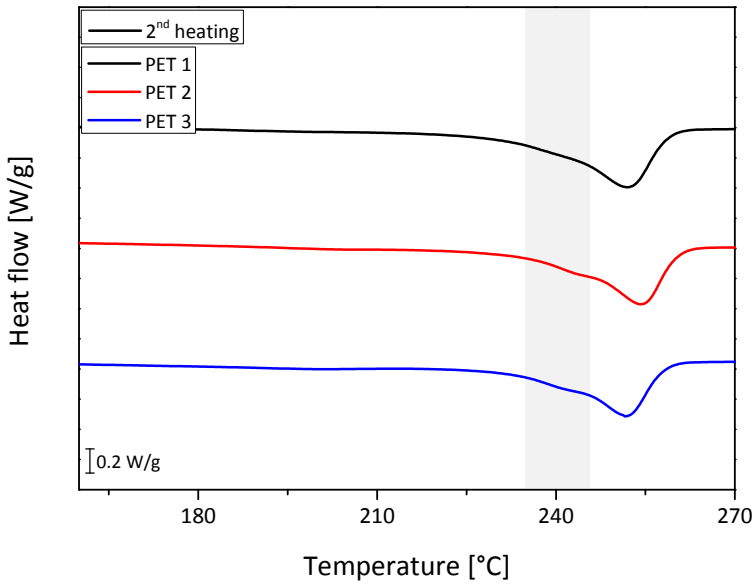

Figure 2.6. Thermograms of the second heating of all unaged PET samples.

Neither the peak position for the melting peak in the first run, nor an alteration of the peak shape could be observed after ageing. This indicates that the crystal heterogeneity was not influenced during degradation [40]. However, the degree of crystallinity changed as a function of exposure time, which is plotted in Figure 2.7 for PET 1. With a value of more than 45.5 ± 0.4% PET 1 showed a high degree of crystallinity. The capacity to crystallise is also induced by the structure [41]. Additionally a high amount of crystallinity can be caused by orientation, where more oriented chains can contribute to a higher amount of crystallinity [6]. Compared to oriented PET, the molecules of standard PET films exhibit a higher mobility due to less orientation and distortion of the intermolecular bonds, like the van der Walls attraction [42]. The behaviour of the crystalline fraction after ageing indicated orientation. All materials showed the same behaviour: after the first 1000 h of testing the value for the degree of crystallinity decreased. Further ageing caused no significant changes, except after oven ageing at 65°C and 85°C, where the value decreased to

around 34.3 ± 2.0% and 31.5 ± 0.1%, respectively. Therefore, the level of physical degradation of the sample cannot be evaluated only by the change in the degree of crystallinity [40].

The decrease in the degree of crystallinity can be caused by the fact that the material was oriented during processing (molecule chains are arranged in machine direction during the extrusion process) and the ageing caused a relaxation which accompanied an increased value of disorder and a decrease in the crystalline fraction. Admittedly, crystallisation during degradation might be affected differently by various factors. A decrease in the degree of crystallinity can indicate a strong bulk degradation by different mechanisms, such as hydrolysis, thermo-oxidation etc. [43]. But after additional 1000 h of ageing the values remained almost unchanged. Another reason can be the decrease in molecular mobility, which would be evident by an increase in the glass transition temperature leading to suppressed crystallisation [40].

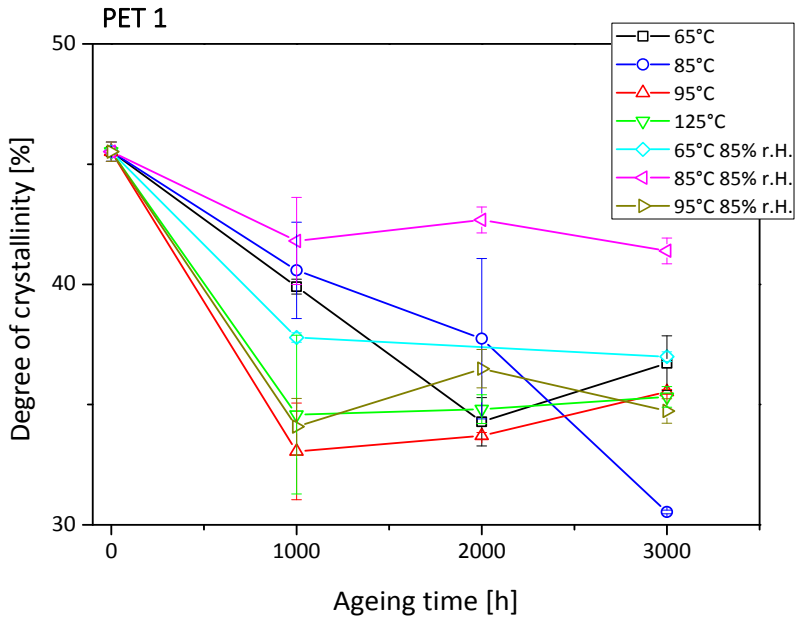

Figure 2.7. Change of degree of crystallinity of PET 1.

After 1000 h of ageing a small secondary melting peak can be found for nearly all ageing types except for 95°C at a relative humidity of 85%. The peak was always below 2% degree of crystallinity and the secondary melting peak temperature is shown in Figure 2.8. Further ageing time caused no significant increase of this peak temperature. Oven ageing led to a lower secondary peak temperature than ageing under the influence of humidity. This can be observed for 65°C and 85°C as well. Ageing at 125°C caused the highest secondary peak temperature with 157°C. Multiple melting endotherms are common and observed via DSC with semi-crystalline polymers [37]. A variety of interpretations have been made, such as the presence of more than one crystallographic

form, the presence of melting, re-crystallisation and re-melting, changes in morphology (lamella thickening and crystal perfection), changes in the orientation and effects of molecular weight distribution [37, 44]. Bell et al. reported two endotherms and proposed that the lower one was related to the melting of imperfect, smaller crystals with partially extended chains and the higher endotherm was caused by melting of folded chain crystals [45, 46]. Later it was suggested that partial melting and re-crystallisation took place during heating, which led to two endotherms, where the one at lower temperature was due to the melting of crystals formed at the crystallisation temperature [37, 47]. The one at higher temperature was suggested to have been caused by the melting of crystals produced by annealing on heating [37, 47]. Galli et al. reported that chain segments in the trans-conformation can crystallise even below T_G [8, 48, 49]. As the testing conditions, e. g. heating rate, were the same for all experiments the influence of variable parameters can be dismissed. Therefore the differences in the temperature were caused by the different types of ageing.

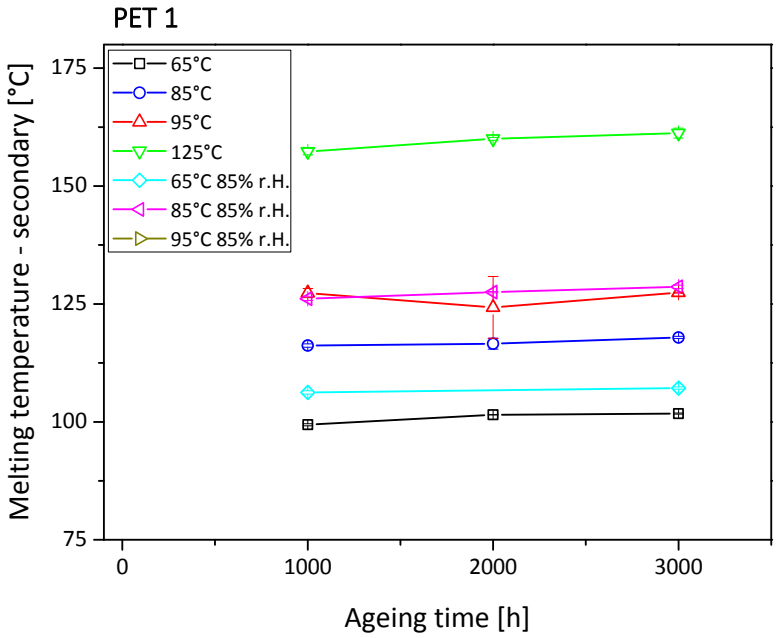

Figure 2.8. Change of secondary melting temperature of PET 1.

Ajji and Cole showed that drawing causes significant change in the crystallisation temperature – it decreases significantly as the draw ratio is increased [6]. This could not be verified in the crystallisation temperature of PET 2 compared to PET 1 and PET 3, which would be another indication that PET 1 and PET 3 were also oriented. Figure 2.9 exemplarily shows the crystallisation temperature of PET 3. Ageing only at 85°C and 95°C, both at 85% r. H., caused a strong increase of the crystallisation temperature. Due to the fact that the melt only crystallises when the

temperature is below the melting temperature, the crystallisation peak temperature is always lower than the melting temperature. An increase in the crystallisation temperature can be caused by a decrease in molar mass. Due to shorter chains an increased solidification can occur because the increased number of chain ends can act as nucleating agents [26, 50]. This can be seen as evidence for chemical ageing caused by hydrolysis, which causes chain scission. These results correspond well to the GPC results, where ageing at 85°C and 95°C, both at 85% r. H. caused a significant decrease of the molar mass.

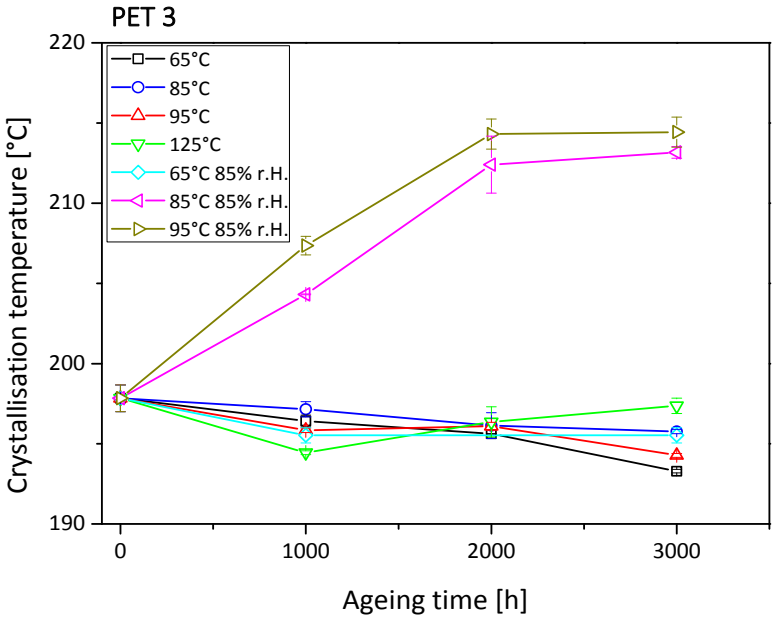

Figure 2.9. Change of crystallisation temperature of PET 3.

The optical properties were unaffected by ageing, except for those tests which were made at high temperatures (125°C). Figure 2.10 shows the hemispherical transmittance for PET 3 characterised via UV/Vis/NIR spectroscopy. Only ageing at 125°C after 3000 h led to a significant decrease in transmittance. The polymer thermally degrades causing yellow or brown colour due to conjugated structures, such as quinones [36, 51]. It is assumed that only exposure temperatures above glass transition caused discolouration. Discolouration can be an important indicator for polymer degradation, however it need not necessarily occur [12, 52, 53].

The changes in microstructure are caused by chemical changes at molecular level, which can basically be evaluated via IR spectroscopy. In general all spectra consisted of typical peaks before and after ageing caused by the amorphous and crystalline phases, see Table 2.3 [1, 2, 5]. The comparison of unaged and aged IR spectra showed differences only for samples aged at high

temperatures (95°C, 125°C and 95°C 85% r. H.). For example the spectra for unaged and aged PET 3 (95°C and 95°C 85% r. H.) are shown in Figure 2.11 in order to illustrate the influence of humidity.

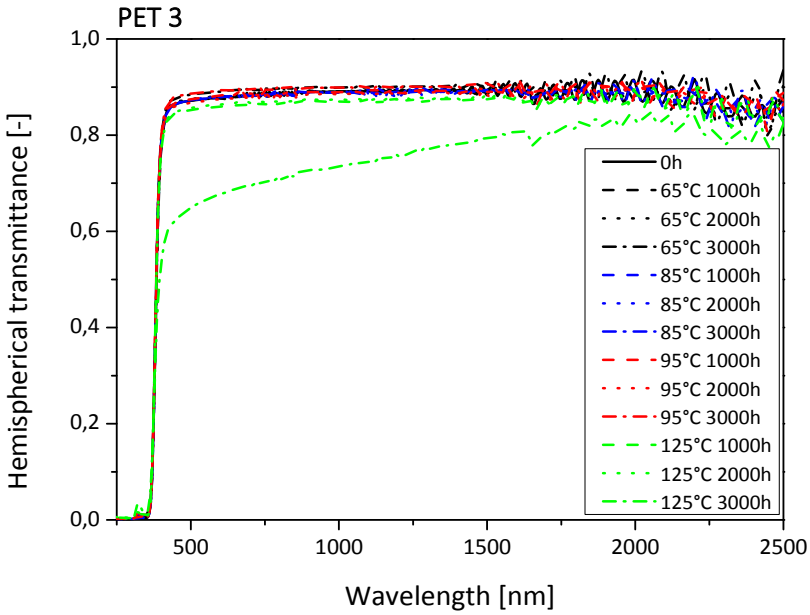

Figure 2.10. Hemispherical transmittance of PET 3.

Ageing at 95°C 85% r. H. caused significant changes in the area from 1800 to 800 cm^{-1}. In detail the intensity slightly increased for the absorption peaks at 1589, 1533 and 1261 cm^{-1}. The increase of the peaks at 1448 and 1370 cm^{-1} can be caused by the decrease in crystallinity, as these peaks correspond to the amorphous fraction [31]. Besides an increase for the peak at 1240 cm^{-1} a shift was observed, which moved after ageing under temperature (95°C) to 1245 cm^{-1} and after ageing with additional humidity (95°C 85% r. H.) to 1250 cm^{-1}, respectively. This wavenumber corresponds to the C(=O)-O stretching, aromatic ester CC stretching and C=O in-plane bending vibration [54]. A shift to higher wavenumbers can be correlated to an increase in the amorphous region [54]. Venkatachalam et al. reported an increase in carboxyl terminated species during the formation of coloured species [36]. Only the samples aged at 125°C became discoloured and these had the highest increase in the band at 1245 cm^{-1}. Under high humidity levels hydrolysis cause chain scission in PET. The reaction is a random chain scission at ester linkage, which induces hydroxyl and carboxyl end groups [1, 12]. However, no significant changes in the spectra at around 3400 cm^{-1} could be detected, which would correspond to the OH group. For the aged materials at lower temperatures, such as 65°C and 85°C, independent of the humidity level, no significant differences compared to the unaged one were visible. In this case ATR characterisation has not shown the required results and was insufficient to characterise chemical degradation for PET films.

Table 2.3. Wavenumbers and assignments of the IR bands of PET [1, 2, 5, 54].

Wavenumber [cm^{-1}]	**Assignment**
3000-2855	CH and CH_2 stretching
1715	C=O stretching
1579	Aromatic CC stretching
1505	Aromatic CH in-plane bending Aromatic CC stretching
1470	CH_2 bending
1457	CH_2 bending OCH bending
1410	Aromatic CH in-plane bending Aromatic CC stretching
1370	CH_2 wagging
1340	CH_2 wagging OCH bending
1245	C(=O)-O stretching Aromatic ester CC stretching C=O in-plane bending
1178	Aromatic CH in-plane bending
1119	O-CH_2 stretching Aromatic CC stretching Aromatic CH in-plane bending
1099	C-O stretching
1048	C-O stretching
1018	Aromatic CCC bending Aromatic CC stretching Aromatic CH in-plane bending
971	O-CH_2 stretching C(=)-O stretching
898	CH_2 rocking
872	Aromatic CH out-of-plane bending Aromatic ester CC out-of-plane bending C=O out-of-plane bending Ring torsion
848	Aromatic CC stretching Aromatic ester CC stretching CCH bending COC bending C(=O)-O stretching C=O in-plane bending CH_2 rocking
793	Aromatic CH out-of-plane bending C=O rocking CCO bending
724	C=O out-of-plane bending Ring torsion Aromatic CH out-of-plane bending

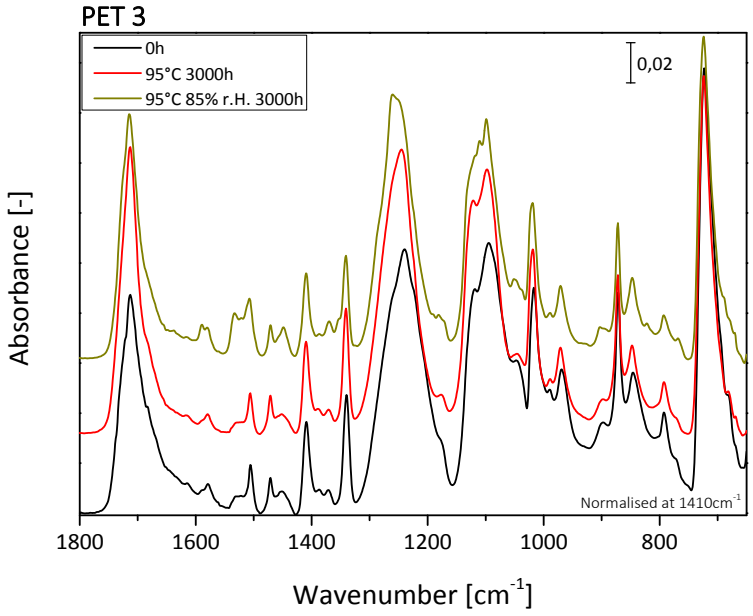

Figure 2.11. Change of crystallisation temperature of PET 3.

The rigidity is a particularity for this polymer and goes along with the low intermolecular interactions due to the absence of polar functional groups [55]. The low flexibility of PET is caused by its coplanar structure, which includes phenylene rings and coplanar ester groups. These are linked by short ethylene groups, see Figure 2.12. Its properties are mainly due to its chemical structure, but also depend on the crystallinity, orientation, molecular weight etc. [38]. That is the reason, why PET exhibited a relatively high modulus in the DMA tests compared to other standard polymers [56, 57].

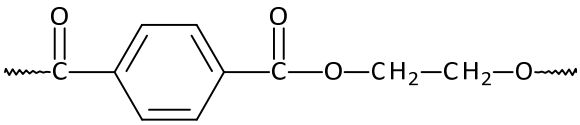

Figure 2.12. Structure of PET.

DMA results of the unaged PET films are shown in Figure 2.13. At 30°C PET 3 exhibited the highest storage modulus with a value of 4.51 GPa compared to PET 1 with 3.15 GPa and PET 2 with 2.55 GPa. The differences in storage modulus at 30°C between the samples can be caused by the fact, that the clamping of such thin samples is not trivial and that the sample preparation was done by the film producer. With that it cannot be excluded that not all of the samples were cut in machine direction. This can lead to a deviation in the storage modulus values. When reaching the glass transition temperature (T_G), where the mobility in the amorphous phase of the main chain is

increasing, the modulus dropped to below 0.24 GPa at 175°C. This corresponds to the loss tangents, which remained low below 60°C, indicating that only a small amount of energy is dissipated. Above 60°C the loss tangents increased and peaked at 99°C and 106°C, respectively. It is interesting that the curves for PET 2 showed no hints of the 3 layer construction, which means there were no additional steps in the modulus or any additional peaks in the loss tangent. However, the transition temperatures are more independent of the sample orientation during the DMA experiment than the modulus.

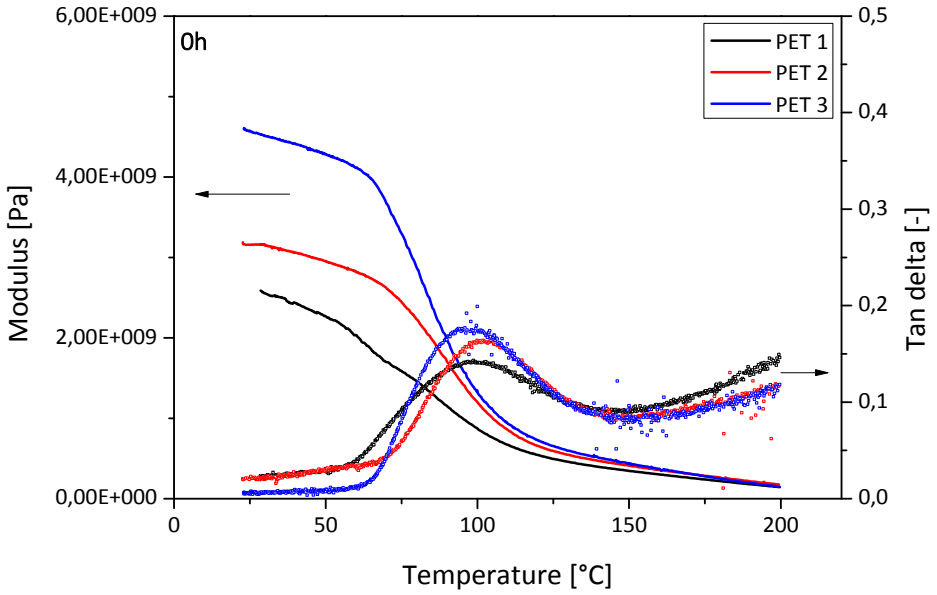

Figure 2.13. Storage modulus and loss tangent of all unaged PET films.

In general the loss tangent reflects the mobility of molecules, which means that a bigger value signals higher mobility of molecules [42, 57]. As PET is a semi-crystalline polymer it consists of a crystalline and an amorphous phase. However, only the amorphous phase determine T_G which is based on disordered macromolecules. The structure of the side chains influences T_G which means that the more space a side chain needs, the higher is T_G. This effect is called steric hindrance [56]. The ability of deformation in the amorphous phase is defined by the density of the entanglements and the mobility caused by temperature [50]. At temperatures below T_G the mobility of macromolecules is generally frozen and the deformation behaviour is energy-elastic. In the region of T_G the chains become more flexible, so that frozen orientations can relax. If the temperature increase further the mobility of the chains in the amorphous phase increase and become entropy-elastic. In PET it is possible that rotation could occur along the junctions in the backbone of the

chain, such as the –O– bond [42]. These effects are associated with the increase of the free volume [50, 56, 58].

The glass transition was determined by the maximum of the loss tangent and were located at 99°C, 106°C and 99°C for PET 1, PET 2 and PET 3, respectively. This compares to values in the literature where the measured values are in the range of 70°C to 140°C [4, 5, 42, 59]. There can be various reasons for the high glass transition temperature of PET 2 compared to the other samples: it could be the three layered construction, the biaxial orientation but also a different chemical structure with a higher steric hindrance due to side chains. However, the glass transition relaxation is very sensitive to the crystalline fraction [41]. Due to restraints in the amorphous region, molecular motions induced by the crystalline phase shift toward higher values as the crystallinity increases [4, 41]. In the literature this was only seen below a degree of crystallinity of 30% [41, 60]. Exceeding a value of 30% the glass transition is shifted back to lower temperatures [41, 60]. The T_G also very much depends on the thermal history, like the processing conditions [42, 56]. Ajji and Cole showed that drawing causes no significant change in T_G [6, 42].

The development of the glass transition temperature (T_G) over the ageing duration of PET 2 is exemplarily shown for all films in Figure 2.14. Samples aged at 95°C 85% r. H. for 2000 h and 3000 h were too brittle to be tested via DMA measurements. Ageing at 85°C, 95°C, 85°C 85% r. H. and 95°C 85% r. H. caused an increase of T_G. Because the glass transition is affected by the molecular mobility in the amorphous part, the changes implied a suppression of molecular mobility [40]. The suggested structural changes can probably be attributed to the interaction between functional groups, such as carboxyl acid groups and alcohol groups produced through hydrolysis degradation reactions [40]. However, the glass transition temperature can also change with the degree of crystallinity [4]. Anyway, as the degree of crystallinity decreased after the first 100 h of ageing, the increase in T_G and yield stress was not caused by post-crystallisation. It can rather be caused by the decrease in free volume. Hagihara et al. and Ehrenstein and Pongratz showed that the free-volume hole size in the amorphous part was reduced during degradation, which can influence the glass transition [12, 40]. Interestingly T_G only slightly increased for ageing conditions at 65°C, 65°C 85% r. H. and 125°C. A reason may be that 65°C was below the glass transition temperature. However, no explanation could be found for the changes after ageing at 125°C. The same behaviour can be observed for all three PET materials.

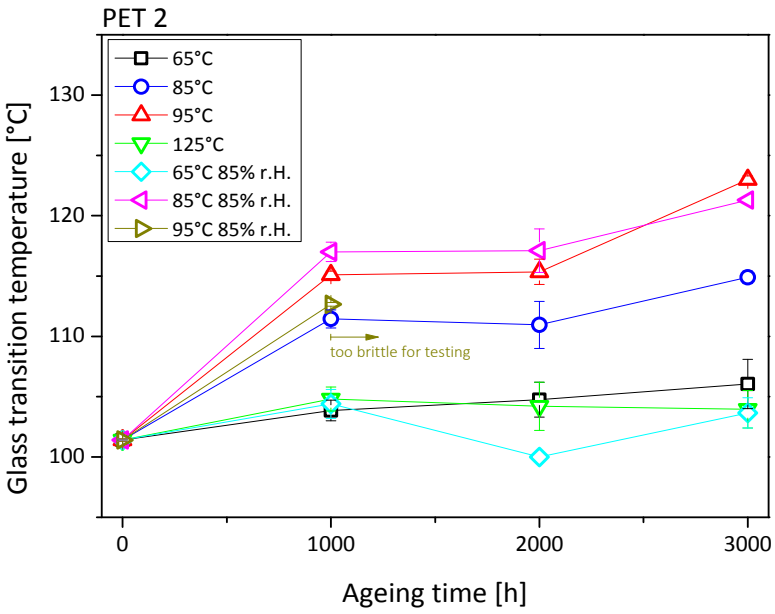

Figure 2.14. Change of T_G of PET 2 after ageing.

Figure 2.15 shows the stress-strain curves of all PET materials in the initial state. A ductile behaviour with distinct yield points can be observed for all unaged films. PET 1 and PET 2 exhibited almost the same behaviour, except a difference at the strain at break value. The difference between PET 1 and PET 2 compared to the storage modulus values of the DMA experiments can be explained by the influence of the sample clamping in the DMA test procedure and by the sample preparation. PET 3 showed, with a higher modulus, a stiffer behaviour – 5000 MPa compared to 4000 MPa, respectively. The literature stated that the crystallinity is considered as the single most important characteristic of a polymer in determining its mechanical properties [2, 37, 61, 62]. In general the orientation in machine direction of PET can lead to very high mechanical strengths with a decrease in the elongation [42]. This result of stretching is because the chain segments in the amorphous regions are already extended in a variety of directions, which limits the freedom that can occur during additional stretching, which happens during tensile tests [42]. Even though only the data sheet of PET 2 stated a biaxial orientation, it is probable that the other films were also oriented based on the results so far.

Noticeable was a high deviation of the unaged material. This may have been caused by the sample preparation, which was unfortunately done by the film producer. It cannot be excluded that not all of the samples were cut in machine direction which would explain the higher deviation of the values. Nevertheless, tensile tests of the aged samples were conducted in order to verify if a certain trend was detectable.

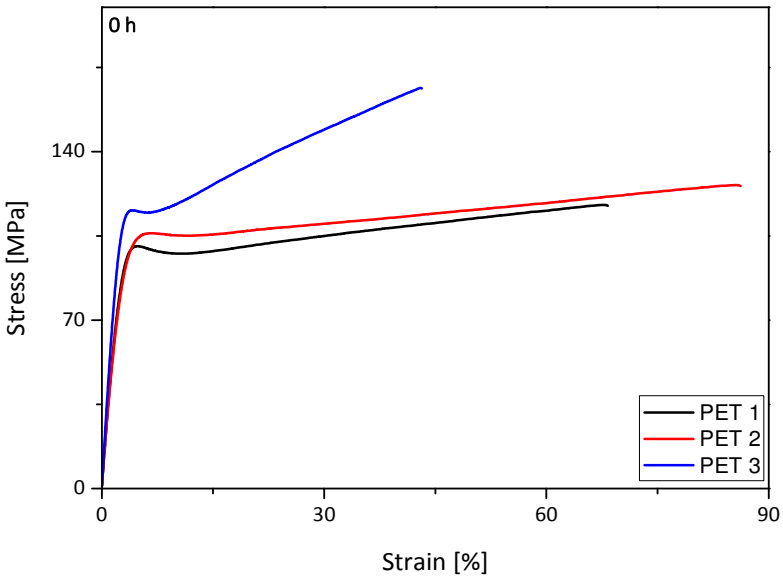

Figure 2.15. Stress-strain curves of all unaged materials.

The Young's modulus exhibited no significant changes after ageing for any of the materials, but an increase of the yield stress was observed, see Figure 2.16. In general the increase of the yield stress is an indicator for physical ageing processes, such as post-crystallisation and decrease in free volume [12]. However, the DSC results showed no post-crystallisation. Some of the samples showed a disappearance of the yield point and were very brittle after a certain time of ageing.

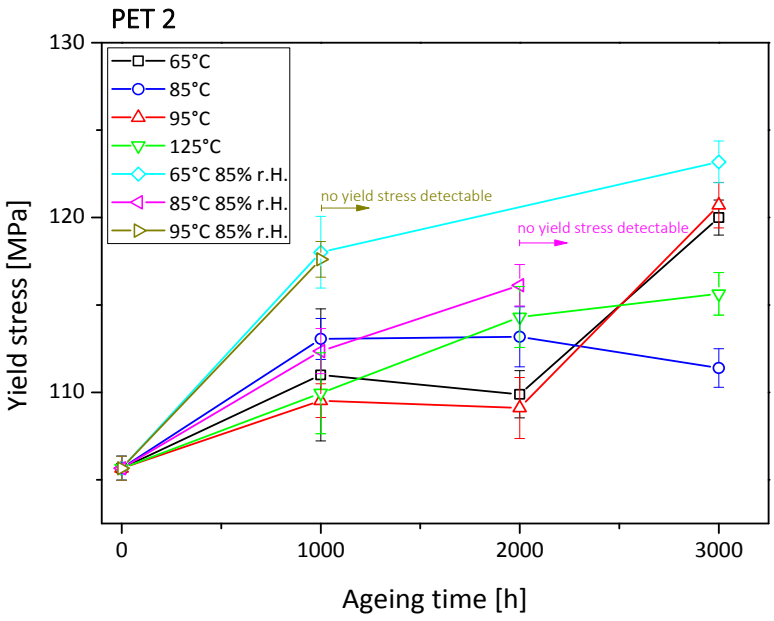

Figure 2.16. Change of yield stress of PET 2 after ageing.

A decrease of the strain at break was detected for all PET materials aged under 85°C and 95°C, both at 85% r. H., see Figure 2.17. This indicates chemical ageing including chain scission [26, 63, 64]. Hydrolysis which causes a decrease in molecular weight could be the reason for these changes, which was confirmed by the GPC results. Especially after ageing above T_G (99°C for unaged PET 3) and at high humidity levels, a stronger decrease of the strain at break value can be seen. Starting at a temperature of around 100°C, hydrolysis of the ester bond sets in [12]. The values decreased below 1% for 85°C 85% and 95°C 85% r. H. after 3000 h and 2000 h, respectively. The high standard deviation can be explained due to the fact that the fracture of samples during tensile tests starts at a defect which has a notching effect. This defect can be due to sample preparation, enclosures, bubbles, different thickness distributions, density differences occurring due to hydrolytic degradation, etc. Furthermore the sample preparation is the reason which is more likely for this high standard deviation; not all samples may be cut in machine direction. Nevertheless, a decreasing trend with ageing time at high temperature and humidity levels is obvious. This is more pronounced the higher the ageing temperature was.

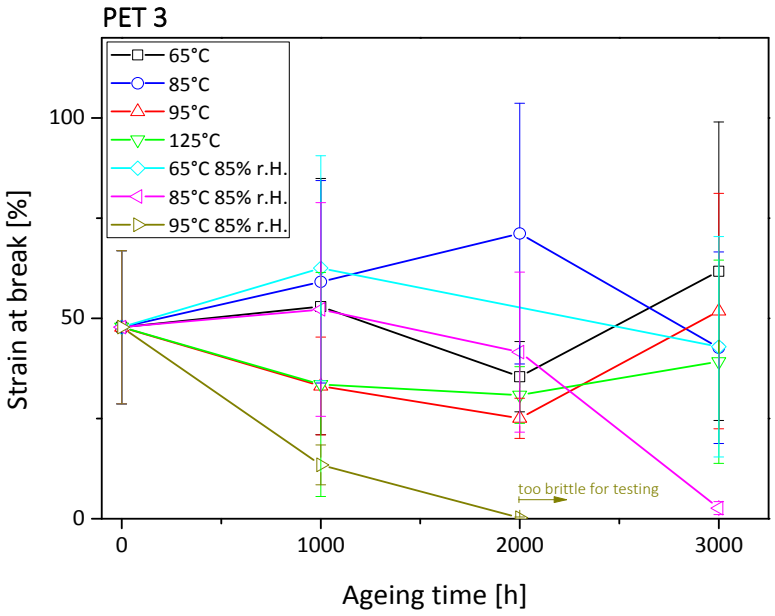

Figure 2.17. Change of strain at break value of PET 3.

When comparing characterisation methods a significant correlation between the molar mass and the crystallisation temperature of the DSC results was observed, see Figure 2.18. The samples aged at 85°C 85% r. H. and 95°C 85% r. H. showed similar linear decreases of the molar mass with the crystallisation temperature probably due to a similar degradation mechanism. Ageing at 125°C caused a different gradient, indicating a different ageing mechanism than that for ageing at high

humidity level. 3000 h at 125°C caused approximately the same decrease in molar mass as ageing at 85°C 85% r. H. for 1000 h. The other ageing types caused no significant change in molar mass or in crystallisation temperature. Obviously, the crystallisation temperature is a more sensitive and reliable indicator for chain scission via hydrolysis than, for example, the strain at break value, which was not as sensitive as the temperature in this research. In general the disadvantage of mechanical testing is that the fracture of the sample starts at a defect, generated e. g. via sample preparation, different thickness distributions, enclosures, bubbles, density differences, etc. [26]. This makes the DSC results more independent of such external influences.

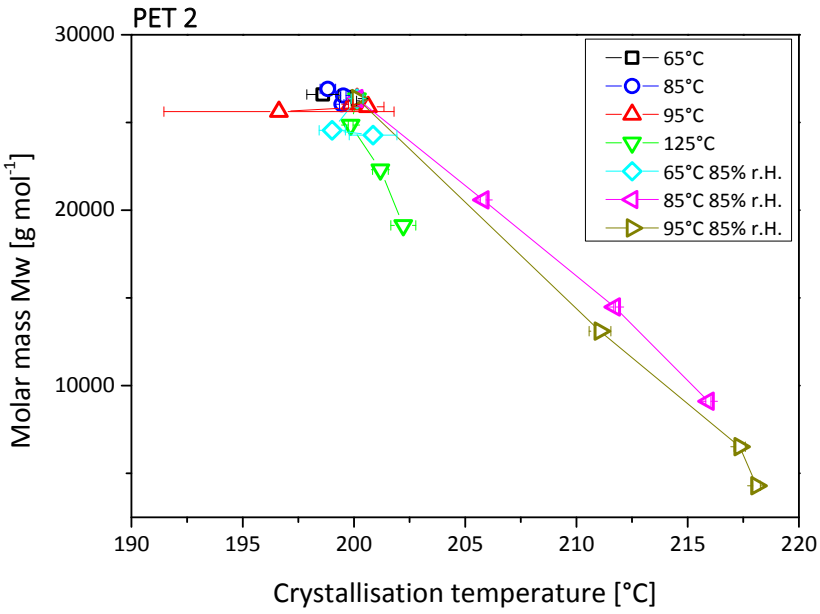

Figure 2.18. Molar mass over crystallisation temperature of PET 2.

2.4. Summary and conclusion

The effects of different types of artificial ageing on various polyethylene terephthalate (PET) films were discussed. PET films were chosen, as they are widely used as a component in a backsheet for PV modules. The results could help to enhance the existing knowledge of the ageing behaviour of PET films dependent on temperature and humidity level. Furthermore it might help to draw additional conclusions about the complex ageing behaviour of PET-based multilayer backsheets. Therefore different PET films were aged with a heating furnace and a climatic chamber under different temperature and humidity conditions. The materials' chemical, thermal, optical, thermo-mechanical and mechanical properties were characterised using water absorption tests, GPC measurements, DSC, IR spectroscopy, UV/Vis/NIR spectroscopy, DMA and tensile tests.

A significant water uptake could not be detected. The degree of crystallinity decreased after the first 1000 h, implying a high orientation for all materials. Optical changes could only be found for 125°C after 3000 h, which led to the conclusion that no visible discolouration does not mean no degradation took place. In this case ATR measurements were not a suitable method to characterise chemical degradation, as no significant changes caused by hydrolysis were visible. The glass transition temperatures T_G increased with increasing ageing duration, maybe caused by a decrease of the free volume. The strain at break value decreased with higher temperature and humidity levels caused by chemical degradation (hydrolysis). This was confirmed by the increase in crystallisation temperature and furthermore by the GPC results, where a decrease of the molar mass for high temperatures and humidity levels could be detected. For PET 1 aged at 125°C curing reactions could be detected. A sensitive and more reliable indicator for chain scission via hydrolysis was the crystallisation temperature compared to mechanical testing.

2.5. References

[1] Dubelley, F., Planes, E., Bas, C., Pons, E., Yrieix, B., and Flandin, L. 2017. The hygrothermal degradation of PET in laminated multilayer. *European Polymer Journal* 87, 1–13.

[2] Aljoumaa, K. and Abboudi, M. 2016. Physical ageing of polyethylene terephthalate under natural sunlight. Correlation study between crystallinity and mechanical properties. *Appl. Phys. A* 122:6, 6, 1–10.

[3] Scheirs, J. and Long, T. E. 2003. *Modern polyesters*. *Chemistry and technology of polyesters and copolyesters*. Wiley series in polymer science. John Wiley & Sons, Hoboken, N.J.

[4] Dong, W., Zhao, J., Li, C., Guo, M., Zhao, D., and Fan, Q. 2002. Study of the amorphous phase in semicrystalline poly(ethylene terephthalate) via dynamic mechanical thermal analysis. *Polymer Bulletin* 49, 2-3, 197–203.

[5] Awaja, F. and Pavel, D. 2005. Recycling of PET. *European Polymer Journal* 41, 7, 1453–1477.

[6] Ajji, A., Legros, N., and Dumoulin, M. M. 1998. High Performance Materials from Oriented Plastics. *Advanced Performance Materials* 5, 117–136.

[7] Allen, N. S., Edge, M., Mohammadian, M., and Jones, K. 1994. Physicochemical aspects of the environmental degradation of poly(ethylene terephthalate). *Polymer Degradation and Stability* 43, 2, 229–237.

[8] Lu, X. and Hay, J. 2001. Crystallization orientation and relaxation in uniaxially drawn poly(ethylene terephthalate). *Polymer* 42, 19, 8055–8067.

[9] Peike, C., Hülsmann, P., Blüml, M., Schmid, P., Weiß, K.-A., and Köhl, M. 2012. Impact of Permeation Properties and Backsheet-Encapsulant Interactions on the Reliability of PV Modules. *ISRN Renewable Energy* 2012, 1–4, 1–5.

[10] Oreski, G. and Pinter, G. 2013. Accelerated weathering of multi-layer films - effect of specimen preperation. In *The proceedings of the Austrian--Slovenian Polymer Meeting 2013*, Centre of Excellence PoliMaT, Ed. Narodna in univerzitetna knjižnica, Ljubljana, 40–42.

[11] Grassie, N. and Scott, G. 1988. *Polymer Degradation & [and] stabilisation*. Cambridge Univ. Press, Cambridge u.a.

[12] Ehrenstein, G. W. and Pongratz, S. 2007. *Beständigkeit von Kunststoffen*. Carl Hanser Verlag, Munich.

[13] Badia, J., Strömberg, E., Karlsson, S., and Ribes-Greus, A. 2012. The role of crystalline, mobile amorphous and rigid amorphous fractions in the performance of recycled poly (ethylene terephthalate) (PET). *Polymer Degradation and Stability* 97, 1, 98–107.

[14] Edge, M., Hayes, M., Mohammadian, M., Allen, N. S., Jewitt, T. S., Brems, K., and Jones, K. 1991. Aspects of poly(ethylene terephthalate) degradation for archival life and environmental degradation. *Polymer Degradation and Stability* 32, 2, 131–153.

[15] Lechat, C., Bunsell, A., and Davies, P. 2011. Tensile and creep behaviour of polyethylene terephthalate and polyethylene naphthalate fibres. *J Mater Sci* 46, 528–533.

[16] Pieter Gijsman, Guido Meijers, and Giacomo Vitarelli. 1999. Comparsion of the UV-degradation chemistry of polypropylene, polyethylene, polyamide 6 and polybutylene terephthalate. *Polymer Degradation and Stability,* 65, 433–441.

[17] McMahon, W., Birdsall, H. A., Johnson, G. R., and Camilli, C. T. 1959. Degradation Studies of Polyethylene Terephthalate. *J. Chem. Eng. Data,* 4, 57–79.

[18] Ito, K., Haraguchi, Y., Hayakawa, S., and Toda, A. 2008. Enhanced Crystallization of Blended Poly(ethylene terephthalate) and Poly(butylene terephthalate). *Polym J* 40, 10, 992–995.

[19] Chen, Z., Hay, J. N., and Jenkins, M. J. 2013. The thermal analysis of poly(ethylene terephthalate) by FTIR spectroscopy. *Thermochimica Acta* 552, 123–130.

[20] Hosseini, S. S., Taheri, S., Zadhoush, A., and Mehrabani-Zeinabad, A. 2007. Hydrolytic degradation of poly(ethylene terephthalate). *J. Appl. Polym. Sci.* 103, 4, 2304–2309.

[21] Assadi, R., Colin, X., and Verdu, J. 2004. Irreversible structural changes during PET recycling by extrusion. *Polymer* 45, 13, 4403–4412.

[22] Holland, B. J. and Hay, J. N. 2002. The thermal degradation of PET and analogous polyesters measured by thermal analysis-Fourier transform infrared spectroscopy. *Polymer,* 43, 1835–1837.

[23] Foulc, M., Bergeret, A., Ferry, L., Ienny, P., and Crespy, A. 2005. Study of hygrothermal ageing of glass fibre reinforced PET composites. *Polymer Degradation and Stability* 89, 3, 461–470.

[24] Planes, E., Yrieix, B., Bas, C., and Flandin, L. 2014. Chemical degradation of the encapsulation system in flexible PV panel as revealed by infrared and Raman microscopies. *Solar Energy Materials and Solar Cells* 122, 15–23.

[25] Oreski, G. and Wallner, G. M. 2005. Delamination behaviour of multi-layer films for PV encapsulation. *Solar Energy Materials and Solar Cells* 89, 2-3, 139–151.

[26] Knausz, M., Oreski, G., Eder, G. C., Voronko, Y., Duscher, B., Koch, T., Pinter, G., and Berger, K. A. 2015. Degradation of photovoltaic backsheets: Comparison of the aging induced changes on module and component level. *J. Appl. Polym. Sci.* 132, 42093, 1–8.

[27] Allen, N. S., Edge, M., Rodriguez, M., Liauw, C. M., and Fontan, E. 2000. Aspects of the thermal oxidation of ethylene vinyl acetate copolymer. *Polymer Degradation and Stability,* 68, 363–371.

[28] Allen, N. S., Edge, M., Rodriguez, M., Liauw, C. M., and Fontan, E. 2001. Aspects of the thermal oxidation, yellowing and stabilisation of ethylene vinyl acetate copolymer. *Polymer Degradation and Stability,* 71, 1–14.

[29] Weisskopf, K. 1988. Characterization of Polyehtylene Terephthalate by Gel Permeation Chromatography (GPC). *Journal of Polymer Science* 26, 1919–1935.

[30] International Organisation for Standardisation, ISO 11357-3. 1999. *Plastics - Differential scanning calorimetry (DSC) Part 3: Determination of temperature and enthalpy of melting and crystallization,* 11357-3.

[31] Miyake, A. 1959. The infrared spectrum of polyethylene terephthalate. I The effect of crystallization. *J. Polym. Sci.* 38, 134, 479–495.

[32] International Organisation for Standardisation, ISO 527-3. 1995. *Plastics - Determination of tensile properties: Part 3: Test conditions for films and sheets,* 527-3.

[33] Lahokallio, S., Saarinen, K., and Frisk, L. 2013. Effect of High-Humidity Testing on Material Parameters of Flexible Printed Circuit Board Materials. *Journal of Elec Materi* 42, 9, 2822–2834.

[34] Bin, Y., Oishi, K., Yoshida, K., Nakashima, T., and Matsuo, M. 2004. Orientation Distribution Functions of the Three Principal Crystallographic Axes as well as Crystallites of Poly(ethylene terephthalate) Films under Biaxially Stretching. *Polym J* 36, 5, 394–402.

[35] Wintermantel, E. and Ha, S.-W. op.1998. *Biokompatible Werkstoffe und Bauweisen*. *Implantate für Medizin und Umwelt*. Springer, Berlin, Heidelberg.

[36] Venkatachalam, S., G., S., V., J., R., P., Rao, K., and K., A. 2012. Degradation and Recyclability of Poly (Ethylene Terephthalate). In *Polyester*, H. E.-D. Saleh, Ed. InTech. DOI=10.5772/48612.

[37] Kong, Y. and Hay, J. N. 2003. Multiple melting behaviour of poly(ethylene terephthalate). *Polymer,* 44, 623–633.

[38] Karagiannidis, P. G., Stergiou, A. C., and Karayannidis, G. P. 2008. Study of crystallinity and thermomechanical analysis of annealed poly(ethylene terephthalate) films. *European Polymer Journal* 44, 5, 1475–1486.

[39] Hamid, S. H., Ed. 1992. *Handbook of polymer degradation*. Environmental science and pollution control series 2. Dekker, New York u.a.

[40] Hagihara, H., Oishi, A., Funabashi, M., Kunioka, M., and Suda, H. 2014. Free-volume hole size evaluated by positron annihilation lifetime spectroscopy in the amorphous part of poly(ethylene terephthalate) degraded by a weathering test. *Polymer Degradation and Stability* 110, 389–394.

[41] Cristea, M., Ionita, D., and Simionescu, B. C. 2010. A new insight in the dynamo-mechanical behavior of poly(ethylene terephthalate). *European Polymer Journal* 46, 10, 2005–2012.

[42] Bhushan, B., Ma, T., and Higashioji, T. 2002. Tensile and dynamic mechanical properties of improved ultrathin polymeric films. *J. Appl. Polym. Sci.* 83, 10, 2225–2244.

[43] Boukezzi, L., Boubakeur, A., and Lallouani, M. Effect of Artificial Thermal Aging on the Crystallinity of XLPE Insulation Cables: X-ray Study. *Proceedings of Annual Report Conference on Elctrical Insulation nand Dielectric Phenomena* 2007.

[44] Medellin-Rodriguez, F. J., Phillips, P. J., Lin, J. S., and Campos, R. 1997. The triple melting behavior of poly(ethylene terephthalate). Molecular weight effects. *J. Polym. Sci. B Polym. Phys.* 35, 11, 1757–1774.

[45] Bell, J. P. and Dumbleton, J. H. 1969. Relation between melting behavior and physical structure in polymers. *J. Polym. Sci. A-2 Polym. Phys.* 7, 6, 1033–1057.

[46] Bell, J. P. and Murayama, T. Relations between dynamic mechanical properties and melting behavior of nylon 66 and poly(ethylene terephthalate). *Journal of Polymer Science, Polymer Physisc Edition* 1969, 7 (6).

[47] Holdsworth, P. J. and Turner-Jones, A. 1971. The melting behaviour of heat crystallized poly(ethylene terephthalate). *Polymer* 12, 3, 195–208.

[48] Huang, J., Chu, P. P., and Chang, F.-C. 2000. Conformational changes and molecular motion of poly(ethylene terephthalate) annealed above glass transition temperature. *Polymer* 41, 5, 1741–1748.

[49] Galli, R., Canetti, M., Sadocco, P., Seves, A., and Vicini, L. 1983. Preoriented poly(ethylene terephthalate) yarns. Influence of the gauche-trans transformation on crystallization. *J. Polym. Sci. Polym. Phys. Ed.* 21, 5, 717–723.

[50] Frick, A. and Stern, C. 2006. *DSC-Prüfung in der Anwendung*. Carl Hanser Verlag, Munich.

[51] Edge, M., ALLEN, N., Wiles, R., MCDONALD, W., and MORTLOCK, S. 1995. Identification of luminescent species contributing to the yellowing of poly(ethyleneterephthalate) on degradation. *Polymer* 36, 2, 227–234.

[52] Gambogi, W. J., Heta, Y., Hashimoto, K., Kopchick, J. G., Felder, T., MacMaster, S. W., Bradley, A., Hamzavytehrany, B., Garreau-Iles, L., Aoki, T., Stika, K. M., Trout, T. J., and Sample, T. 2014. A Comparison of Key PV Backsheet and Module Performance from Fielded Module Exposures and Accelerated Tests. *IEEE J. Photovoltaics* 4, 3, 935–941.

[53] Liu, F., Jiang, L., and Yang, S. 2014. Ultra-violet degradation behavior of polymeric backsheets for photovoltaic modules. *Solar Energy* 108, 0, 88–100.

[54] Donelli, I., Freddi, G., Nierstrasz, V. A., and Taddei, P. 2010. Surface structure and properties of poly-(ethylene terephthalate) hydrolyzed by alkali and cutinase. *Polymer Degradation and Stability* 95, 9, 1542–1550.

[55] Perepelkin, K. E. 2001. Physicochemical Nature and Structural Dependence of the Unique Properties of Polyester Fibres. *Fibre Chemistry* 33, 5, 340–352.

[56] Menges, G., Haberstroh, E., Michaeli, W., and Schmachtenberg, E. 2002. *Werkstoffkunde Kunststoffe*. Carl Hanser, Munich.

[57] Menard, K. P. 2002. Dynamic Mechanical Analysis. In *Encyclopedia of Polymer Science and Technology*. John Wiley & Sons, Inc. DOI=10.1002/0471440264.pst102.

[58] Struick, L. C. E. 1977. Physical Aging in Plastics and Other Glassy Materials. *Polymer Engineering and Science* 17, 3.

[59] Rwei, S.-P. 1999. Properties of poly(ethylene terephthalate)/poly(ethylene naphthalate) blends. *Polym. Eng. Sci.* 39, 12, 2475–2481.

[60] Illers, K. H. and Breuer, H. 1963. Molecular motions in polyethylene terephthalate. *Journal of Colloid Science* 18, 1, 1–31.

[61] Kong, Y. and Hay, J. N. 2002. The measurement of the crystallinity of polymers by DSC. *Polymer* 43, 14, 3873–3878.

[62] Chaari, F. and Chaouche, M. 2004. Rheooptical investigation of the crystallization of poly(ethylene terephthalate) under tensile strain. *J. Polym. Sci. B Polym. Phys.* 42, 10, 1915–1927.

[63] Oreski, G. and Wallner, G. M. 2005. Aging mechanisms of polymeric films for PV encapsulation. *Solar Energy* 79, 6, 612–617.

[64] Oreski, G. Accelerated indoor durability testing of polymeric photovoltaic encapsulation materials. In *SPIE Solar Energy + Technology, San Diego, USA, 2010. DOI*=10.1117/12.860390.

3. Comparison of natural and artificial weathering of polymeric multilayer films

The following chapter deals with the comparison of natural and artificial weathering tests of photovoltaic (PV) backsheets. As already stated, natural weathering is the method of choice when it comes to application relevant reliability testing of PV module materials. However, the PV industry still uses artificial ageing methods in order to verify the ageing behaviour and the reliability of polymer materials, such as encapsulants or backsheets. This is the reason why it is necessary to investigate the different influences of natural and artificial weathering.

3.1. Introduction to natural and artificial weathering on polymeric multilayer films

As the importance of renewable energy sources is growing the development of PV modules has been proceeded [1]. A high quality product standard is required and as a result module lifetimes of 20 years and more are guaranteed with a limited loss in functionality [2, 3]. Therefore not only the module itself but also the components of a PV module have to be tested concerning their quality. The advantage of testing on component level is the easier handling with a lower effort and therefore lower costs compared to testing the whole part [4]. The additional drive to lower component and testing costs led to new materials and artificial ageing of the components of a PV module [5]. Backsheets in particular need to provide mechanical stability, protection against weathering, electrical insulation and a selective barrier function against water vapour, oxygen and acetic acid over the whole lifetime of a PV module. Additionally a good adhesion to the encapsulation material is necessary [6]. In order to fulfil these requirements multilayer laminates are standard for backsheets consisting of different polymer and barrier layers [5]. Polymeric materials are used due to their low costs and good processability compared to other materials [7]. A typical backsheet structure includes three layers, where the inner layer (facing to the solar cell) is usually ethylene vinyl acetate (EVA), polyethylene (PE), polyamide (PA), polyethylene terephthalate (PET) or a fluoropolymer. This layer is responsible for the adhesion to the encapsulation and should protect the core layer against ultraviolet light. The core layer is often made of PET or PA for mechanical stability, electrical insulation and should act as a selective barrier function for atmospheric gases since it is usually the thickest layer. The outer layer (air side) of the backsheet protects the other layers and the PV module against weathering and can be made of PA,

PET or fluoropolymers [8]. However, polymers are associated with a certain percentage of failures in the field [6, 9]. Especially PV backsheets are critical to the performance and reliability of silicon photovoltaic modules [10, 11]. Therefore the ageing behaviour of the backsheet is crucial for the whole PV module because it influences cell corrosion and the encapsulant degradation and can lead to the breakdown of the whole PV module [6, 8, 10, 12–15]. Thus, the type of backsheet highly affects the reliability over the whole life cycle of a PV module. A gradual degradation and loss in performance due to environmental stresses, such as temperature, humidity and UV radiation of PV modules and components have been observed [2, 4, 10, 14, 16–22, 22–26]. Several studies have been carried out concerning the ageing behaviour of single backsheets as well as backsheets incorporated in PV modules [4, 15]. The examinations confirmed that the differences are negligible for polyester-based backsheets [4].

For accelerated lifetime predictions artificial weathering tests are usually conducted with the benefit of less time consumption and therefore faster results under controlled conditions and elimination, or rather control, of sample contamination compared to natural weathering tests [2, 10, 11, 27]. Mostly studies without irradiation were conducted and only some research on backsheets has been done with regard to artificial ageing with and without irradiation [8, 11, 12, 19, 21]. But, Gambogi et al. already stated that the existing qualification tests in the PV industry can be used only to verify infant mortality failures in module design and materials [28]. With regard to application conditions, diffuse irradiation should not been ignored, since not only the inner side is stressed by UV light, but also the back side due to scattering and reflection [29]. For example snow reflects 63 to 79% of all wavelengths [29]. Even if the intensity is small the incoming light might induce photo-degradation.

The weathering performance of polymeric backsheet materials is most accurately assessed by outdoor exposure to natural weathering at different locations and examination of their performance characteristics by observing changes in physical and chemical properties [5, 29]. Although natural weathering is the most reliable exposure method to examine long-term performance, its major disadvantage is the extremely long exposure time required to achieve the corresponding service lifetime of the components. In order to decrease the testing time significantly for the purpose of more rapid prediction of long-term weathering performance, it is necessary to use accelerated artificial weathering and ageing tests followed by measurements of physical and chemical changes or changes in performance. Certainly there are still open questions concerning the comparability of artificial and natural weathering of backsheets. It is necessary to establish

connections between field performance of polymer products and accelerated materials durability testing in order to better predict the service life of a polymer product [5].

Therefore the main focus of this chapter is to evaluate the influence of natural and different artificial weathering tests on the behaviour of several multilayer backsheets and furthermore to verify the comparability of these test results.

3.2. Experimental procedure

Seven commercially available backsheet multilayer films were investigated; all of them consisted of different material layers, see Table 3.1. The unaged and aged materials were characterised in order to verify the influence of ageing time and type and subsequently to compare them. Natural weathering on the roof of the university in Leoben (AT) was conducted and the results were compared to the outcomes of artificial weathering via Xenotest Beta LM and UVTest (Atlas, Linsengericht, DE). The artificial ageing with the Xenotest (Xe) device was conducted with xenon arc lamps and the UV ageing with fluorescence lamps type UV-A. In Table 3.2 the ageing parameters are listed. The main difference between the artificial ageing tests was that only the UV ageing consisted of a dark cycle, whereas at Xe ageing the samples were irradiated according to ISO 4892 constantly [30, 31]. So for the Xe ageing dry and rain cycles, both with irradiation alternated and for the UV ageing light and dark condensation cycles alternated.

All backsheets were faced with the inner side (facing to solar cell) to the sun and irradiation, respectively, like in real application. The following characterisation methods were used in order to quantify and qualify changes in optical, thermal, mechanical and thermo-mechanical properties: water absorption tests, microscopy, Ultraviolet/Visual light/Near-Infrared (UV/Vis/NIR) spectroscopy, differential scanning calorimetry (DSC), dynamic mechanical analysis (DMA), tensile tests and Fourier transform infrared (FTIR) spectroscopy. All samples were prepared and cut before they were aged to minimise the errors induced by cutting brittle materials for mechanical testing [32].

Table 3.1. Investigated backsheets.

Material	Layer thickness in µm	Layer construction		
		Inner layer	Core layer	Outer layer
AAA	25/300/25	PA	PA	PA
APA	25/250/25	PA	PET	PA
TPT	37/250/37	Polyvinyl fluoride (PVF)	PET	PVF
KPK	19/250/19	Polyvinyliden fluoride (PVDF)	PET	PVDF
THV	-	EVA	PET	Tetrafluoroethylene (TFE) Hexafluoropropylene (HFP) Vinylidene fluoride (VDF) (THV)
PPE 1	125/190/50	PE-EVA	PET	PET
PPE 2	100/125/50	PE-EVA	PET	PET

Table 3.2. Ageing parameters

Parameters	Natural weathering (NW)	Xenon ageing (Xe) ISO 4892-1 [30]	UV-A ageing (UV) ISO 4892-3 [31]
Cycles	Day Night	Light Light + spray	Light Dark
Light source	Sun	Xenon arc lamp 300 – 400 nm	Fluorescence lamp UV-A 345 nm
Irradiance intensity in W m^{-2}	Ambient conditions	60	0.76
Temperature in °C	Ambient conditions	65	60 50
Relative humidity in % (r. H.)	Ambient conditions	50	Not controlled

Water absorption tests were done on square-shaped samples (60 x 60 mm). They were stored at 23°C and 50% relative humidity (r. H.). Subsequently the samples were dried in an oven at 50°C and 350 mbar and frequently weighed until the mass remained constant. A Vötsch climate chamber type VC 7020 (Balingen, DE) was used and the samples were weighed regularly. For each material three samples were used.

Microscopy pictures were taken with a Zeiss Stemi 2000-C Microscope (Oberkochen, DE) in combination with a Canon Power Shot G9 (Tokio, JP) under daylight settings and a magnification of 1.25. All pictures were taken with the same settings in order to make them more comparable.

UV/Vis/NIR spectroscopy was carried out on a Perkin Elmer Lambda 950 (Waltham, US). The wavelength range was between 250 and 2500 nm with a measuring interval of 5 nm. Hemispherical transmission measurements were done with an Ulbricht sphere. Additionally the colour values for

all samples were calculated with the colour software WinColour based on standard light C between 780 and 380 nm under an angle of observation of 2°.

FTIR spectra were collected in attenuated total reflection (ATR) mode using a Spectrum GX spectrometer (Perkin Elmer, Waltham, US). The transmittance spectra were recorded from 4000 to 650 cm^{-1} with a resolution of 4 cm^{-1}.

DMA was performed using a Perkin Elmer DMA 8000 (Waltham, US) in tension mode. The samples, with the dimensions of 10 x 4 mm, were heated from -80°C to 200°C with a rate of 3 K min^{-1}. A frequency of 1 Hz was used and at least two samples were measured in machine direction.

The thermal behaviour was analysed via DSC using a Perkin Elmer DSC 4000 (Waltham, US) over the range of -40 to up to 270°C with a heating rate of 10 K min^{-1}. Approximately 10 mg of samples were cut and put in 50 µl pans with perforated lids. A Nitrogen atmosphere was used in order to prevent further oxidation processes. In order to identify reversible and irreversible processes two heating runs were conducted. Peak temperatures and enthalpies were evaluated according to ISO 11357-3 [33]. Three samples were used to obtain an average.

Tensile tests on rectangular samples (15 x 100 mm) were carried using a Zwick-Roell Z001 (Ulm, DE) at ambient temperature according to EN ISO 527-3 [34]. A testing speed of 50 mm min^{-1} and a gauge length of 50 mm was used. The samples were tested in machine direction. The Young's modulus, yield point, strain at break and stress at break were determined for at least seven specimens for each test series.

3.3. Results and discussion

Polycondensates, such as PA and PET, are prone to chemical degradation via hydrolysis and therefore the ability to absorb water has a significant influence on the ageing behaviour [35–37]. Therefore water absorption tests were conducted on the virgin materials and plotted in Figure 3.1. The backsheet PPE 2 with the lowest thickness (275 µm) showed the lowest mass. Even though AAA exhibited the highest thickness with a value of 350 µm, it had the second lowest overall mass. A reason is that this backsheet consisted only of PA layers and PA has a lower density compared to PET, which is the core layer in all other backsheets [38]. After the first day of drying the samples showed a small decrease of the mass with around 0.02 mg for APA. However, no significant changes could be detected compared to the starting mass after almost two weeks of drying. The mass of KPK was 1.70 ± 0.01 g at the beginning and after 14 days of drying it exhibited a value of 1.69 ± 0.01 g. This means that no detectable water absorption took place. Admittedly, the

absorption of water is not necessarily required for hydrolysis reactions, the humidity available in the surrounding air can be enough to lead to chain scission via hydrolysis [37].

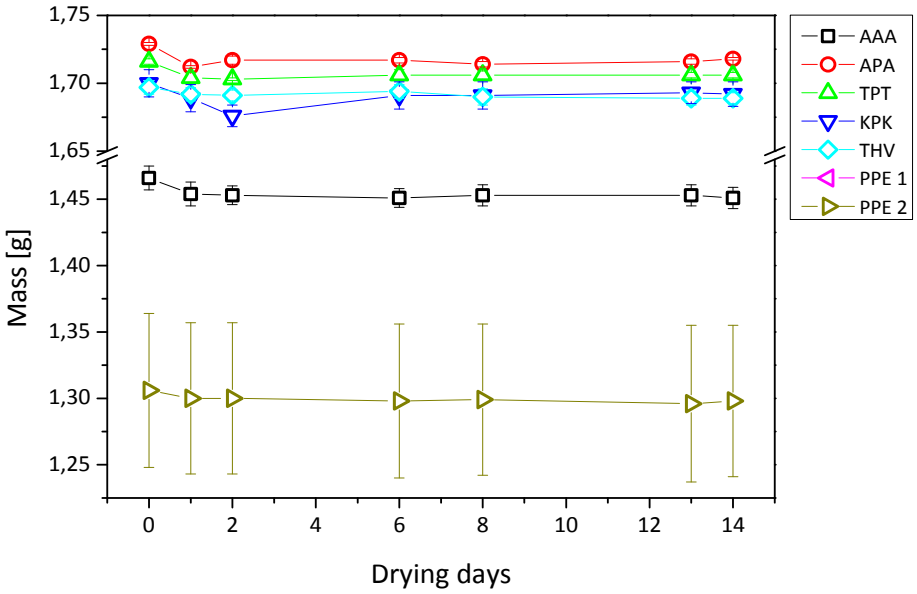

Figure 3.1. Mass development during drying for all virgin backsheets.

A classification of the backsheets depending on the layer material was done in order to better compare the samples. The following material classes for the inner front layers could be identified, see Table 3.3.

Table 3.3. Material class and belonging backsheets for inner layers (front side).

Material class inner layer	**Backsheet**
PA	AAA, APA
Fluoropolymers	TPT, KPK
Polyolefins	THV, PPE 1, PPE 2

In order to verify changes in optical properties UV/Vis/NIR spectra were recorded. Figure 3.2 shows exemplarily the spectra of unaged and aged AAA, front sides. Especially natural weathering caused a decrease in reflectance in the visual light region. The naturally aged samples were cleaned with purified water and measured again in order to verify whether this discoloration was due to soiling or not. The comparison of the original, weathered surface to the cleaned one revealed an influence of soiling. This can be seen for all backsheets except for APA, where there is no significant difference. A smoother surface and a different surface energy might be possible for this type of backsheet. Only the backsheets with PA-based front layers showed an increase in the reflectance

in the UV region after UV-A ageing of the front side, which indicates a consumption of possible UV absorbers. Fluoropolymer and polyolefin layers showed no changes in the UV region.

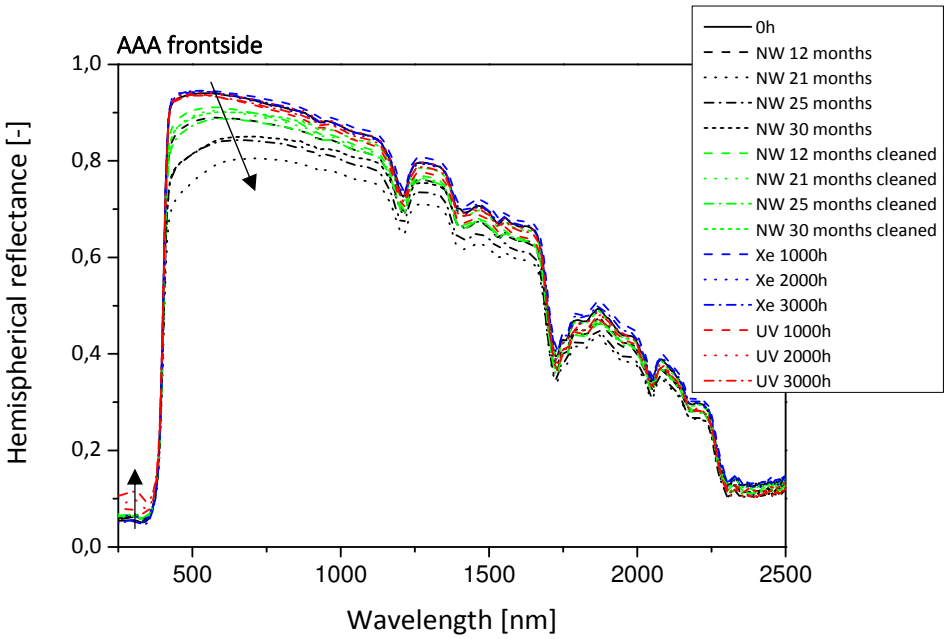

Figure 3.2. Hemispherical reflectance of aged AAA.

The colour value b* corresponds to the blue-yellow axis according to CIE Lab System and can be a representative indicator for ageing, due to the formation of chromophoric groups during ageing and its direct relation to yellowness [8]. It can be a severe problem for PV backsheets in the field which can lead to a strong absorption of irradiation and thus high operation temperatures of the PV module, depending on the spacing from the roof and available reflected light and location [5, 8]. Higher temperatures lead to accelerated degradation processes [8, 35]. Even though it is a significant factor, research on UV degradation mechanisms of backsheets is rare in literature [8, 14]. The previous research was mostly focused on degradation without UV irradiation, such as thermo-oxidative degradation [8, 11, 12, 14, 19, 21, 39]. The dominant mechanism for yellowing may be photo-oxidation, which is why the UV-dose was used instead of the time axis to compare the different ageing types. In general after natural ageing the front side became discoloured – the b* value increased with increasing ageing time and UV dose, respectively, see Figure 3.3. This was also visible in the decrease of reflectance in the spectra in the blue region of the visible light. Backsheets with PA front layers showed no significant changes of colour after artificial ageing at all, neither after Xe nor after UV ageing independent of the middle layer (PA or PET). Only natural weathering caused an increase of the b* value of 1.4 ± 0.0 after 30 months on the cleaned front side. Soiling was responsible for an additional colour change up to a delta of 3.8 ± 0.0 after

21 months. Literature showed that oxidation processes of hindered phenolic oxidants are associated with an increase in yellowing [40, 41]. Apparently, artificially ageing with irradiation is not sufficient to cause the same deteriorations in optical properties as natural weathering did for PA front sides, which means that different ageing mechanism occurred for this material class.

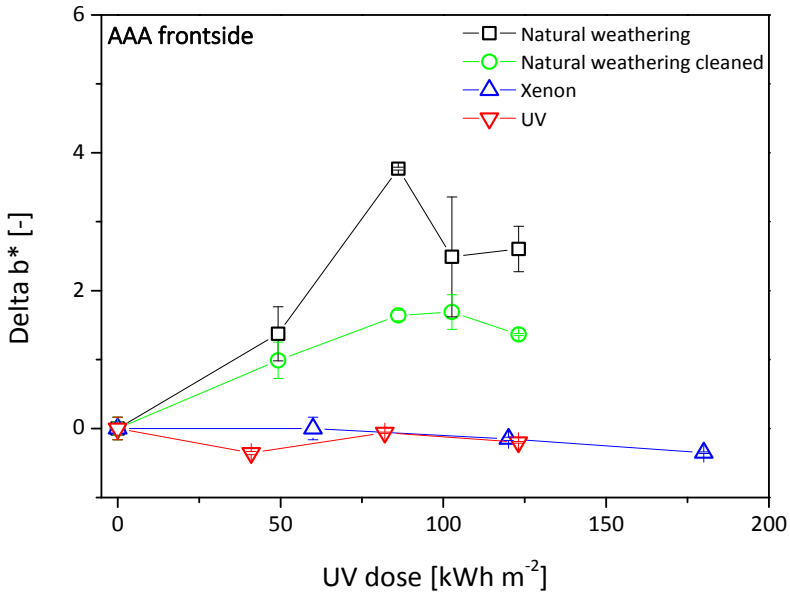

Figure 3.3. Delta of the colour value b for aged AAA front side.*

Also backsheets with fluoropolymers on the front side (PVF, PVDF) and PET middle layer showed no significant changes in yellowing after Xenon ageing. However, for these materials natural and UV ageing caused a significant increase of the b* values, see Figure 3.4. It is probable that, in PVDF a small amount of degradation which can cause conjugated groups can lead already to visible discolouration. For this material class the test design of UV ageing including light and dark cycles was effective in causing the same amount of discolouration as natural weathering. An alternative explanation may be the discolouration of the PET core layer which could be simultaneously measured via reflectance, because of the low thickness of the fluoropolymer layer. Hydrolysis processes in the PET core layer could be possible during natural and UV ageing, due to a high level of humidity and this could lead to yellowing. This may be the reason why the comparable ageing test with continuous irradiation (Xe ageing) did not cause the same amount of discolouration. Additionally, soiling was responsible for an increase in the b* value up to 3.2 ± 1.0 after 21 months of natural weathering. Further exposure time led to a decrease for which a phase of rain could be responsible. This “cleaning phase” can be observed for all naturally weathered samples, independent of the material.

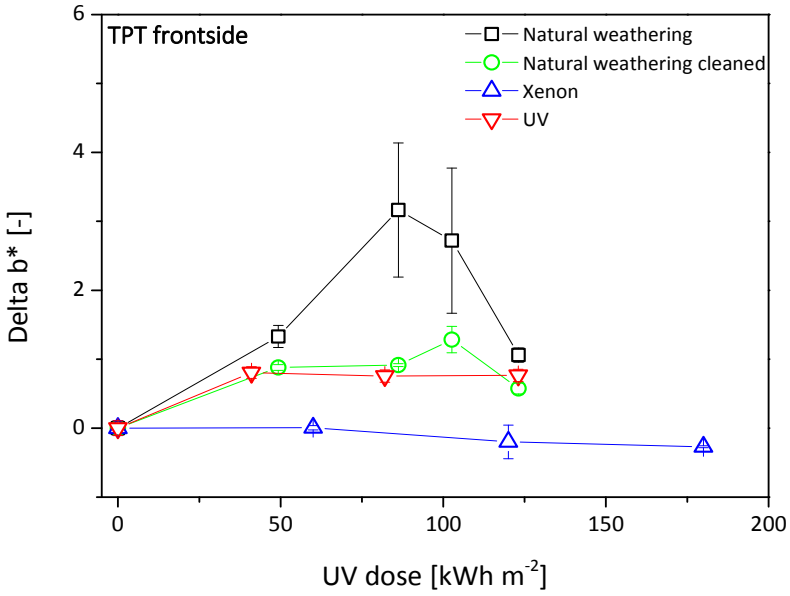

Figure 3.4. Delta of the colour value b for aged TPT front side.*

Polyolefin-based front layers showed a different behaviour compared to the other material classes, which can be seen in Figure 3.5. This material class exhibited the largest changes in colour. Artificial ageing caused an increase of the b* value for all ageing types up to a value of 4.7 ± 3.0 after 3000 h of UV ageing. Compared to the quite stable fluoropolymer front sides, polyolefins are more prone to photo-degradation, which would explain the discolouration also after Xe ageing [35]. However, it is the only material which exhibited a comparable amount of discolouration after natural and artificial ageing. Besides the change in colour, cracks were observed across the machine direction on the surface beginning after 1000 h of UV and Xe ageing and after 30 months of natural weathering for PPE 1 and PPE 2, respectively. Cracks and delamination in backsheets are the worst failures, because it allows enhanced water vapour and oxygen ingress leading to a higher level of hydrolysis in the polyester core layers and oxidation [4, 42]. Responsible for the surface cracking is the UV irradiation, which induced an embrittlement of the surface polyolefin layer [43]. Cracks can lead to loss in isolation properties and is a severe safety problem. In addition water vapour in a PV module can cause potential induced degradation (PID), corrosion of metal and cell parts and can enhance the degradation of encapsulants, which drastically reduce the performance and the lifetime of a PV module [4, 44, 45]. Pictures of PPE 1 samples are exemplarily shown in Figure 3.6, where the development of discolouration and cracks can be seen. UV aged samples showed the most significant yellowing and a large number of cracks after 3000 h (123 kWh m^{-2}). Lin et al. already showed that humidity in combination with UV light plays a synergistic effect on surface

erosion of PPE backsheets [43]. The UV ageing consisted of dark condensation cycles which enhanced this chemical degradation process and influenced the surface roughness.

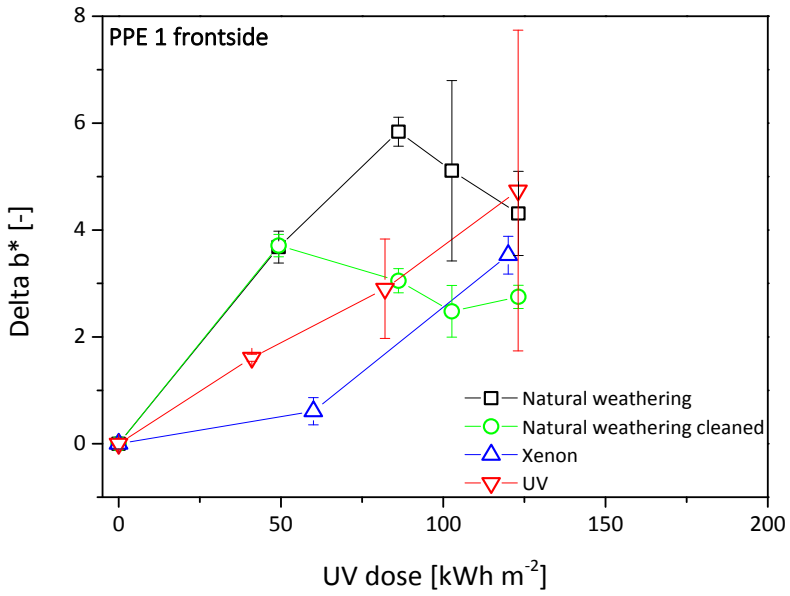

Figure 3.5. Delta of the colour value b for aged PPE 1 front side.*

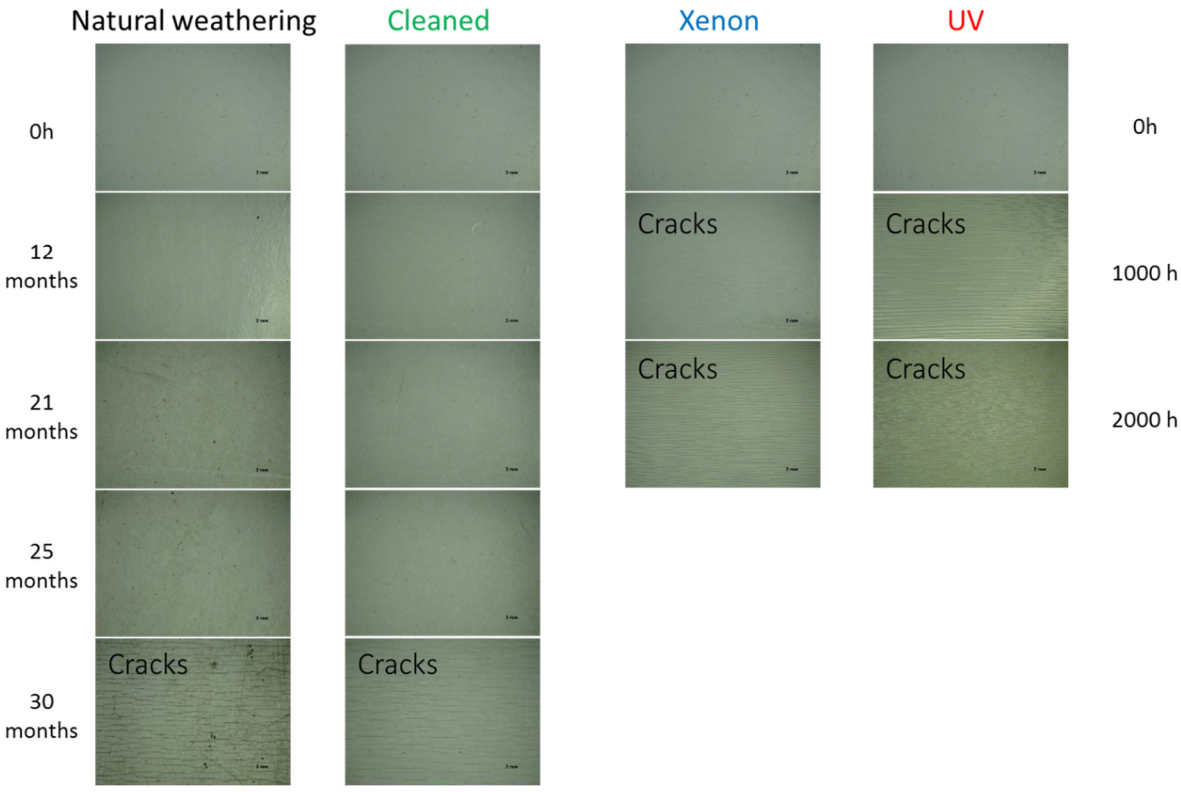

Figure 3.6. Microscope pictures of aged PPE 1 front sides.

THV was the only backsheet which behaved differently compared to all other samples – after a certain amount of ageing time the EVA front layer delaminated. Figure 3.7 shows the microscopy pictures of aged THV samples. Additionally, UV ageing seemed to cause different and more severe ageing mechanisms of the EVA layer, which burned onto the PET layer. This happened although the ageing test was conducted in accordance to the standard [31]. Nevertheless, the energy input was too high for this material.

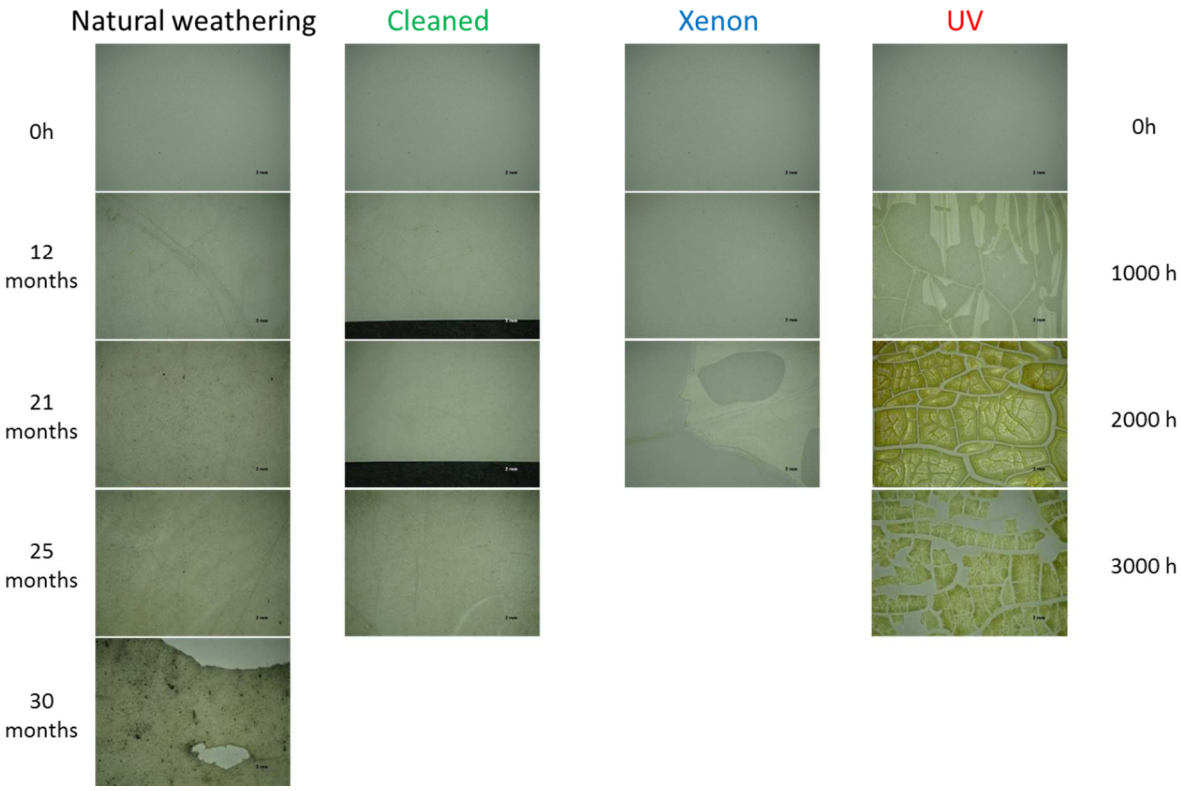

Figure 3.7. Microscope pictures of aged THV front sides.

The back side of all backsheets showed no significant changes in the reflectance spectra. A smaller amount of discolouration could be observed compared to the front sides, see Table 3.4. This might be due to the fact that the intensity of the reflected and scattered light was too low to cause an amount of degradation leading to discoloration, independent of the material class. Wypych already showed that the reflected or scattered light is dependent on the albedo and it highly varies with the underground material and wavelength of the light [29]. Another influence could be the device design, such as the position and the design of the sample holders, etc. in the artificial ageing devices.

Table 3.4. Material class and belonging backsheets for outer layer (back side).

Material class outer layer	Backsheet	Δ b*
PA	AAA, APA	< 1.0
Fluoropolymers	TPT, KPK, THV	< 0.5
PET	PPE 1, PPE 2	< 1.0

In general Xe aged samples showed no similarity in the development of b* compared to the natural aged samples, except for polyolefin front sides. The fluoropolymer and polyolefin-based front sides which were UV aged exhibited approximately the same amount of yellowness as the natural ones. The test and cycle design influenced the ageing behaviour of the materials – UV ageing included a dark condensation phase whereas the samples were continuously irradiated during Xe ageing. However, the main degradation mechanism (hydrolysis, photo-degradation, etc.) of the material played an important role on the effectiveness of the artificial ageing test.

In order to characterise the changes in chemical structure on the surface due to photo-oxidation processes, IR spectra were recorded and are shown in Figure 3.8 for the front side of AAA. Typical bands of PA were found at 2919, 2850 and 1465 cm^{-1} for the CH_2 vibration and at 3288 cm^{-1} and 1553 cm^{-1} for the CN and NH vibration, respectively. The absorption peak at 1638 cm^{-1} was caused by the carboxyl (C=O) and amide group [46–50]. Ageing related changes for PA-based front layers were found in the area between 1300 and 1000 cm^{-1} possibly caused by soiling after natural weathering, which was confirmed as the cleaned sample did not show these changes anymore. Only Xe aged samples exhibited differences in the region from 1300 to 1000 cm^{-1} compared to the unaged one. As soiling can be excluded, these peaks correspond to skeletal motions or so called fingerprint region and indicate structural changes [49, 51]. The photo-oxidation process of PA starts with the formation of hydro-peroxides at the carbon atom close to the nitrogen atom and is the general process of the formation of radicals for polymers [35, 52]. This process leads to the formation of amide and carboxyl end groups [35]. However, in this research an increase in intensities in the corresponding absorbance bands could not be observed.

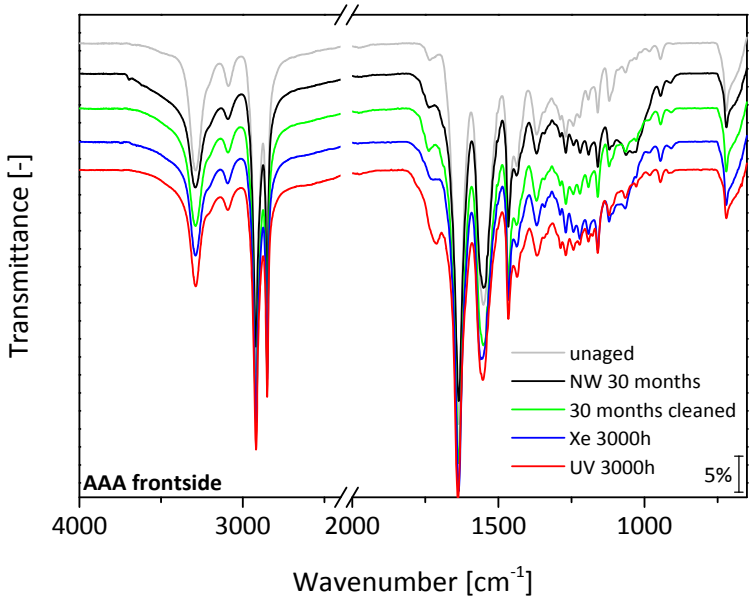

Figure 3.8. IR spectra of aged AAA.

Fluoropolymer front layers exhibited no significant changes in IR spectra, which corresponded well to the low amount of discolouration characterised via UV/Vis/NIR spectroscopy. Reasons for that are that the fluorine atom has a high bonding energy which makes it very rare to re-bond with other atoms. Additionally, fluorine atoms are bigger than hydrogen atoms and surround the carbon chain like a protective shell, which is responsible for a high physical and chemical resistance [35, 53].

Polyolefin-based front layers exhibited significant absorbance bands of polyethylene with additional ketone and ester groups, see Figure 3.9. The absorbance at 2916, 2849, 1471, 1370 and 717 cm^{-1} corresponds to the stretching and deformation vibrations of CH_2 [50, 51]. Carboxyl groups were responsible for the peak at 1735 cm^{-1}. The peaks at 1241 and 1021 cm^{-1} were caused by the ester vibration of C(=O)O and C-O groups and deformation of the methylene unit, respectively [51]. This indicates that a certain amount of EVA might be mixed in the polyolefin layer. Ageing caused changes in the carboxyl area at around 1730 cm^{-1} due to the formation of ketone and lactone carbonyl groups and esters [51, 54, 55]. Additional peaks at 1713 and 1171 cm^{-1} were detected for all ageing types, which was induced by oxidation processes [51, 54, 55]. Both artificially weathering tests caused absorption at 1413 cm^{-1}. UV aged PPE 1 additionally exhibited a peak at 1169 cm^{-1} and a shoulder at 1462 cm^{-1}. Differences between the uncleaned and cleaned naturally weathered samples were caused by soiling. This can be seen in the decrease of the peak at around 1000 cm^{-1}. Ageing in general caused an increase at 3399 cm^{-1} which corresponds to OH vibration [51]. Altogether the aged spectra exhibited a significant degree of oxidation, but the artificial ageing tests

on the front sides could not cause the same change in the chemical structure in the material analysed by IR spectroscopy as the natural weathering did.

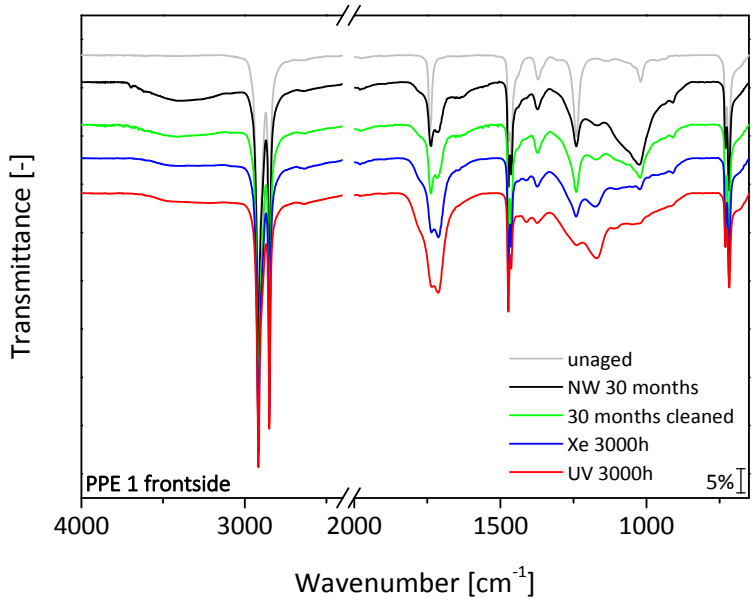

Figure 3.9. IR spectra of aged PPE 1.

All PA-, fluoropolymer- and PET-based back sides of the samples showed no significant changes in the chemical structure via IR spectroscopy after weathering. For AAA, soiling could also be detected at the naturally aged back side, due to a coarser surface structure. The only exception was THV, where two distinct peaks at 2918 and 2850 cm^{-1} (vibrations of CH_2) and an additional one at 1737 cm^{-1} were detected for the 2000 h Xe aged samples. The last corresponds to the carboxyl group and indicates oxidation processes [56]. However, if changes were visible due to ageing, artificial ageing could not cause the same behaviour in the optical properties of all backsheets.

DMA measurements were conducted in order to validate the changes in the thermo-mechanical behaviour due to ageing. As the mechanical stability is mainly determined by the thickest layer of the multilayer films – the core layer – it is a good method to analyse the influence of degradation on this layer. In Table 3.5 the material class and the accompanying backsheets are listed. Concerning the storage modulus no significant changes could be observed due to ageing.

Table 3.5. Material class and belonging backsheets for core layer.

Material class core layer	Backsheet
PA	AAA
PET	APA, TPT, KPK, THV, PPE 1, PPE 2

An advantage of the DMA is the fact that it is more sensitive for the detection of transition temperatures compared to thermal analysis via DSC [57]. In the case of multilayer backsheets it is possible to individually analyse the glass transition temperatures (T_G) of each layer if the two temperatures are not at a similar temperature and within the measured range. The glass transition temperature is important because the physical properties of the polymer changes drastically due to the fact that the material goes from a hard glassy to a rubbery state. Therefore it defines the end of the operating range over which the thermoplastic, amorphous polymer should be used [57]. In the case of a semi-crystalline PV module backsheet where strength and a certain amount of stiffness are required for the core layer, this temperature needs also to be considered, as the use above T_G can also enhance ageing processes. In general T_G is the temperature where the chains in the amorphous parts begin to coordinate large-scale motions. Therefore the amorphous parts are responsible for T_G [57]. Changes in the transition temperature can be traced back to changes in free volume, which is influenced by e. g. chemical structure, molar mass, ageing [57]. Figure 3.10 shows the T_G of the PET layer of KPK exemplarily for all PET core layers. As photo-oxidation was not the main degradation mechanism for the core layer, but probably thermo-oxidation and hydrolysis processes were, the time axis was used for the comparability of the different ageing types. After ageing – independent of the type – a decrease in T_G could be observed. For the PET layer in KPK the reduction of the value was around 1°C after 30 months of natural weathering, 4°C after 3000 h UV ageing, and around 8°C after 3000 h Xe ageing, respectively. The decrease in temperature implied an increase of molecular mobility after ageing, which was the highest for Xe aged samples [58]. This behaviour was observed for all PET core layers and is in contrast to existing research work where the T_G is increased due to post-crystallisation and/or reduction of the free volume during ageing, as well as relaxation processes [35, 58, 59]. In general it can be stated that the degree of crystallinity influences the T_G of PET – an increase of the degree of crystallinity leads to an increase in T_G for crystallinity values below 30% [59]. An increase was only observed for all fluoropolymer outer layers (TPT and KPK). The T_G of PA core layers were not significantly influenced by ageing, whether when PA was used as outside nor as core layer. As already shown in the optical results THV delaminated and it was not possible to analyse it via DMA. According to the DMA results, no significant distinction by the type of ageing could be found based only on the material class of the core layer. This means that artificially and naturally aged samples exhibited similar changes verified by DMA.

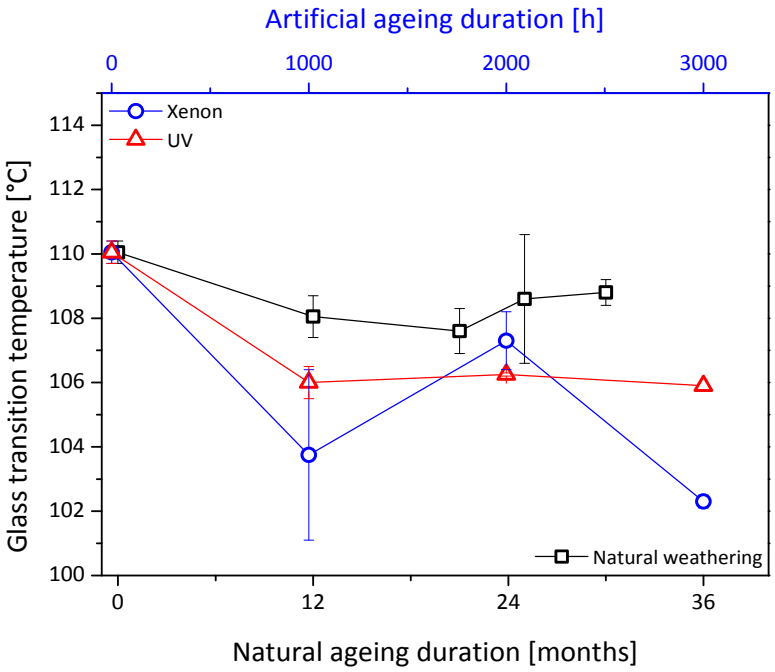

Figure 3.10. Glass transition temperature of the PET layer of KPK.

Due to tensile mode and the relatively low melting temperature of the polyolefin layers of PPE 1 and PPE 2, the temperature range for these backsheets was limited to 100°C as the upper limit. Up to this temperature no transition temperature was visible. Therefore the onset temperature of the melting of the polyolefin layer was analysed, see Figure 3.11. This onset temperature relates to the temperature values of the melting of the DSC experiments for the polyolefin layer. Only UV ageing caused an increase of around 14°C after 3000 h. Xe ageing did not lead to significant changes, nor did natural weathering up to 25 months. Additional 5 months of natural weathering led to a decrease of around 4°C. The increase in melting onset temperature indicated the formation of bigger and more perfect crystalline regions with a possible higher lamella thickness due to ageing [38, 60]. Unfortunately, it gives no information about the core layer. The ageing effect of artificial and natural weathering showed differences concerning thermo-mechanical properties.

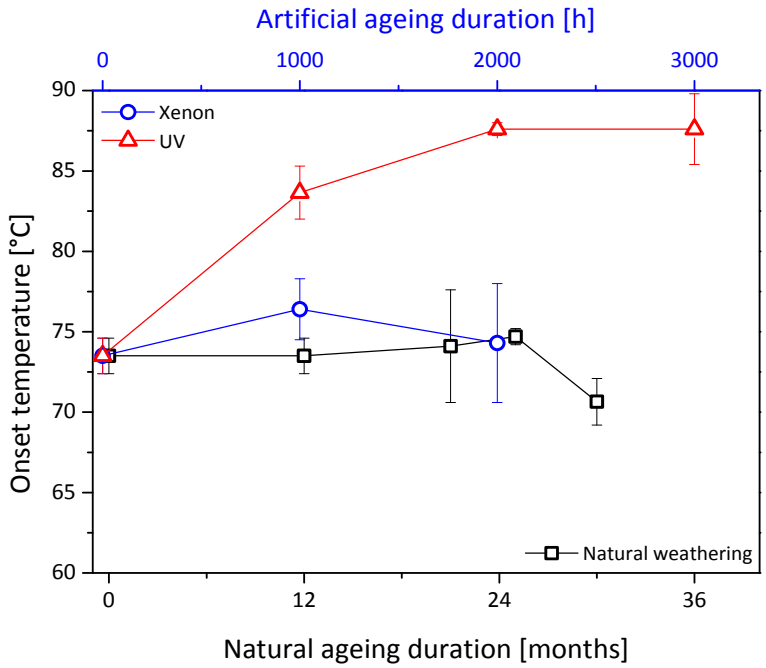

Figure 3.11. Onset temperature of PPE 2.

Thermal analysis via DSC showed no significant changes in the melting behaviour for all core layers of the multilayer films, which means no changes in melting temperature or enthalpy except for TPT. Foulc et al. stated that two coexistent phenomena may affect the crystallinity and therefore also the mechanical properties [61]: on the one hand the preferred decrease of the amorphous fraction during ageing results in an increase in crystallinity of the remaining material. On the other hand crystalline lamellae can be also partially attacked by hydrolysis inducing a decrease of crystallinity [61]. However, according to literature this should go along with a decrease in melting temperature, assigning either a decrease of lamellar thickness or a change in amorphous-crystal surface energy, which was not observed for all materials [61]. TPT was the only material which showed a different behaviour compared to the other PET-based materials. The melting enthalpy of the PET layer of TPT increased by around 20 J g^{-1} for the longest ageing durations (3000 h and 30 months, respectively), see Figure 3.12. This increase is equal to an increase in the degree of crystallinity because these values are proportional to each other. It is interesting that neither the storage modulus nor the T_G were influenced by the strong increase in the degree of crystallinity.

The THV back layer only showed an implied melting peak at around 150°C with an enthalpy of below 0.5 J g^{-1}. This fluoropolymer is a terpolymer of TFE, HFP and VDF and is highly amorphous due to the fact that VDF in combination with its other monomers disrupts the high crystallinity which is typical of PVDF homo polymer [62, 63].

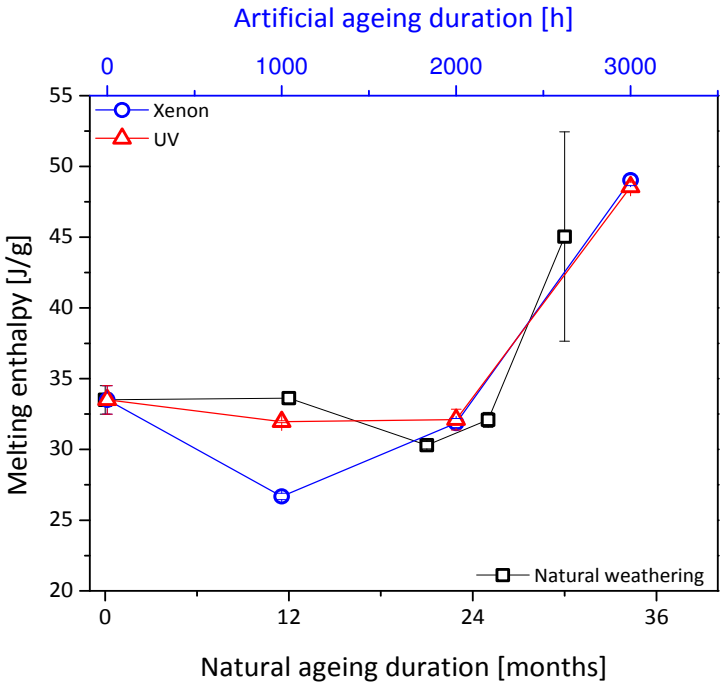

Figure 3.12. Melting enthalpy of the PET layer of TPT.

In contrast to the melting behaviour, significant signs of chemical degradation via chain scission could be observed in the cooling behaviour for all PA, PET and polyolefin materials independent of the type of layer (front, core or back side). An indicator for the molar mass is the crystallisation temperature, see Figure 3.13 for example [60]. A decrease in molar mass can cause an increase in the crystallisation temperature. The reason is that shorter chains lead to an increase of the amount of chain ends and they can act as a nucleating agent, which cause an increased solidification [4, 60, 64]. Unfortunately, no statement of a specific trend of the different test types could be made, since this was not observable within one material class, even though the crystallisation temperature increased after all ageing types.

Interestingly, a disappearance of the crystallisation peak was observed for the PVF layer of TPT after ageing in the cooling run, see Figure 3.14. The degree of crystallinity is controlled by a varying number of parameters, such as molecular weight, polymerisation method, thermal history and cooling rates [38, 65, 66]. Obviously, ageing prevented the crystallisation of PVF, except in the case of 12 months of natural weathering [67].

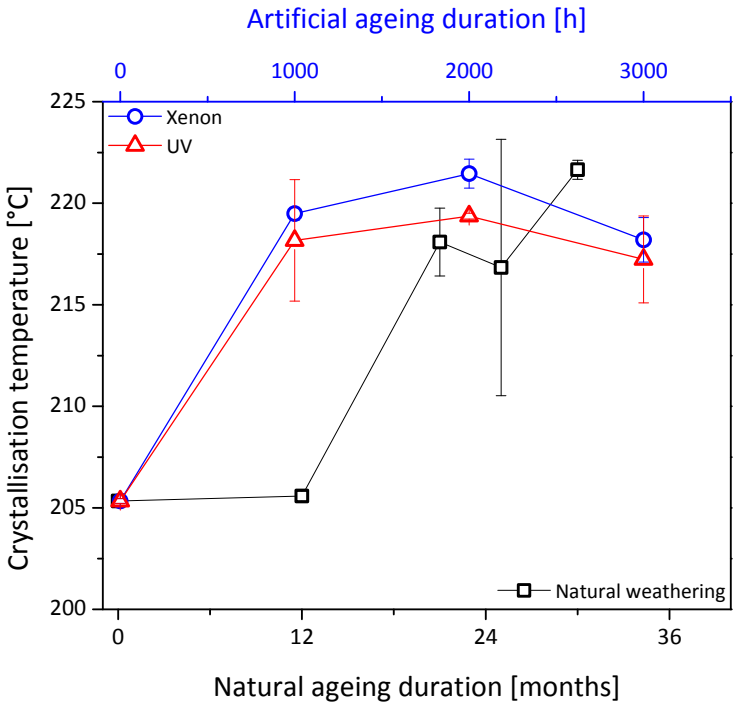

Figure 3.13. Crystallisation temperature of the PET layer of TPT.

Tensile tests also provided an understanding of the changes in the core layer, as the core layer is responsible for the mechanical stability due to its greater thickness. In general all backsheet materials showed a similar behaviour – a ductile behaviour with a yield point could be observed, see Figure 3.15. Before reaching the yield point, intermolecular forces work against the deformation. The yield point is the point at which plastic deformation starts. Further load leads to an increase in stress, as the polymer chains are fully oriented in load direction. This causes the absorption of the load by the main valence bonds. Therefore the strain at break value is a good indicator for chemical degradation via hydrolysis, due to the fact that it depends on the polymer chain length as well as on the resulting entanglements [4, 14, 67, 68].

After ageing a typical behaviour for polymers could be seen for all backsheets, namely that the materials became brittle with an increase in yield stress, see again Figure 3.15. This is an indicator for physical ageing processes, such as post-crystallisation and decrease in free volume and is well known in the literature [4, 14, 35]. Probably a reduction in the free volume was responsible for the increase in yield stress, as no significant increase in the melting enthalpy could be detected to demonstrate post-crystallisation. After a further increase of the ageing duration for UV ageing up to 2000 and 3000 h the materials became even more brittle and they broke without reaching a yield point at very low strain values. This indicates that especially UV ageing caused a higher amount of chain scission via hydrolysis in the materials, than Xe or natural ageing. This can be explained by the

different test designs of UV and Xe ageing. UV ageing includes a dark phase for condensation, which is not the case for Xe ageing. The differences in yield stress between natural, Xe and UV ageing could not been detected via the crystallisation temperature of the PET core layer in the DSC studies, where the values increased for UV and Xe aged samples at the same amount. A reason can be the multilayer construction which has an effect in mechanical testing. This effect makes tensile tests more sensitive for differences caused by different ageing types.

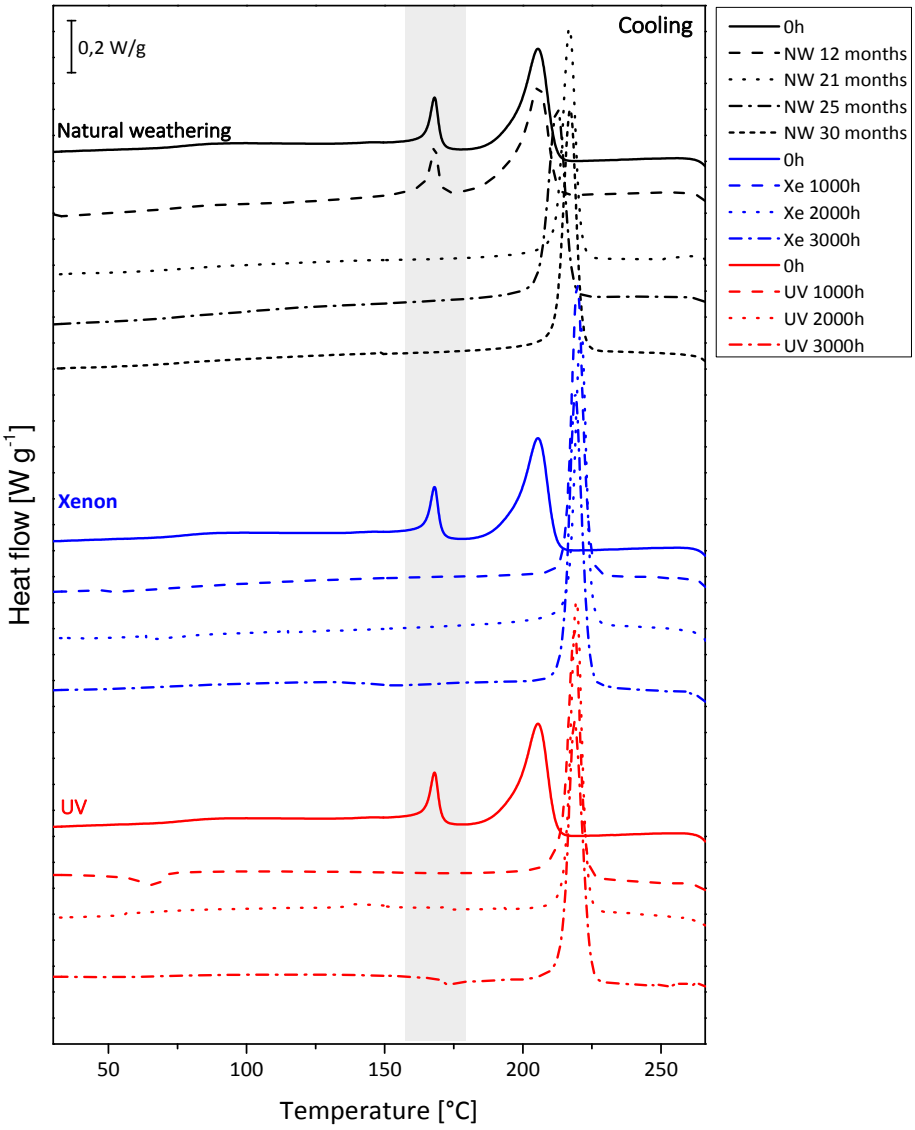

Figure 3.14. Thermograms of the cooling of TPT.

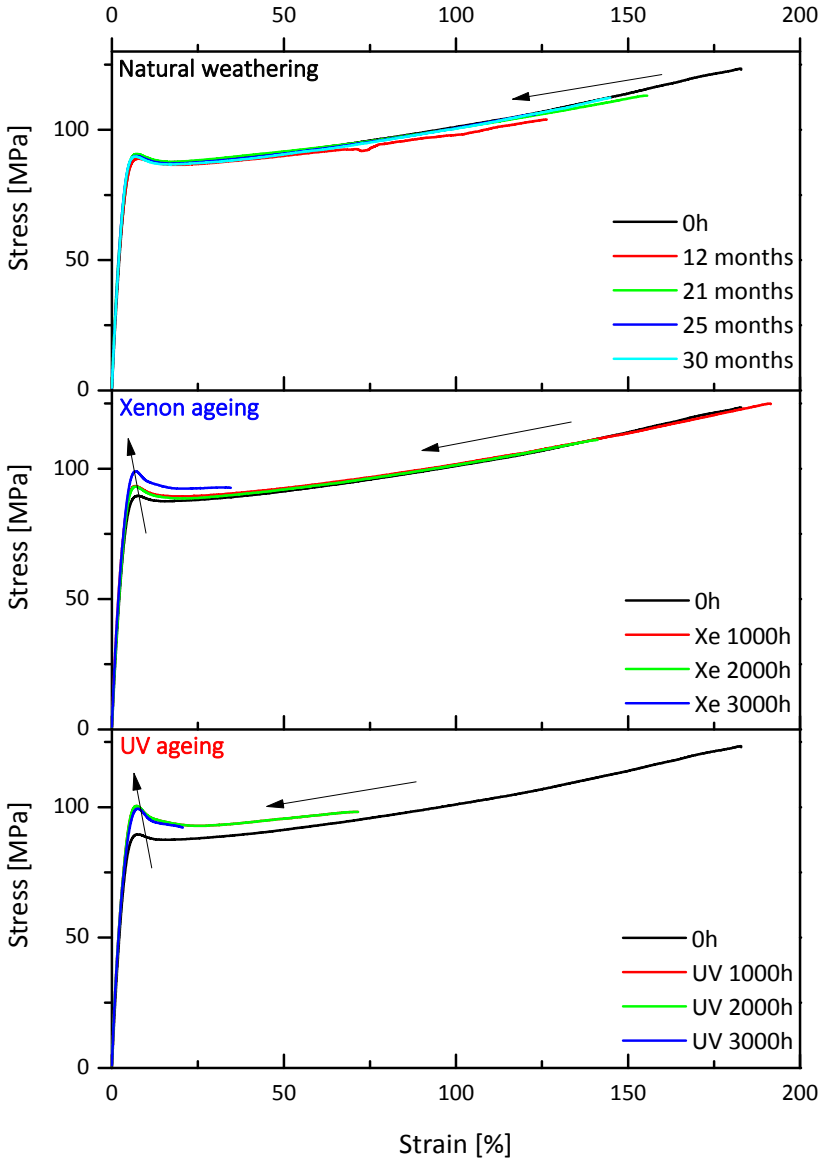

Figure 3.15. Stress-strain curves of aged KPK.

The PA-based backsheet (AAA) showed no changes in Young's modulus or yield stress which are indicators for physical ageing processes, such as post-crystallisation. However, the material exhibited an almost linear decrease in strain at break to a minimum of 85% which was similar for all weathering types. In contrast to that, the PET-based backsheets (APA, TPT, KPK, THV, PPE 1 and PPE 2) showed differences depending on the type of ageing. UV ageing seemed to be more severe concerning mechanical properties than natural or Xe ageing, see Figure 3.16. The value for the strain at break decreased already after 2000 h of UV ageing to a value below 5% indicating a strong decrease in molar mass due to chemical degradation processes, such as hydrolysis. Pickett and

Coyle stated that only 1-2% of the units need to be hydrolysed in order to lead to a significant embrittlement of the polymer [37]. The material became brittle and no yield stress was detectable. All PET-based backsheets showed a similar development of the strain at break value. This does not correlate to the crystallisation temperature, which increased almost independently of the ageing type. Changes in Young's modulus or in yield stress were not observable for APA, KPK and THV.

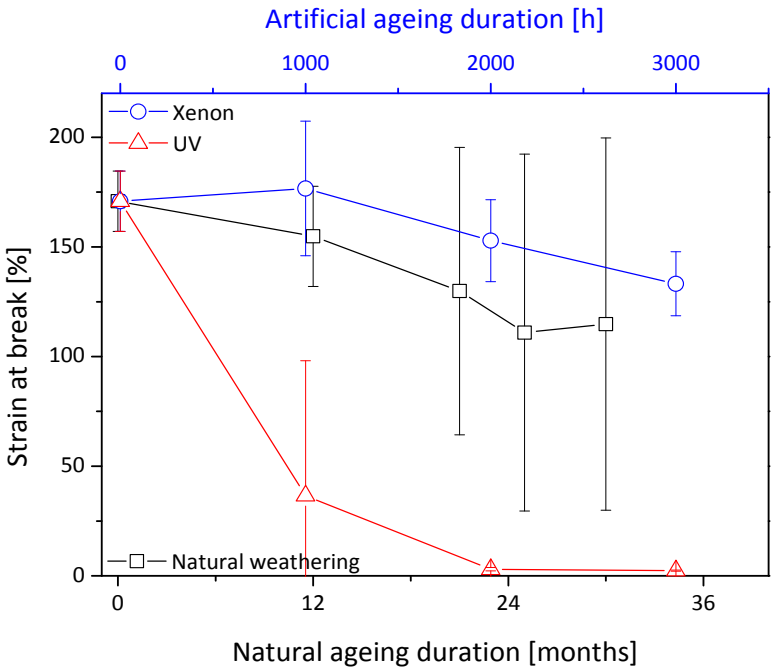

Figure 3.16. Strain at break value of aged APA.

TPT mechanically behaved differently compared to the other PET-based materials, like the thermal behaviour. It showed, in addition to the changes in strain at break, also changes in Young's modulus and yield stress, see Figure 3.17 and Figure 3.18, respectively. The Young's modulus decreased from an original value of 3200 MPa to around 2900 MPa and remained constant after 1000 h and 12 months, respectively. This indicates a decrease in melting enthalpy (crystallinity), an increase in free volume and relaxation processes, respectively. Due to processing via extrusion the molecular chains are oriented in machine direction. The cooling step after processing can freeze this high level of orientation and the material is not in its equilibrium state. Ageing can reduce the degree of orientation because of relaxation processes. A reduction in melting enthalpy was only observed for the 1000 h Xe aged samples. However, the maximum ageing duration of 3000 h and 30 months, respectively, caused a strong increase in melting enthalpy and therefore in crystallinity which could obviously not influence the Young's modulus.

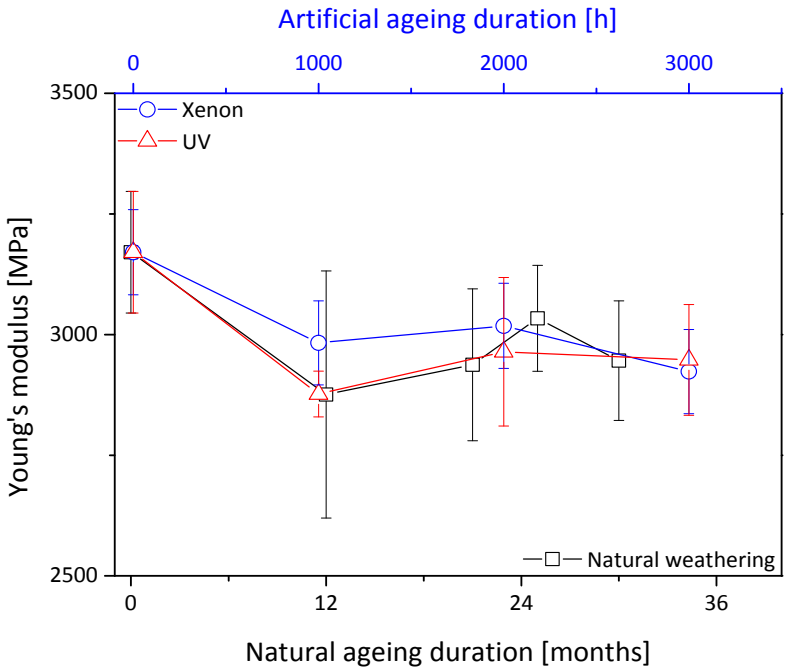

Figure 3.17. Young's modulus of aged TPT.

The mechanical properties of all backsheets showed a different degree of deterioration depending on the type of weathering. UV ageing caused a stronger decrease in the strain at break values, indicating a more severe chemical degradation of the material than natural or Xe ageing. A reason may be the test design which included a dark condensation phase, whereas during Xe ageing the samples were continuously irradiated.

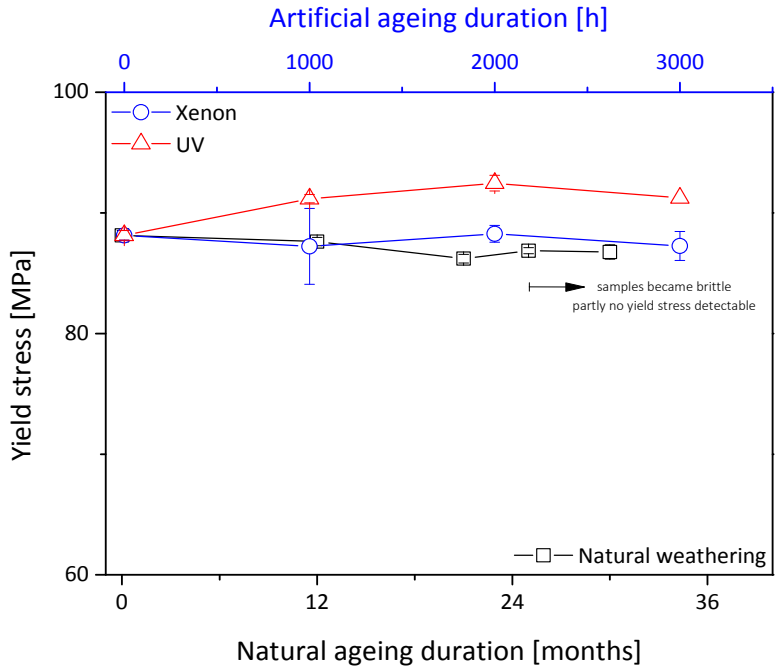

Figure 3.18. Yield stress of aged TPT.

3.4. Summary and conclusion

The main focus of this part was to evaluate the effect of artificial and natural ageing on multilayer backsheet films for PV modules. For this reason different backsheet films were naturally and artificially aged. Subsequently the optical, thermal, thermo-mechanical and mechanical properties were characterised.

Significant differences in the ageing behaviour of backsheet materials were found, depending on the type of backsheet and on the type of ageing. Water absorption tests showed no significant changes after drying for any of the materials. The colour value b* was chosen as representative indicator for ageing, due to its direct relation to yellowness. The results of the b* value of Xe aged samples showed different behaviour compared to the naturally aged ones. Only UV aged PA-based backsheets exhibited similar behaviour compared to the naturally aged samples. Thermal analysis revealed a significant increase of the crystallisation temperature which is an indicator for chain scission, probably via hydrolysis. Even though only minor optical changes could be detected, major deterioration in mechanical properties were observed. The backsheets became brittle and the strain at break value decreased for all materials. However, modulus or yield point changes could not been observed, except for TPT. UV ageing showed similar changes in the optical properties, whereas Xe ageing led to comparable deterioration of the mechanical properties to natural weathering. Even though degradation by photo-oxidation is mainly located on the side of the backsheet exposed to UV radiation, it is not the main factor causing a failure of backsheets.

It could be shown that with natural and artificial ageing tests different degradation results were achieved. Natural weathering in Leoben was not as harmful as the standardised artificial ageing tests. Probably longer exposure times in natural weathering would cause a further decrease in properties. However, the ageing mechanisms were different. A reason for the different behaviour of artificial ageing tests compared to natural weathering may be the different test designs. During Xe weathering the samples were continuously irradiated, whereas UV ageing tests exhibited light and dark cycles. The dark cycles are condensation phases during UV ageing, which allow humidity to ingress into the backsheet and therefore can cause a higher amount of degradation due to hydrolysis of the inner PA or PET layer. These results are especially interesting as Xe testing is usually taken as environmental simulation and UV ageing only as an accelerated ageing method. The main degradation mechanism (hydrolysis, photo-degradation, etc.) of the material has to be taken into account when designing effective artificial ageing tests. Xe and UV testing need to be adapted to adequately address backsheet performance in the outdoor environment in order to insure durability.

3.5. References

[1] REN21. 2016. *Renewables 2016*. *Global status report*.

[2] Li, H., Kikuchi, R., Kumagai, M., Amano, T., Tang, H., Lin, J.-M., Fujiwara, K., and Ogawa, N. 2012. Nondestructive estimation of strength deterioration in photovoltaic backsheets using a portable near infrared spectrometer. *Solar Energy Materials and Solar Cells* 101, 0, 166–169.

[3] Schultz, O., Glunz, S. W., and Willeke, G. P. 2004. SHORT COMMUNICATION. ACCELERATED PUBLICATION: Multicrystalline silicon solar cells exceeding 20% efficiency. *Prog. Photovolt: Res. Appl.* 12, 7, 553–558.

[4] Knausz, M., Oreski, G., Eder, G. C., Voronko, Y., Duscher, B., Koch, T., Pinter, G., and Berger, K. A. 2015. Degradation of photovoltaic backsheets: Comparison of the aging induced changes on module and component level. *J. Appl. Polym. Sci.* 132, 42093, 1–8.

[5] Fu, O., Hu, H., Gambogi, W. J., Kopchick, J. G., Felder, T., Babak, H., Alex, B., Yushi, H., and John, T. Understanding backsheet durability through field studies and accelerated stress testing. In *SNEC 2014*.

[6] Jorgensen, G. J., K. M. Terwilliger, J. A. DelCueto, S. H. Glick, M. D. Kempe, J. W. Pankow, F. J. Pern, and T. J. McMahon. 2006. Moisture transport, adhesion, and corrosion protection of PV module packaging materials. *Solar Energy Materials & Solar Cells* 90, 2739–2775.

[7] Oreski, G., Wallner, G. M., and Lang, R. W. 2009. Ageing characterization of commercial ethylene copolymer greenhouse films by analytical and mechanical methods. *Biosystems Engineering* 103, 4, 489–496.

[8] Liu, F., Jiang, L., and Yang, S. 2014. Ultra-violet degradation behavior of polymeric backsheets for photovoltaic modules. *Solar Energy* 108, 0, 88–100.

[9] IEA Task 13. 2014. *Degradation Behaviour of PV Modules under Different Accelerated Stress Conditions Based on Stress Conditions Evaluated from Real-time Outdoor Testing*. *Report IEA-PVPS T13-04:2014 Degradation Behaviour of PV Modules under Different Accelerated Stress Conditions Based on Stress Conditions Evaluated from Real-time Outdoor Testing*.

[10] Kim, N., Kang, H., Hwang, K.-J., Han, C., Hong, W. S., Kim, D., Lyu, E., and Kim, H. 2014. Study on the degradation of different types of backsheets used in PV module under accelerated conditions. *Solar Energy Materials and Solar Cells* 120, 543–548.

[11] Namsu Kim, Seoungsoo Lee, Xing Guan Zhao, Dajung Kim, Chulmin Oh, and Hanjun Kang. 2016. Reflection and durability study of different types of backsheets and their impact on c-Si 5PV6 module performance. *Solar Energy Materials and Solar Cells* 146, 91–98.

[12] Lewandowski, S., Rejsek-Riba, V., Bernès, A., Perraud, S., and Lacabanne, C. 2016. Influence of the environment during a photodegradation of multilayer films. *J. Appl. Polym. Sci.* 133, 41, 51.

[13] Michael D. Kempe. 2006. Modeling of rates of moisture ingress into photovoltaic modules. *Solar Energy Materials and Solar Cells* 90, 16, 2720–2738.

[14] Oreski, G. and Wallner, G. M. 2005. Aging mechanisms of polymeric films for PV encapsulation. *Solar Energy* 79, 6, 612–617.

[15] Peike, C., Hülsmann, P., Blüml, M., Schmid, P., Weiß, K.-A., and Köhl, M. 2012. Impact of Permeation Properties and Backsheet-Encapsulant Interactions on the Reliability of PV Modules. *ISRN Renewable Energy* 2012, 1–4, 1–5.

[16] Gambogi, W., Fu, O., Bradley, A., Stika, K. M., Hamzavy, B., Smith, R., and Sample, T. 2012. *The Impact of Materials Properties on PV Module Performance and Durability*. 27th European Photovoltaic Solar Energy Conference and Exhibition.

[17] Gambogi, W. J. Comparative Performance of Backsheets for Photovoltaic Modules. In *25th European Photovoltaic Solar Energy Conference and Exhibition, Valencia, Spain, 2010*, 4079–4083.

[18] Gambogi, W. J., Heta, Y., Hashimoto, K., Kopchick, J. G., Felder, T., MacMaster, S. W., Bradley, A., Hamzavytehrany, B., Garreau-Iles, L., Aoki, T., Stika, K. M., Trout, T. J., and Sample, T. 2014. A Comparison of Key PV Backsheet and Module Performance from Fielded Module Exposures and Accelerated Tests. *IEEE J. Photovoltaics* 4, 3, 935–941.

[19] Gambogi, W. J., Kopchick, J. G., Felder, T. C., MacMaster, S. W., Bradley, A. Z., Hamzavy, B., Kathmann, E. E., Stika, T. J., Trout, T. J., Garreau-Iles, L. G., and Sample, T. Backsheet and Module Durability and Performance and Comparison of Accelerated Testing to Long Term Fielded Modules. In *28th European Photovoltaic Solar Energy Conference and Exhibition, Paris, France, 2013*.

[20] Kim, W. G. and Lee, J. Y. 2002. Contributions of the network structure to the cure kinetics of epoxy resin systems according to the change of hardeners. *Polymer,* 43, 5713–5722.

[21] Oreski, G. and Wallner, G. M. 2005. Delamination behaviour of multi-layer films for PV encapsulation. *Solar Energy Materials and Solar Cells* 89, 2-3, 139–151.

[22] Ryu, C.-M., Pang, B.-L., Kim, H.-I., Kim, K.-M., Lee, S.-W., Kim, H.-J., and Park, J.-W. 2013. Effect of side chain on wettability and adhesion performance of acrylic pressure-sensitive adhesives on thin silicon wafer. *Journal of Adhesion Science and Technology* 27, 10, 1136–1145.

[23] Voronko, Y., Eder, G., Chernev, B., Knausz, M., Oreski, G., Koch, T., and Berger, K. Analytical Evaluation of the Ageing Induced Changes of the Adhesive within Photovoltaic Backsheets. In *28th European Photovoltaic Solar Energy Conference and Exhibition, Paris, France, 2013*.

[24] Voronko, Y., Eder, G. C., Knausz, M., Oreski, G., Koch, T., and Berger, K. 2015. Correlation of the loss in photovoltaic module performance with the aging behaviour of the backsheets used. *submitted to Progress in Photovoltaics: Research and Applications*.

[25] Voronko, Y., Eder, G. C., Knausz, M., Oreski, G., Koch, T., and Berger, K. A. Influence of environmental factors on the ageing behaviour of photovoltaic backsheets. In *European Weathering Symposium, Bratislava, Slowakei, 2013*.

[26] Voronko, Y., Eder, G. C., Knausz, M., Oreski, G., Koch, T., and Berger, K. A. 2015. Correlation of the loss in photovoltaic module performance with the ageing behaviour of the backsheets used. *Prog. Photovolt: Res. Appl.* 23, 11, 1501–1515.

[27] Kusato Hirota. 2012. *Backsheet reliability test according to IEC61730-1 Ed.2 Draft*.

[28] Gambogi, W. J., Yushi, H., Kopchick, J. G., Felder, T., MacMaster, S. W., Bradley, A. Z., Hamzavytehrany, B., Yu, B.-L., Stika, K. M., Trout, J. T., Garreau-Iles, L., Fu, O., and Hu, H. Assessment of PV Module Durability Using Accelerated and Outdoor Performance Analysis and Comparisons. In *40th IEEE Photovoltaic Specialists Conference, Denver, USA, 2014*.

[29] Wypych, G. 2008. *Handbook of material weathering*. Chem Tec Publ, Toronto.

[30] DIN, Normausschuss Kunststoffe (FNK). *DIN EN ISO 4892-2 - Kunststoffe - Künstliches Bestrahlen oder Bewittern in Geräten: Teil 2: Xenonbogenlampen,* 4892-2.

[31] International Organisation for Standardisation, ISO 4892-3. 2006. *Kunststoffe - Künstliches Bestrahlen oder Bewittern in Geräten Teil 3 Fluoreszenzlampen: Part 3: Fluorescent UV lamps,* 4892-3.

[32] Oreski, G. and Pinter, G., Eds. 2013. *Aging Characterization of Multi-Layer Films Used as Photovoltaic Module Backsheets*. 28th European Photovoltaic Solar Energy Conference and Exhibition; 3050-3054 4AV.4.13.

[33] International Organisation for Standardisation, ISO 11357-3. 1999. *Plastics - Differential scanning calorimetry (DSC) Part 3: Determination of temperature and enthalpy of melting and crystallization,* 11357-3.

[34] International Organisation for Standardisation, ISO 527-3. 1995. *Plastics - Determination of tensile properties: Part 3: Test conditions for films and sheets,* 527-3.

[35] Ehrenstein, G. W. and Pongratz, S. 2007. *Beständigkeit von Kunststoffen*. Carl Hanser Verlag, Munich.

[36] Launay, A., Thominette, F., and Verdu, J. 1994. Hydrolysis of poly(ethylene terephthalate). A kinetic study. *Polymer Degradation and Stability* 46, 3, 319–324.

[37] Pickett, J. E. and Coyle, D. J. 2013. Hydrolysis kinetics of condensation polymers under humidity aging conditions. *Polymer Degradation and Stability* 98, 7, 1311–1320.

[38] Ehrenstein, G. W., Riedel, G., and Trawiel, P. 2004. *Thermal analysis of plastics*. *Theory and practice*. Carl Hanser Verlag, Munich.

[39] Wallner, G. M., Geretschläger, K. J., Dankl, M., and Hinersteiner, I. Aging Behavior of Polyamide Based Backsheet Films. In *28th European Photovoltaic Solar Energy Conference and Exhibition, Paris, France, 2013*.

[40] Beißmann, S., Stiftinger, M., Grabmayer, K., Wallner, G., Nitsche, D., and Buchberger, W. 2013. Monitoring the degradation of stabilization systems in polypropylene during accelerated aging tests by liquid chromatography combined with atmospheric pressure chemical ionization mass spectrometry. *Polymer Degradation and Stability* 98, 9, 1655–1661.

[41] Klaus J. Geretschläger, Gernot M. Wallner, and Jörg Fischer. 2016. Structure and basic properties of photovoltaic module backsheet films. *Solar Energy Materials and Solar Cells* 144, 451–456.

[42] Tracy, J., Bosco, N., Novoa, F., and Dauskardt, R. 2017. Encapsulation and backsheet adhesion metrology for photovoltaic modules. *Prog. Photovolt: Res. Appl.* 25, 1, 87–96.

[43] Lin, C.-C., Lyu, Y., Hunston, D. L., Kim, J. H., Wan, K.-T., Stanley, D. L., and Gu, X., Eds. 2015. *Cracking and delamination behaviors of photovoltaic backsheet after accelerated laboratory weathering* 9563. SPIE.

[44] Reid, C., Ferrigan, S. A., Martinez, J. I., and Woods, J. T. Contribution of PV Encapsulant Composition to Reduction of Potential Induced Degradation (PID) of Crystalline Silicon PV Cells. In *28th European Photovoltaic Solar Energy Conference and Exhibition, Paris, France, 2013*.

[45] Stollwerck, G., Schoeppel, W., Graichen, A., Jaeger, C., and Kollesch, M. Polyolefin Backsheet Protects Solar Modules for a Life Time. In *28th European Photovoltaic Solar Energy Conference and Exhibition, Paris, France, 2013*.

[46] Chernev, B. S. and Eder, G. C. 2011. Spectroscopic Characterization of the oligomeric surface structures on polyamide Materials formed during accelerated aging. *Applied Spectroscopy* 10, 65.

[47] Ishikawa, T. and Nagai, S. 1980. Effect on casting conditions on polymorphism of nylon-12. *Journal of Polymer Science,* 18, 291–299.

[48] Ogunniran, E. S., Sadiku, R., Sinha Ray, S., and Luruli, N. 2012. Morphology and Thermal Properties of Compatibilized PA12/PP Blends with Boehmite Alumina Nanofiller Inclusions. *Macromol. Mater. Eng.* 297, 7, 627–638.

[49] Rhee, S. and White, J. L. 2002. Crystal Structure and Morphology of biaxially oriented polamide 12 films. *Journal of Polymer Science: Part B: Polymer Physics* 40, 1189–1200.

[50] Verleye, G. A. L., Roeges, N. P. G., and De Moor, M. O. 2001. *Easy Identification of Plastics and Rubbers*. Rapra Technology, Shawbury.

[51] Günzler, H. and Heise, M. H. 1996. *IR-Spektroskopie*. *Eine Einführung*.

[52] Pieter Gijsman, Guido Meijers, and Giacomo Vitarelli. 1999. Comparsion of the UV-degradation chemistry of polypropylene, polyethylene, polyamide 6 and polybutylene terephthalate. *Polymer Degradation and Stability,* 65, 433–441.

[53] Krebs, C., Leu, K. W., and Krebs-Avondet-Leu, Eds. 1999. *Langzeitverhalten von Thermoplasten*. *Alterungsverhalten und Chemikalienbeständigkeit*. Hanser, München.

[54] Grabmayer, K., Wallner, G. M., Beißmann, S., Braun, U., Steffen, R., Nitsche, D., Röder, B., Buchberger, W., and Lang, R. W. 2014. Accelerated aging of polyethylene materials at high oxygen pressure characterized by photoluminescence spectroscopy and established aging characterization methods. *Polymer Degradation and Stability* 109, 40–49.

[55] Jin, J., Chen, S., and Zhang, J. 2010. UV aging behaviour of ethylene-vinyl acetate copolymers (EVA) with different vinyl acetate contents. *Polymer Degradation and Stability* 95, 5, 725–732.

[56] Senna, M., Aly, H., Ali, Z., and El-Naggar, A. 2001. Structure-property behaviour of electron beam irradiated polytetrafluoroethylene and polytetrafluoroethylene-co-hexafluoropropylene. *Polymer Degradation and Stability,* 71, 53–60.

[57] Menard, K. P. 2002. Dynamic Mechanical Analysis. In *Encyclopedia of Polymer Science and Technology*. John Wiley & Sons, Inc. DOI=10.1002/0471440264.pst102.

[58] Hagihara, H., Oishi, A., Funabashi, M., Kunioka, M., and Suda, H. 2014. Free-volume hole size evaluated by positron annihilation lifetime spectroscopy in the amorphous part of poly(ethylene terephthalate) degraded by a weathering test. *Polymer Degradation and Stability* 110, 389–394.

[59] Dong, W., Zhao, J., Li, C., Guo, M., Zhao, D., and Fan, Q. 2002. Study of the amorphous phase in semicrystalline poly(ethylene terephthalate) via dynamic mechanical thermal analysis. *Polymer Bulletin* 49, 2-3, 197–203.

[60] Frick, A. and Stern, C. 2006. *DSC-Prüfung in der Anwendung*. Carl Hanser Verlag, Munich.

[61] Foulc, M., Bergeret, A., Ferry, L., Ienny, P., and Crespy, A. 2005. Study of hygrothermal ageing of glass fibre reinforced PET composites. *Polymer Degradation and Stability* 89, 3, 461–470.

[62] Hirschmann, B., Oreski, G., and Pinter, G. 2014. Thermo-mechanical characterisation of fluoropolymer films for concentrated solar thermal applications. *Solar Energy Materials and Solar Cells* 130, 615–622.

[63] Scheirs, J. 1997. *Modern fluoropolymers*. *High performance polymers for diverse applications*. Wiley series in polymer science. Wiley, Chichester, New York.

[64] Ottersböck, B., Oreski, G., and Pinter, G. 2017. Comparison of different microclimate effects on the aging behavior of encapsulation materials used in photovoltaic modules. *Polymer Degradation and Stability*.

[65] Elkordy, A. A., Ed. 2013. *Applications of Calorimetry in a Wide Context - Differential Scanning Calorimetry, Isothermal Titration Calorimetry and Microcalorimetry*. InTech.

[66] Liu, J., Lu, X., and Wu, C. 2013. Effect of Preparation Methods on Crystallization Behavior and Tensile Strength of Poly(vinylidene fluoride) Membranes. *Membranes* 3, 4, 389–405.

[67] Oreski, G. 2004. *Untersuchung des Delaminationsverhaltens von Folienverbunden für die Einkapselung von PV-Modulen*. Master thesis, Montanuniversität Leoben.

[68] Grellmann, W. and Seidler, S. 1998. *Deformation und Bruchverhalten von Kunststoffen*. VDI-Buch. Springer.

4. Ultra-accelerated ageing of polymeric multilayer films

This chapter focuses on the influence of weathering types on polymer degradation. Special emphasis was given on the ultra-acceleration of artificial ageing. A feasibility study was conducted in order to verify whether climate chamber ageing can be correlated with ultra-accelerated pressure cooker ageing for polyethylene terephthalate (PET)-based photovoltaic (PV) backsheets. These both tests are state of the art in the PV industry, however, research work on the correlation of these tests has not been conducted yet. This work is published in the Journal of Applied Polymer Science 133 (2016), 47, 44230, with the title “Correlation study of damp heat and pressure cooker testing on backsheets”.

4.1. Introduction to ultra-accelerated ageing of polymeric multilayer films

Considerable research and progress have been made in the development of PV modules and the incorporated components to increase the reliability and service life. This benefits the market growth of renewable energy directly generated by the sun [1, 2]. To collect radiant flux cheaply by PV modules, relatively high module lifetimes are necessary. For PV modules high product standards are required and, as a result, module lifetimes of 20 years and more are guaranteed with a limited loss in functionality of the component. Weathering stability is the key factor for the reliability of PV modules. The main critical parts concerning degradation are polymeric materials used as protective frontsheet, sealant, encapsulation and backsheet in a module [1, 3–7].

There are different approaches to test the lifetime of a PV module. One option is to test the performance of the whole PV module. This is not only the most expensive option, but also requires the most effort. Testing on the material and component level, however, is less costly, has simplified sample preparation and more testing options. In the case of encapsulations, the advantages of testing film samples are merely applicability, pre-selection or process improvements. The reason is that some interactions like reaction rates, interdependency, ageing mechanisms, etc. of the components can hardly be reproduced. But for backsheets consisting of polyester, Knausz et al. already showed that differences in material properties, whether the backsheet is aged as a single film or incorporated within a PV module, are negligible if the microclimate is comparable [8]. Due to the different installation situation of the backsheet compared to the encapsulation fewer degradation cases occur in combination with other PV module components, which makes the single film testing of PET-based backsheets suitable. This is an advantage especially for fast material testing.

Backsheets in general have to provide mechanical stability and electrical insulation and should act as a protection against weathering and as a selective barrier for atmospheric gases, such as water vapour, oxygen, acetic acid, etc. [5]. Thus, the type and therefore the different degradation behaviour of a backsheet component highly affects the long-term stability of the whole PV module [1, 3–5, 8–11]. Generally multilayer laminates are utilised as backsheets. In many standard backsheets PET is used as the core layer to offer mechanical stability and sufficient electrical insulation [1, 8]. The core layer is used in combination with protective outer layers, e.g. fluoropolymers, polyamides (PA), highly stabilised PET or other polymeric materials. The loss of functionality of the core layer can result in delamination of the backsheet, decreased or insufficient electrical insulation properties or critical changes in permeation properties and subsequently can lead to the breakdown of the whole module. Consequently the ageing behaviour of the core layer is crucial for the lifetime of a backsheet and therefore for the whole PV module during its intended life of more than 20 years [8, 12, 13].

For the investigation of the ageing behaviour and its influence on the material properties in a reasonable period, accelerated ageing tests were conducted. In the case of polycondensates as core layer in backsheets, like PET or PA, hydrolysis is the dominating ageing factor [5, 12–15]. The activation energy for thermal degradation is on average 197 kJ mol^{-1} [16]. By comparison, the value is lower for hydrolysis, around 136 kJ mol^{-1}, depending on temperature and humidity level [17]. Looney et al. showed that the activation energy is even lower at around 111 kJ kg^{-1} mol^{-1} for PET hydrolysis [12]. This indicates that hydrolysis is dominating in all degradation cases, but with contributions from other reactions, like oxidative degradation, thermal esterification, etc. [12].

Polymers with functional groups like amides and esters such as in Polyesters, can degrade via hydrolysis under the presence of water und acids [18]. Ester bonds are susceptible to hydrolysis especially at elevated temperatures and moisture. The reaction leads to chain scission at the ester bond, which decreases the molecular weight [16]. Additionally the concentration of carboxyl end groups increases. However, the lower the value of carboxyl end groups in the origin material the higher the hydrolysis resistance as they support hydrolytic degradation [12, 16]. Anti-hydrolysis additives for polyesters can be based on carbodiimide (HN-C-NH) to chemically react with free moisture during processing and service and act as acid- and water scavengers, converting them into non-reactive urea structures [16]. Phenylenebisoxazonie (PBO) is as well an effective scavenger, it reacts with acid end groups and couples PET chains, thus increasing the polymer molecular weight [16].

In general hydrolysis leads to chain scission which results in embrittlement, but also physical ageing processes (e.g. post-crystallisation), which can lead to a loss in mechanical properties [5, 8, 19]. This can be simulated by hot and humid tests, like damp heat (DH) storage (85°C and 85% relative humidity (r. H.)). In the PV industry DH tests are often applied for up to 1000 h in order to evaluate the quality of backsheets of PV modules. DH testing is included in IEEE 1262 as a qualification test for up to 1000 h and also in the standard IEC 61215 and 61730 [20, 21]. However, as Looney et al. already stated, DH testing is not adequate to safely predict field lifetimes of PV modules, especially due to the fact that UV degradation is neglected [12]. Though, due to the shielding outer layers, like fluoropolymers, the core layer is protected to a certain degree. Furthermore the UV radiation on the backsheet is of minor importance compared to the stress of the frontsheet and depends on the location and on the type of mounting and ground [22, 23]. Additionally differences in the microclimate can cause different ageing behaviours.

Even though the DH test exhibits drawbacks, as stated above, it is a useful test to evaluate material quality and infant material failures, especially for materials which are sensitive to hydrolysis [7, 12]. This was also shown by Gambogi et al., Looney et al. and Gong et al. [7, 12, 24].

Usually DH testing for 2000 h and more is conducted in the PV industry. This equals approximately 3 months, which takes too long for a fast material pre-selection. A decrease in the development time of backsheets can be achieved by an increase of temperature, humidity and pressure. A saturated vapour pressurisation test or pressure cooker test (PCT), which is standardised (DIN EN 60749-33) and commonly used in the semiconductor and printed circuit boards (PCB) industry offers these specific environmental conditions [7]. PCT testing is already used for backsheets to evaluate weather resistance, in particular resistance to hydrolysis [12, 25, 26]. However, it has not been clarified if the ageing mechanisms and effects on the material properties are equal to DH test exposure. This is particularly because the PCT exposure is high above the glass transition temperature of PET (around 80°C), which is in contrast to DH exposure.

Hence the objective of this work was to investigate and to correlate the ageing behaviour of PET-based PV backsheets after exposure under DH and PCT conditions. Moreover a correlation between the results of the DH test and the further accelerated PCT was conducted.

4.2. Experimental procedure

A standard composite backsheet film, consisting of polyvinyl fluoride (PVF) and PET was investigated. The PVF layer was approximately 30 µm thick and the PET layer was approximately

200 µm thick. Samples were artificially aged under damp heat test conditions up to 2000 h and under pressure cooker test conditions up to 96 h, see Table 4.1.

Table 4.1. Ageing parameters.

Parameter	**Damp Heat Test (DH)**	**Pressure cooker test (PCT)**			
Temperature in °C	85	100	110	120	140
Rel. Humidity in % r. H.	85	100	100	100	100
Pressure in bar	Ambient	4	4	4	4
Duration in h	500 1000 2000	12 24 48	12 24 48	12 24 48 96	12 24

To analyse and verify differences in thermal, mechanical and chemical properties the ageing behaviour was investigated by differential scanning calorimetry (DSC), tensile tests and infrared (IR) spectroscopy. As already shown in the literature, PVF exhibited no significant changes after artificial weathering [14, 18]. Additionally the thickness of the PVF layer is about 14% of the PET layer. These were the reasons why only ageing results of PET will be discussed. Due to the targeted test duration of around 5 days (120 h) the relation of the two time abscissas was fixed in order to better compare the two test types (96 h of PCT equals 2000 h of DH testing).

Thermal analysis was used to characterise ageing effects on the morphology of the polymeric backsheet. The tests were performed using a Perkin Elmer DSC 4000 (Waltham, US). Indium and Zinc standards were used to do temperature and enthalpy calibration. Samples of around 10 mg were cut and put into 50 µl pans with perforated lids. Thermograms were recorded under nitrogen atmosphere from 25°C to 300°C. A heating rate of 10 K min^{-1} was chosen for a proper investigation of melting and crystallisation processes [27, 28]. In order to identify reversible (physical ageing effects) and irreversible (chemical ageing effects) processes, two heating runs and one cooling run were conducted. Peak temperatures and enthalpies were evaluated for the purpose of characterising ageing effects on the polymer morphology according to ISO 11357-3 [29]. For every evaluation at least two sample runs were evaluated.

Tensile tests on rectangular samples were carried out by using a Z010 testing machine (Zwick-Roell, Ulm, DE) according to EN ISO 527-3 [30]. All samples had a width of 15 mm, a gauge length of 50 mm and an overall sample length of 100 mm. The samples were cut after artificial ageing and tested in machine direction. The tests were conducted with a crosshead speed of 50 mm min^{-1}. Average values for elastic modulus and yield strength were deduced via force values and crosshead speed from a total of at least seven specimens for each test series.

In order to characterise the chemical structure and its changes after artificial ageing, IR measurements were conducted. IR analysis was carried out in attenuated total reflection (ATR) mode using a Spectrum GX FTIR spectrometer (Perkin Elmer, Waltham, US). The ATR unit contained a zinc selenide (ZnSe) crystal (Pike Technologies, Madison, US). The transmittance spectra were recorded between 4000 and 650 cm^{-1}. Each spectrum is an average of 12 spectra measured at a resolution of 4 cm^{-1}. For a better comparison all ATR spectra were normalised to 1408 cm^{-1} according to Urban, which corresponds to the ring in-plane deformation [31, 32].

4.3. Results and discussion

In the following section the results of the ageing tests are discussed. DSC is a versatile tool to determine physical ageing processes, like post-crystallisation. The melting enthalpy is directly proportional to the degree of crystallinity which is an indicator for ageing processes. But also chemical degradation, like chain scission, can be detected by DSC measurements [18, 27, 28]. An increase in melting enthalpy as well as a shift to higher melting temperatures can be a result of post-crystallisation. In contrast, chain scission due to hydrolysis results in a shift of the crystallisation temperature as well as in an increase of the crystallisation enthalpy [8, 27].

Figure 4.1 exemplarily shows thermograms (first heating, cooling and second heating) of an unaged and DH 2000 h aged sample. With increasing temperature the melting endotherms of the first heating were decreasing slightly. At about 192°C the curves resulted in a small endothermic peak, caused by the melting of the 30 µm thick PVF layer. The 200 µm thick PET layer melted at around 258°C. These values are according to literature [27]. No glass transitions and cold-crystallisation temperatures for PET could be observed which indicates a highly crystalline material [27]. In the crystallisation curves, the first crystallisation peak is attributed to PET (194°C) and the second to PVF (168°C). At the second heating run PVF showed a melting peak at 191°C and PET at 255°C. As mentioned before, PVF exhibited no significant ageing effects within the designated time. Distinctive changes in the initial melting and cooling behaviour of PET were observed after ageing – a significant increase of the melting enthalpy and crystallisation temperature could be observed during the first heating and cooling.

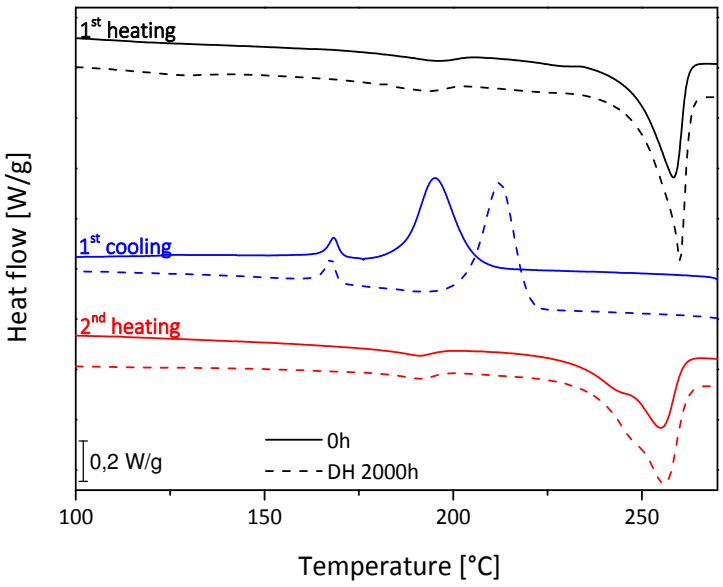

Figure 4.1. Thermograms of unaged and aged samples.

As PET is a polymer made via a condensation process under elimination of water, it is therefore sensitive to chain scission due to hydrolysis [18]. In general, polymers with functional groups like amides and esters can degrade via hydrolysis in the presence of water und acids [18]. However, as it is used as a PV backsheet material, it should be resistant to hydrolysis. This can be accomplished by increasing the degree of crystallinity by heat treatment as well as by addition of suitable stabilisers (nucleating agents). A higher degree of crystallinity is also desirable when PET is subjected to elevated temperatures [16].

In Figure 4.2 the PET melting enthalpies for all unaged and aged samples are depicted. In general with rising test duration the melting enthalpy increased. For the DH test samples the value increased from originally 38.9 J g^{-1} to 44.8 J g^{-1} after 2000 h. An increase in melting enthalpy can be caused by physical as well as chemical ageing processes. One obvious physical effect is post-crystallisation [18, 33]. Post-crystallisation takes place especially in imperfectly crystallised materials. In general semi-crystalline polymers, like PET, exhibit no crystalline equilibrium due to the process conditions of the industrial production. During artificial ageing changes in the physical structure may happen which lead to an increase of the degree of crystallinity and of the lamella thickness. Furthermore a refinement of the crystalline structure occurs, where amorphous molecules near the crystallite surface are attached to the crystallite regions. This process is accelerated with temperatures above the glass transition temperature (PET around 80°C), due to a

higher mobility of the molecular chains. As a result of the increased degree of crystallinity a higher melting enthalpy can be observed [18, 33].

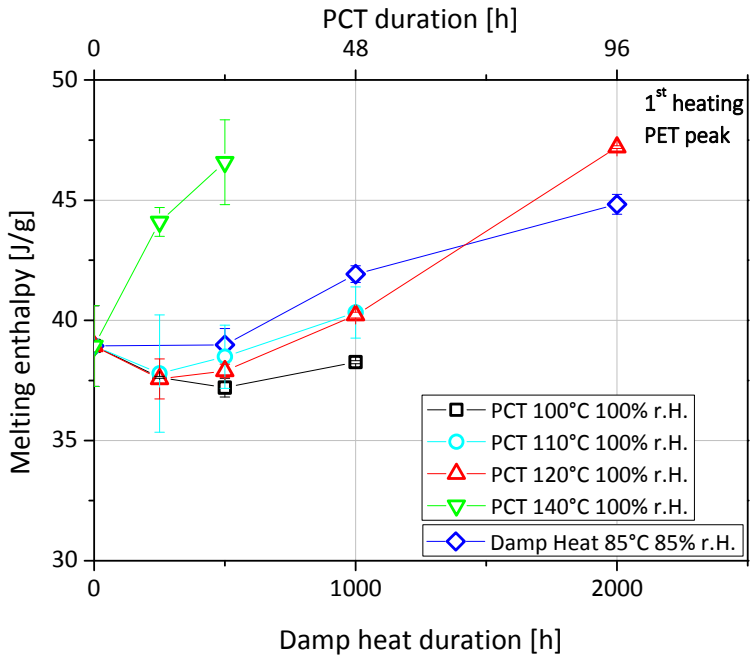

Figure 4.2. PET melting enthalpies.

PCT testing at temperature levels of 100°C, 110°C and 120°C showed no significant changes in melting enthalpy up to 24 h. With longer exposure times (>24 h) the melting enthalpy of 110°C and 120°C aged samples increased to values almost similar to the damp heat test. After 96 h of PCT exposure at 120°C the enthalpy showed a slightly higher value (47.2 J g^{-1}) than the damp heat 2000 h sample (44.8 J g^{-1}). In general it should be considered that enthalpies are not as precise as temperature values due to the fact that the whole weight of the multilayer film was used for calculation of the enthalpy which leads to larger uncertainty. Also differences in layer thicknesses highly influence the enthalpy results, which could not be excluded.

The samples aged under PCT conditions at 140°C exhibited the strongest melting enthalpy increase of 7.7 J g^{-1} to a value of 46.6 J g^{-1} after 24 h. Presumably, an ageing temperature of 140°C was too harsh for the material. Additionally, already after 24 h a strong embrittlement was observed. The degradation rate depends on the humidity level, the temperature and of course also on the morphology of the polymer and the degree of crystallinity. The polymeric chains in the amorphous phase were shortened and therefore exhibited a higher mobility. Short chains located next to lamella surfaces could attach themselves to the crystallite region. This so called chemo-crystallisation process occurs preferably under high molecular mobility – above glass transition temperature, which was the case in the conducted ageing tests [18, 34]. As a result the density can

change, like Planes et al. showed, and the melting enthalpy increased [35]. This led to the assumption that in the case of 140°C exposure, chemical ageing processes are more dominating than at exposures at lower temperatures (100-120°C).

In contrast to the melting enthalpy, the melting peak temperature was almost unaffected by different ageing conditions and durations. However, the crystallisation temperature of all aged samples increased after ageing, see Figure 4.3. In addition the higher the temperature level the higher was the crystallisation temperature. 100°C of PCT were probably too low to cause the same change in crystallisation temperature as DH – the crystallisation temperature increased to a value of 199°C after 48 h of exposure. PCT at 110°C showed good similarity up to 24 h compared to DH. After 48 h the value stagnated at around 201°C, which was 10°C below the crystallisation temperature of the DH test after 1000 h. PCT samples aged at 120°C showed almost similar behaviour to the damp heat test, with deviations of a maximum of 4°C of the mean value after 48 h of ageing. Samples aged at 140°C exhibited the strongest increase of the crystallisation temperature after artificial ageing – from a value of 194°C to 215°C after 24 h. As already described in the literature by Frick and Stern, the crystallisation temperature is affected by molar weight and therefore by chemical changes in the polymer [28]. The reason is that shorter chains, previously formed by chain scission, exhibited higher flow ability. This led to a higher mobility of the shorter chains and with it a better form energy of crystallites. This effect corroborated the previously stated assumption that the samples aged at 140°C showed dominating effects of chemical degradation (hydrolysis). Similar behaviour could be observed for the crystallisation enthalpy – higher exposure temperatures and longer exposure time led to a higher increase of crystallisation enthalpy. Nonetheless an Arrhenius plot of the crystallisation temperature revealed a linear behaviour – a constant activation energy, due to the fact that hydrolysis is the main ageing process which is detected by the crystallisation temperature.

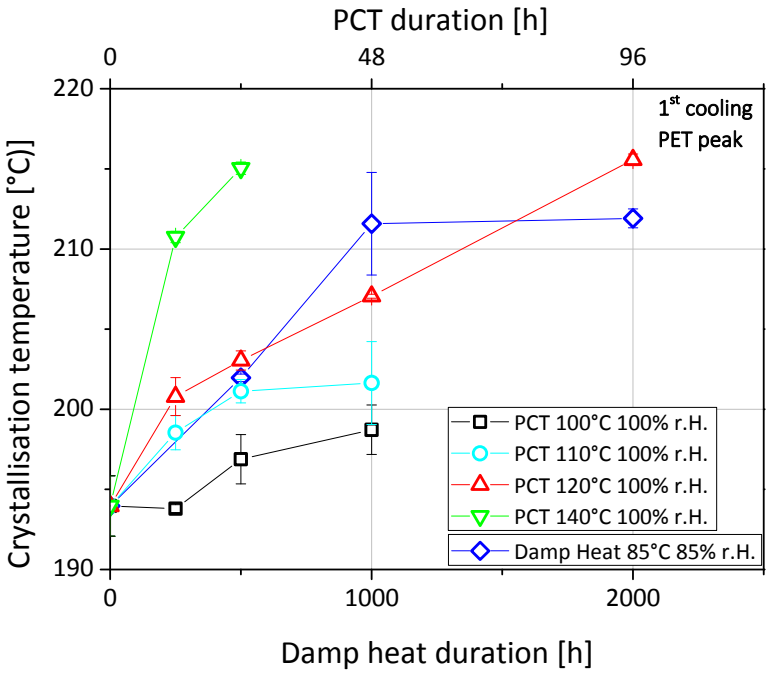

Figure 4.3. PET crystallisation temperatures.

For the purpose of analysing the influence of ageing on the mechanical behaviour, tensile tests were conducted. This was done in order to get information about physical and chemical ageing processes. Physical ageing processes, like post-crystallisation, are mainly visible before and in the yield region. Whereas for chemical ageing effects, like chain scission due to hydrolysis, the region of the breaking point can be used as an indicator [19, 33]. Unaged film samples exhibited ductile material behaviour with a pronounced yield point, see Figure 4.4. As the thickness ratio between the PET and the PVF layer is 200 to 30 µm, the mechanical behaviour is mainly defined by the thicker PET layer. Ageing at elevated temperatures and humidity caused an embrittlement, which led to a significant increase in yield stress and to a significant decrease in stress and strain at break, respectively. An increase in yield stress indicates physical ageing like post-crystallisation [13, 14, 19]. The effect of decreasing strain at break is well known in the literature and can be related to chemical ageing with chain scission and therefore to degradation via hydrolysis, which is supported by the increase of the crystallisation temperature and enthalpy over the ageing time [8, 14, 16].

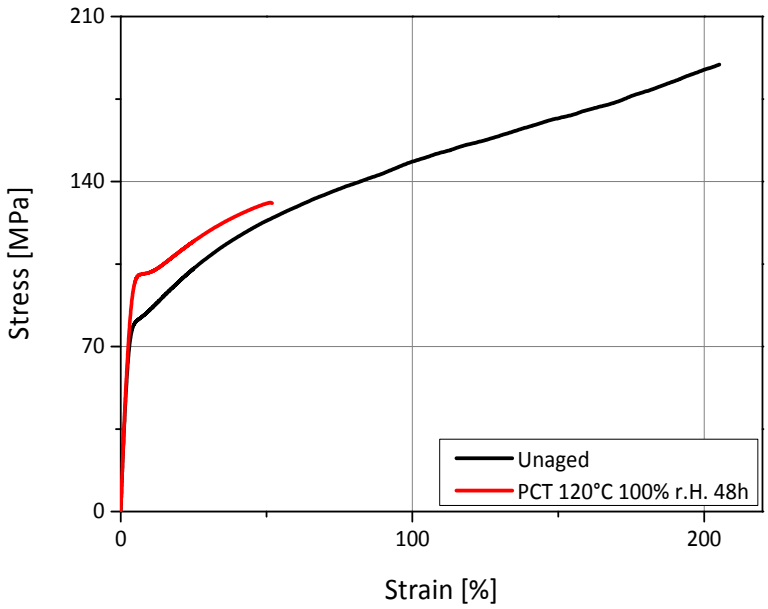

Figure 4.4. Stress-strain curves of an unaged and a PCT 120°C aged sample for 48 h.

In Figure 4.5 the yield stress over ageing duration is plotted. As Oreski et al. already showed, the yield stress is a good indicator for physical ageing processes because it is highly influenced by the degree of crystallinity [5]. With increasing DH ageing duration the yield stress value increased. This is in good accordance with the DSC results, where an increase in melting enthalpy due to post-crystallisation was detected. After 2000 h of DH testing the samples became brittle and failure occurred before reaching yield stress. The PCT samples at 100°C, 110°C, and 120°C showed similar behaviour – with increasing test time the yield stress increased from around 80 MPa to around 95 MPa after 48 h. Samples aged under 120°C for 96 h became brittle and showed a very low yield stress value at around 6.9 MPa. The PCT samples after 12 h at 140°C became too brittle and no yield stress could be detected. After 48 h at 140° PCT the samples became too brittle for mechanical testing. The yield stress results indicated dominating physical ageing processes at lower temperature levels up to 48 h and 1000 h. After longer exposure times (>48 h) chemical ageing processes seemed to be more dominating as the samples became very brittle. In general the yield stress value is a good indicator for ageing processes such as post-crystallisation [14]. However, it was not a suitable parameter to detect differences between PCT at 100°C, 110°C and 120°C.

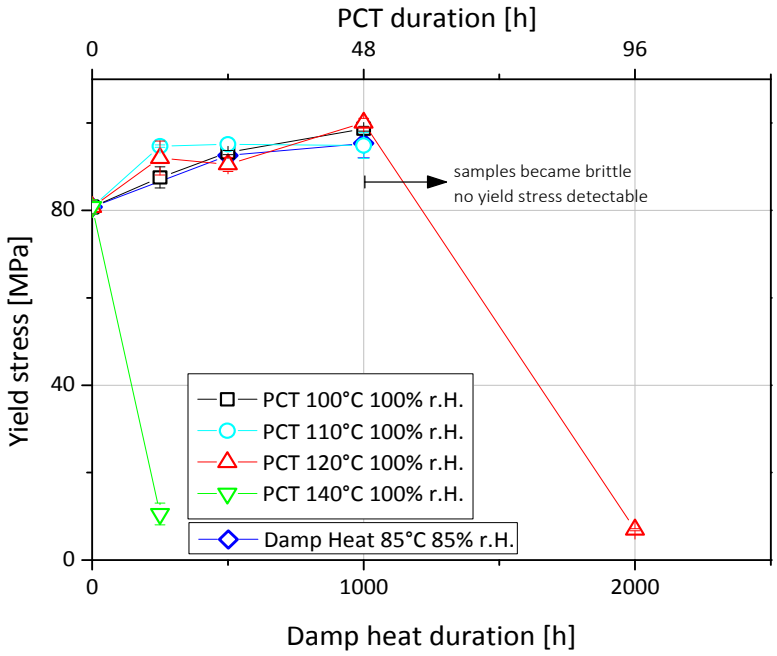

Figure 4.5. Yield stress of all samples.

A suitable and highly sensitive indicator for changes in molar mass is the strain at break value, see Figure 4.6. For that it is necessary to do the testing in the machine direction of the film, which is in contrast to the work of Kim et al. [26]. Polymers, especially films, show anisotropic behaviour, which is generally due to their production process (drawing-off after extrusion process). When testing polymer films in the machine direction a full orientation of the polymer chains in load direction occurs after passing the yield stress. The load gets absorbed via the main valence bonds of the molecular chains and no longer by intermolecular forces. Thus the polymer chain length and the resulting entanglements determine the elongation at break [13, 14, 36, 37]. Consequently the higher the molar mass the longer the chains and the more entanglements can be formed. Therefore chain scission via hydrolysis results in a decrease of elongation at break. If testing in the transverse direction, the load is mainly absorbed by intermolecular forces and not by the main valence bonds of the molecular chain [13, 14, 36, 37].

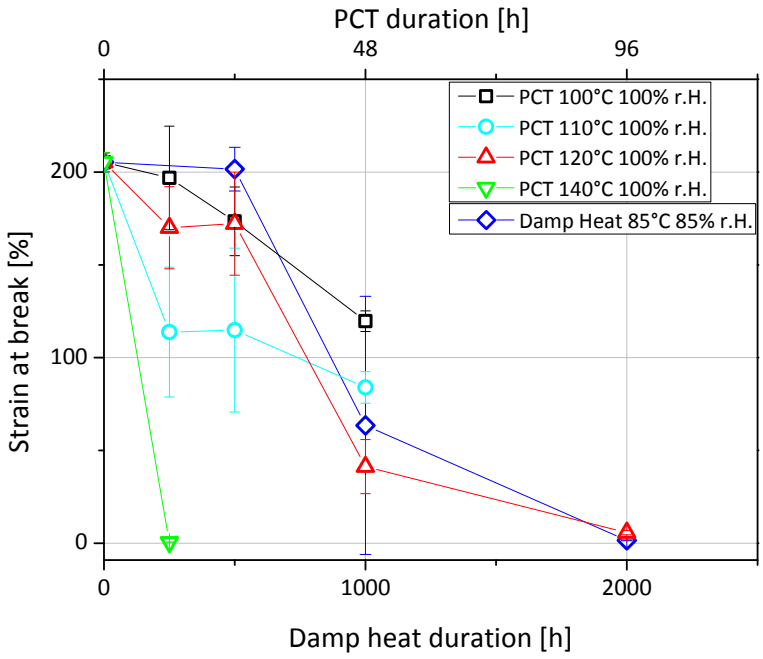

Figure 4.6. Strain at break values of all samples.

A relatively high standard deviation of the strain at break value for all samples was noticeable. The failure of a tensile sample is usually caused by a defect which induced a higher stress concentration (notching effect). A reason for the higher standard deviation could be the fact that the sample preparation was done after artificial ageing, which mechanically generated defects on the edges of the samples. But also different thickness distributions, enclosures, bubbles etc. can be initiators for defects [5, 8].

The damp heat test for 500 h caused no significant changes in the strain at break value (202%), which indicated that mainly physical ageing processes, like post-crystallisation had occurred. Whereas an exposure time of 1000 h led to a significant decrease of strain at break to a value of around 60%, which can be related to chemical ageing with chain scission and therefore to hydrolysis [14]. After 2000 h of damp heat testing the samples were brittle and broke with almost no plastic deformation. Pressure cooker tests at lower temperatures (100 and 110°C) showed slightly different curve progressions compared to the results of the damp heat test in respect to the desired test time. Results of samples aged at 120°C up to 96 h came very close to the damp heat results. Higher exposure temperatures (PCT at 140°C) led to a strong embrittlement of the samples. Chemical ageing processes, such as hydrolysis and chemo-crystallisation, might be more dominating in the case of higher exposure temperatures.

Despite the same order of magnitude of the elongation at break results of DH and PCT 120°C, the comparison of the original stress-strain curves of samples aged at PCT 120°C after 96 h revealed

differences, see Figure 4.7. The samples of DH 2000 h became brittle and broke with almost no plastic deformation at 40.3 MPa and 1.6%. In contrast to that the stress of the PCT 120°C 96 h samples levelled-off to around 8.5 MPa until failure occurred at around 5.8%. This and the fact that a yield stress at around 6.9 MPa could be detected, led to the assumption that the ageing mechanisms of PCT were different at 120°C after 96 h and in a DH test after 2000 h, respectively. Supposedly after DH ageing the PET layer could still contribute to the mechanical load. In contrast to that, the PET layer might be too degraded after PCT 120°C 96 h to contribute to the mechanical load. It appears that the mechanical behaviour is mainly affected by the PVF layer. The assumptions were supported by a slightly higher crystallisation temperature from the DSC results. Similar mechanical behaviour could be found for samples aged at PCT 140°C 12 h. Additionally, an Arrhenius calculation for stress at strain level showed also a non-linear behaviour, due to different ageing mechanisms. Different ageing mechanisms are reasonable as the DH test temperature with 85°C was around glass transition of PET, whereas all PCT experiments were conducted above glass transition temperature and with a higher humidity level than DH. As the purpose of this acceleration is to do a faster material quality test for PET-based backsheets than 2000 h of DH, the differences in degradation mechanisms should be acceptable.

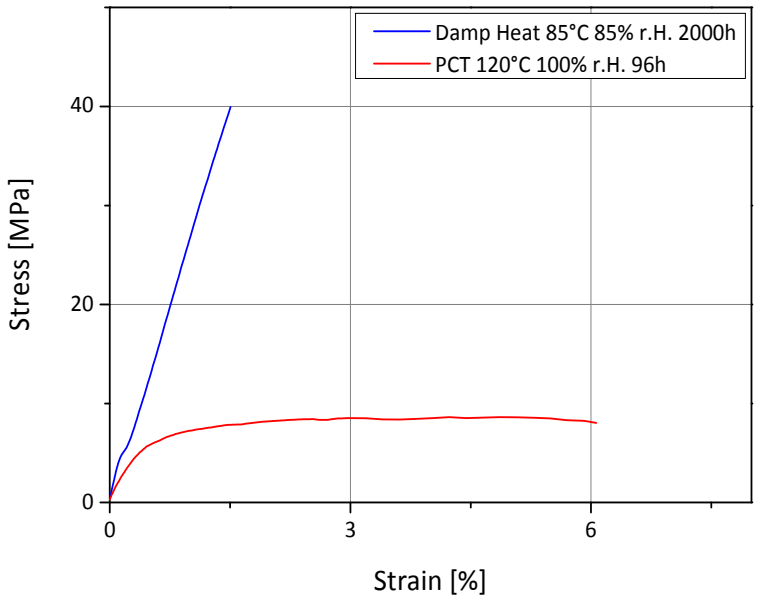

Figure 4.7. Stress-strain curves of a damp heat 2000 h aged sample and of a pressure cooker test 120°C 96 h aged sample.

In order to characterise chemical structure and its changes after artificial ageing, IR measurements were conducted. As an internal standard for normalisation of the spectra the absorbance peak

at 1408 cm^{-1} (in plane deformation of the aromatic ring) was used, as it is considered to be invariant with crystallinity, degree of orientation and ageing [38–40]. Typical spectra for PET were obtained for all samples, see Figure 4.8. Strong absorption bands could be detected in the region between 3000 and 2840 cm^{-1} which corresponds to C-H asymmetric and symmetric stretching vibrations. The peak at 1715 cm^{-1} is assigned to the carboxylic ester group (C=O). The absorption peaks in the region between 1600 and 1325 cm^{-1} were due to aromatic C-C stretching, while the band at 1240 cm^{-1} was caused by an overlap of the stretching of ester groups and the deformation of (=CH) groups. The absorption bands at 1096 cm^{-1} and 1118 cm^{-1} correspond to the stretching of O-C and the deformation of (=CH). The bands at 1017, 970 and 872 cm^{-1} as well were caused by deformation of the (=CH) group. Deformation of the aromatic ring structure caused the strong absorption band at 722 cm^{-1} [13, 14, 39, 41].

After accelerated ageing of the samples only few changes could be detected. Significant differences could be observed for DH 2000h and PCT 120°C 96 h samples compared to the virgin material: an increase of the intensity at 1712 cm^{-1} (C=O), 1683 cm^{-1} (terephthalic acid), 1240 cm^{-1} (ester, carboxyl), 1096 cm^{-1} (ester, carboxyl) as indicators for hydrolysis and an increase of a broad band between 3600 and 2500 cm^{-1}, which marks the deformation of OH groups in a network of hydrogen bonds also due to hydrolysis [24, 40]. Even though there were some changes in IR spectra, significant differences in test temperatures were hard to distinguish.

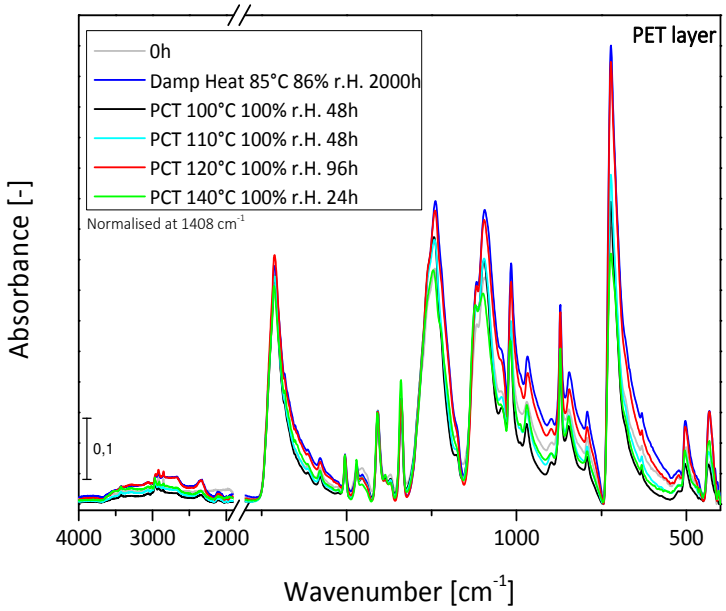

Figure 4.8. IR spectra of unaged and aged samples.

4.4. Summary and conclusion

The objective of this chapter was to investigate and correlate the ageing behaviour of PET-based PV backsheets after exposure under DH and PCT conditions. Moreover a correlation between the results of the DH test and the further accelerated PCT was conducted. For this reason thermal, mechanical and optical properties were characterised.

It was possible to determine ageing related changes by thermal analysis. The lower the exposure temperatures at pressure cooker testing was, the more dominant were physical ageing processes like post-crystallisation. The higher the exposure temperature was, the more dominant were chemical ageing processes like hydrolysis and chemo-crystallisation. The most similar test results to DH testing showed PCT at 120°C. Tensile test results showed significant changes related to ageing – an increase in yield stress, which indicated physical ageing processes like post-crystallisation. Furthermore they revealed a decrease in strain at break values indicating chain scission due to hydrolysis. The mechanical findings are in good accordance with the results of the DSC measurements. In spite of the good similarity of the results of PCT at 120°C and DH test until 48 h and 1000 h, respectively, the failure mechanisms at 96 h (PCT 120°C) and 2000 h (DH) were different. It is assumed that PCT at 120°C for 96 h caused more degradation than DH testing for 2000 h. Even though there are some changes in IR spectra, differences in test temperatures were hard to distinguish.

To summarise, thermal and mechanical properties showed very close order of magnitude between pressure cooker tests at 120°C and damp heat tests, with the constraint of presumable differences in the failure mechanism. Nevertheless, it should be acceptable to use the pressure cooker test at 120°C up to 96 h for fast quality testing to support fast material development for PET-based backsheets instead of 2000 h of damp heat testing. The use of the pressure cooker test (120°C 96h) would lead to an acceleration of the speed of testing by a factor of 21. Pressure cooker testing is proposed to significantly reduce the testing time to four days for material quality and infant failures.

4.5. References

[1] Liu, F., Jiang, L., and Yang, S. 2014. Ultra-violet degradation behavior of polymeric backsheets for photovoltaic modules. *Solar Energy* 108, 0, 88–100.

[2] Swanson, R. M. 2009. Applied physics. Photovoltaics power up. *Science* 324, 5929, 891–892.

[3] Gong, H., Wang, G., and Gao, M. Degradation mechanism analysis of damp heat aged PV modules. 4BV.3.38. In *27th European Photovoltaic Solar Energy Conference and Exhibition, Frankfurt, Germany, 2012*, 3518–3522. DOI=10.4229/27thEUPVSEC2012-4BV.3.38.

[4] Hülsmann, P., Weiß, K.-A., and Köhl, M. 2014. Temperature-dependent water vapour and oxygen permeation through different polymeric materials used in photovoltaic-modules. *Prog. Photovolt: Res. Appl.* 22, 4, 415–421.

[5] Jorgensen, G. J., K. M. Terwilliger, J. A. DelCueto, S. H. Glick, M. D. Kempe, J. W. Pankow, F. J. Pern, and T. J. McMahon. 2006. Moisture transport, adhesion, and corrosion protection of PV module packaging materials. *Solar Energy Materials & Solar Cells* 90, 2739–2775.

[6] Oreski, G. and Pinter, G. Aging Characterization of Multi-Layer Films Used As Photovoltaic Module Backsheets. 4AV.4.13. In *28th European Photovoltaic Solar Energy Conference and Exhibition, Paris, France, 2013*, 3050–3054.

[7] Peike, C., Hülsmann, P., Blüml, M., Schmid, P., Weiß, K.-A., and Köhl, M. 2012. Impact of Permeation Properties and Backsheet-Encapsulant Interactions on the Reliability of PV Modules. *ISRN Renewable Energy* 2012, 1–4, 1–5.

[8] Knausz, M., Oreski, G., Eder, G. C., Voronko, Y., Duscher, B., Koch, T., Pinter, G., and Berger, K. A. 2015. Degradation of photovoltaic backsheets: Comparison of the aging induced changes on module and component level. *J. Appl. Polym. Sci.* 132, 42093, 1–8.

[9] Miyashita, M. and Masuda, A. Correlation between Moisture Ingress and Performance in Photovoltaic Modules. 4CO.9.4. In *28th European Photovoltaic Solar Energy Conference and Exhibitiom*, 2828–2831. DOI=10.4229/28thEUPVSEC2013-4CO.9.4.

[10] Voronko, Y., Eder, G. C., Knausz, M., Oreski, G., Koch, T., and Berger, K. A. 2015. Correlation of the loss in photovoltaic module performance with the ageing behaviour of the backsheets used. *Prog. Photovolt: Res. Appl.* 23, 11, 1501–1515.

[11] Wang, E., Yang, H. E., Yen, J., Chi, S., and Wang, C. 2013. Failure Modes Evaluation of PV Module via Materials Degradation Approach. *Energy Procedia* 33, 256–264.

[12] Looney, K. and Brennan, B. Modelling the correlation between DHT and true field lifetimes for PET based backsheets. In *29th European Photovoltaic Solar Energy Conference and Exhibition, Amsterdam, Netherlands, 2014*, 2467–2470.

[13] Oreski, G. and Wallner, G. M. 2005. Delamination behaviour of multi-layer films for PV encapsulation. *Solar Energy Materials and Solar Cells* 89, 2-3, 139–151.

[14] Oreski, G. Accelerated indoor durability testing of polymeric photovoltaic encapsulation materials. In *SPIE Solar Energy + Technology, San Diego, USA, 2010. DOI*=10.1117/12.860390.

[15] Oreski, G. and Wallner, G. M. 2005. Aging mechanisms of polymeric films for PV encapsulation. *Solar Energy* 79, 6, 612–617.

[16] Scheirs, J. and Long, T. E. 2003. *Modern polyesters*. *Chemistry and technology of polyesters and copolyesters*. Wiley series in polymer science. John Wiley & Sons, Hoboken, N.J.

[17] Pickett, J. E. and Coyle, D. J. 2013. Hydrolysis kinetics of condensation polymers under humidity aging conditions. *Polymer Degradation and Stability* 98, 7, 1311–1320.

[18] Ehrenstein, G. W. and Pongratz, S. 2007. *Beständigkeit von Kunststoffen*. Carl Hanser Verlag, Munich.

[19] Oreski, G., Wallner, G. M., and Lang, R. W. 2009. Ageing characterization of commercial ethylene copolymer greenhouse films by analytical and mechanical methods. *Biosystems Engineering* 103, 4, 489–496.

[20] Internation Organisation of Standardisation, IEC 61215. 2005. *Crystalline silicon terrestrial photovoltaic (PV) modules - Design Qualification and Type Approval*. International Electrotechnical Commission, Geneva, CH, 61215.

[21] VDE Testing and Certification Institute, Ed. 2011. *Safety testing of PV-Modules*. *An overview over the standart IEC 61730-2 and*. A lecture with a small preamble concerning module reliability and lifetime. PV Module Reliability Workshop 2011, Berlin, Berlin.

[22] Michael Köhl. 2015. *Ultra-violet testing of various Backsheets for PV-modules*. PV Module Reliability Workshop 2015 Loughborough, Loughborough.

[23] Zielnik, A. F. and Dumbleton, D. P. 2012. *Photovoltaic Module Weather Durability & Reliability Testing*. *Will your module last outdoors?*

[24] Gambogi, W. J., Heta, Y., Hashimoto, K., Kopchick, J. G., Felder, T., MacMaster, S. W., Bradley, A., Hamzavytehrany, B., Garreau-Iles, L., Aoki, T., Stika, K. M., Trout, T. J., and Sample, T. 2014. A Comparison of Key PV Backsheet and Module Performance from Fielded Module Exposures and Accelerated Tests. *IEEE J. Photovoltaics* 4, 3, 935–941.

[25] Kawashima, K. 2007. *Back sheet for photovoltaic modules and photovoltiac module using the same,* US 2008/0053512 A1.

[26] Kim, N., Kang, H., Hwang, K.-J., Han, C., Hong, W. S., Kim, D., Lyu, E., and Kim, H. 2014. Study on the degradation of different types of backsheets used in PV module under accelerated conditions. *Solar Energy Materials and Solar Cells* 120, 543–548.

[27] Ehrenstein, G. W., Riedel, G., and Trawiel, P. 2004. *Thermal analysis of plastics*. *Theory and practice*. Carl Hanser Verlag, Munich.

[28] Frick, A. and Stern, C. 2006. *DSC-Prüfung in der Anwendung*. Carl Hanser Verlag, Munich.

[29] International Organisation for Standardisation. 1997. *Plastics - Differential scanning calorimetry (DSC) - Part 1: General principles,* 11357-1.

[30] International Organisation for Standardisation, ISO 527-3. 1995. *Plastics - Determination of tensile properties: Part 3: Test conditions for films and sheets,* 527-3.

[31] Badia, J., Strömberg, E., Karlsson, S., and Ribes-Greus, A. 2012. The role of crystalline, mobile amorphous and rigid amorphous fractions in the performance of recycled poly (ethylene terephthalate) (PET). *Polymer Degradation and Stability* 97, 1, 98–107.

[32] Urban, M. W. 1996. *Attenuated total reflectance spectroscopy of polymers*. *Theory and practice*. Polymer surfaces and interfaces series. American Chemical Society, Washington, DC.

[33] Chen, Z., Jenkins, M., and Hay, J. 2014. Annealing of poly (ethylene terephthalate). *European Polymer Journal* 50, 235–242.

[34] Foulc, M., Bergeret, A., Ferry, L., Ienny, P., and Crespy, A. 2005. Study of hygrothermal ageing of glass fibre reinforced PET composites. *Polymer Degradation and Stability* 89, 3, 461–470.

[35] Planes, E., Yrieix, B., Bas, C., and Flandin, L. 2014. Chemical degradation of the encapsulation system in flexible PV panel as revealed by infrared and Raman microscopies. *Solar Energy Materials and Solar Cells* 122, 15–23.

[36] Grellmann, W., Seidler, S., and Alstädt, V. 2011. *Polymer testing*. Carl Hanser Verlag, Munich.

[37] Menges, G., Haberstroh, E., Michaeli, W., and Schmachtenberg, E. 2002. *Werkstoffkunde Kunststoffe*. Carl Hanser, Munich.

[38] Aljoumaa, K. and Abboudi, M. 2016. Physical ageing of polyethylene terephthalate under natural sunlight. Correlation study between crystallinity and mechanical properties. *Appl. Phys. A* 122:6, 6, 1–10.

[39] Chen, Z., Hay, J. N., and Jenkins, M. J. 2013. The thermal analysis of poly(ethylene terephthalate) by FTIR spectroscopy. *Thermochimica Acta* 552, 123–130.

[40] Sammon, C., Yarwood, J., and Everall, N. 2000. An FT-IR study of the effect of hydrolytic degradation on the structure of thin PET films. *Polymer Degradation and Stability,* 67, 149–158.

[41] Verleye, G. A. L., Roeges, N. P. G., and De Moor, M. O. 2001. *Easy Identification of Plastics and Rubbers*. Rapra Technology, Shawbury.

5. Influence of microclimates on the degradation of polymeric films

This chapter focuses on the influence of microclimates on polymer degradation. It deals with the question if it is possible to age encapsulation materials as single film samples and use the results in order to draw conclusions of the material behaviour incorporated in a photovoltaic (PV) module. This work is published in the Journal of Polymer Degradation and Stability 138 (2017) 182-191, with the title “Comparison of different microclimate effects on the aging behaviour of encapsulation materials used in photovoltaic modules”.

5.1. Introduction to the influence of microclimates on the degradation behaviour of polymeric films

Nowadays the demand for alternative energy sources is high and the importance of renewable energy sources is growing. To directly convert sun light into electricity PV modules can be utilised. A relatively high lifetime of 20 years and more is necessary to collect radiant flux cheaply by PV modules. Therefore a high quality product standard for the components is required to guarantee this module lifetimes with a limited loss in functionality.

The important part of a PV module is the solar cell, which is covered by an encapsulation material. The encapsulant must provide electrical insulation, structural support, protection against environmental influences and connect all components. Therefore the following properties are required: high transmittance in a selected spectral region of the solar cell and the incident solar radiation, good thermal conductivity, good adhesion to organic/inorganic materials, low price, good UV resistance and a long lifetime. Furthermore the encapsulant has to deal with different thermal expansions of the materials used in a PV module in order to avoid over-stressing and breakage. Thus encapsulation films need to be made from a low modulus, elastomeric material [1–4].

The long lifetime is a challenging objective particularly for organic encapsulants. During use with terrestrial sunlight and elevated temperatures the material must retain its properties in order to protect the silicon solar cells. This task gets more challenging when the PV modules are used in regions with high solar irradiance, like deserts. Especially the properties of the encapsulant are critical to the long-term behaviour of modules [4].

In the PV industry the encapsulation material mainly used is ethylene vinyl acetate (EVA) copolymer due to its good optical and structural properties, the low-cost production and over 20 years of experience [1, 2, 4, 5]. It consists of polar vinyl acetate (VAc) units randomly dispersed in the ethylene backbone. Depending on the VAc content the material properties can be influenced from plastics to elastomers [1]. Nowadays alternative materials, like thermoplastic polyolefins (TPO) are starting to be in the focus of the PV industry [6–8]. Due to the required module lifetimes the quality and the lifetime of the encapsulant is of high importance. The degradation behaviour of polar ethylene copolymers and thermoplastic polyolefins is well described in the literature [2–4, 9–14]. For example the thermo- and photo-oxidation of crosslinked EVA copolymers can lead to a decrease of the mechanical performance (e.g. enhanced brittleness) and also to yellowing with the consequent loss in performance of the whole PV module [3, 15, 16]. As the main volatile decomposition product acetic acid is formed, which enhances the oxidation process and can lead to corrosion of the metal parts and to an efficiency loss [2]. A reduction in mechanical performance can cause delamination and consequently the breakdown of the whole PV module [16, 17]. These effects are caused by the chain scission mechanism (Norrish type I, II and III reactions) [17]. Typical degradation products are acetic acid, lactones, ketones and acetaldehyde. Additionally, carbonyl groups, hydro-peroxides and anhydrides are formed during the oxidation process. TPOs are also sensitive to thermo- and photo-oxidation, due to remaining catalyst and residual molecules of the production process, which can support the degradation processes. Degradation causes the formation of a variety of oxygen containing groups (carbonyl compounds). Photo-degradation of polyethylene (PE) comes along with chain scission and crosslinking and leads to molecular weight changes [18]. Of course not only chemical ageing processes occur, as described before, but also physical ageing processes; this is to say, changes in the morphology of the material, loss of additives due to migrations, etc. [19].

However, the main task in PV material development is the correlation of natural and accelerated ageing effects, which is of complex nature. The aim is to reduce the testing time in order to verify the material quality. A simple dependence can rarely be found between artificial and natural weathering results, due to possible synergies or anti-synergies. On the one hand the accelerated degradation stresses, like temperature or humidity, highly impact the property changes of the material, as already described in the literature [2, 11, 20–22]. But on the other hand also the microclimate due to sample design (single film or laminated module exposure) can influence the ageing behaviour. The microclimate describes the environment of the sample. It arises from the

combination of the surrounding climate conditions and also from the application specifics (e. g. single polymeric film vs. polymeric film incorporated in a PV module) [23].

No investigations have been done yet dealing with the influence of the microclimate on polymeric encapsulants concerning physical and chemical ageing processes due to the sample set-up. Additionally, damp heat (DH) is the main test for a fast material selection and quality testing in the PV industry. The influence of radiation on the microclimate has been unconsidered in the industry as well as in research work up until now and should be as well verified. Therefore the main focus in this work was to evaluate the influence of different microclimates on the ageing behaviour of encapsulation materials used in PV modules, due to different sample set-ups and ageing types.

5.2. Experimental procedure

Three commercially available standard EVA films (EVA 1 and 3 were fast-cure and EVA 2 was an ultra-fast-cure type) and one TPO were investigated. Czanderna and Pern, Klemchuk et al. described well the composition of their samples, such as additive systems and curing agents and the influence on the ageing behaviour [3, 4]. The ageing behaviour depends not only on the class of the material, but also on the manufacturer and consequently on the specific formulation of the material. Unfortunately the exact chemical composition was not known as only the datasheet was available due to confidential issues. Single films and glass/EVA/backsheet (TPT) modules were laminated with a size of approximately 7 x 25 cm. In this research no solar cells were incorporated in the module samples. The same pre-treatment was used for all samples in a vacuum laminator, see Table 5.1.

Table 5.1. Curing conditions in the vacuum laminator.

Process step	**Time in min**	**Temperature in °C**	**Pressure in mbar**
Closing laminator	0.5	144	atmospheric
Evacuation	6.0	144	atmospheric to 850
Pressure	1.0	144	850
Curing	9.3	144	850
Ventilation	0.3	144	850 to atmospheric
Opening laminator	0.5	144	atmospheric

The backsheet was a commercially available TPT multilayer consisting of poly vinyl fluoride (PVF), polyethylene terephthalate (PET) and PVF. The samples were artificially aged under DH test conditions and under xenon (Xe) test conditions up to 2000 h, see Table 5.2. The description “unaged” or “0 h” means pre-treated (laminated, more specifically cured) but not aged.

Table 5.2. Ageing parameters.

Parameter	**Damp heat test (DH)**	**Xenon test (Xe)**	
Cycle	Humid	Dry	Rain
Cycle time [min]	-	102	18
Irradiation [W m^{-2}]	-	90	90
Temperature [°C]	85	60	60
Humidity [% RH]	85	50	Rain
Duration [h]	500 1000 2000	1000 2000	

For DH conditions a Vötsch climate chamber type VC 7020 (Balingen, DE) was used. An Atlas Xenotest Beta LM (Linsengericht, DE) was utilised with the filter system for outdoor irradiation (similar to the sun) for ageing tests under xenon test conditions. The irradiation was controlled in the wavelength region from 300 to 400 nm. In order to verify physical and chemical degradation effects of ethylene-based PV encapsulants Fourier transform Infrared (FTIR), Ultraviolet (UV)/ visual (Vis)/ near IR (NIR) and Raman spectroscopy were applied. In addition differential scanning calorimetry (DSC) as the detection method was conducted, in order to verify possible changes in the thermal behaviour.

The UV/Vis/NIR measurements were carried out using a Lambda 950 spectrometer from Perkin Elmer (Waltham, US). Spectra were recorded from 250 to 2500 nm with an integrating sphere in order to measure hemispherical transmittance and reflectance. The film samples were measured in transmittance mode. The module samples were measured in reflectance mode, including the glass front cover and the backsheet. All spectra were used to calculate b* values according to the CIE L a* b* colour space. The yellow-blue opponent colours are represented by the b* axis, with blue at negative values and yellow at positive b* values. Standard light source C was used under a 2° observer angle. The axis maximums for L was 100 and for a* and b* 80, respectively.

FTIR analysis was performed in attenuated total reflectance (ATR) mode, using a Spectrum GX FTIR spectrometer (Perkin Elmer, Waltham, US) for film and module samples, respectively. A variable angle ATR device of the type Pike VeeMax II (Pike Technologies, Madison, US) was used with a zinc selenide (ZnSe) crystal. It allowed depth profiling studies thanks to the variable angle of incidence. Angles of 35 to 70° were used which corresponded to different depths, depending on the sample's refractive index and IR wavelength. Film samples were tested on the light facing side after Xe ageing. In contrast to that, the backsheet was removed on all module samples and the measurements were conducted on the back side (side away from the light) of the encapsulant film.

This was done because it was not possible to detach the encapsulant film from the glass layer. The ATR spectra were recorded over the range of 4000 to 650 cm^{-1} for all samples. The measurements were obtained from an average of 16 scans and at a resolution of 4 cm^{-1}. For better comparison all ATR spectra were normalised at the peak at 2850 cm^{-1} [1].

Raman spectra were measured by using a confocal spectrometer LabRAM HR800 (Horiba Jobin Yvon, Bensheim, DE). A green laser was used for excitation at 514.5 nm and scanning was conducted in the range from 650 to 4000 cm^{-1} with an exposure time of 5 s. A diffraction grating with 600 grooves mm^{-1} was used together with a hole size of 500 µm and a slit size of 100 µm. Measurements were conducted on the edge and in the centre of the samples in order to evaluate the influence of possible diffusion processes.

Thermal analysis was carried out using a Perkin Elmer DSC 4000 (Waltham, US). Indium and Zinc were used as standards for temperature and enthalpy calibration. Thermograms were recorded under nitrogen atmosphere. A nitrogen flux of 50 ml min^{-1} was used in order to prevent further oxidative degradation of samples during the heating step [12]. The heating and cooling rate was 10 K min^{-1} for a proper investigation of melting and crystallisation processes [24]. Peak temperatures and enthalpies were evaluated according to ISO 11357-3 [25]. For every evaluation at least three samples were used. Measurements were conducted on the edge and in the centre of the samples in order to evaluate the influence of possible diffusion processes. As the degree of crystallinity is a function of the ethylene content it was assessed by the melting enthalpy of the material in relation to the enthalpy of a perfect PE crystal (ΔH_m = 293 J g^{-1}) [26]. Additionally the degree of curing was calculated by comparing it to the overall crosslinking capability of the uncured EVA [26]. This degree of curing was determined from the reaction enthalpy ΔH_S of the crosslinking reaction of the unaged but cured sample in comparison to the reaction enthalpy ΔH_0 of the uncured EVA reference according to the equation:

$$X_{Curing} = \frac{\Delta H_0 - \Delta H_S}{\Delta H_0}$$

5.3. Results and discussion

Influences on the optical properties from thermo- and photo-oxidative ageing were characterised via UV/Vis/NIR spectroscopy. All EVA film samples showed no significant changes in the measured spectra – independent of DH or Xe ageing, respectively. However significant differences could be observed for EVA module samples especially in the blue wavelength region (490 – 430 nm) after Xe ageing. Therefore data from the spectra were used to determine the colour. According to the

L a* b* colour space the yellow-blue opponent colours are represented by the b* axis, with blue at negative values and yellow at positive b* values. Figure 5.1 shows the b* value for EVA 2 exemplarily. While DH exposure caused yellowing with an increase from 0.8 to a value of 3.0, Xe aged samples exhibited a more pronounced discoloration with an increase of the b* value to 6.1. This discoloration was not caused by long sequences of conjugated double bonds, as it is the case for polyvinylchloride (PVC). As Klemchuk et al. already showed glass/EVA/glass samples that contained benzophenones and phosphites in interaction with peroxides caused discoloration [4, 16]. Unstabilised samples did not discolour significantly [4]. Yellowing in EVA is formed by a combination of ketones and unsaturated double bonds in contrast to PVC where polyenes are responsible for the colour [9].

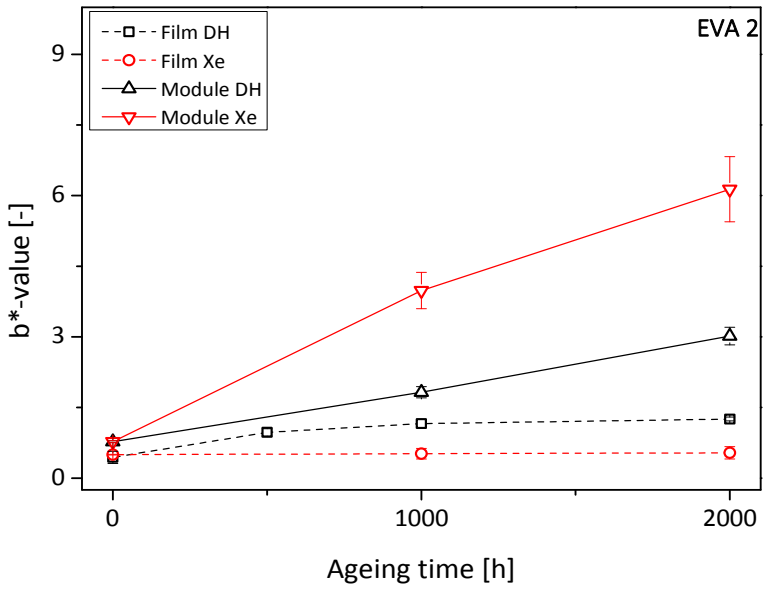

Figure 5.1. Colour value b (blue-yellow axis) according to CIELab of EVA 3 film and module samples.*

Although studies already showed that the degradation rate is bigger under an oxygen atmosphere as is the formation of coloured products, the single films showed no significant yellowing [12]. A reason for the differences may be a photo-bleaching effect, where oxygen and UV irradiation in combination cause the degradation of the chromophoric bonds [3, 4]. Czanderna and Pern reported that photo-bleaching probably precluded most of the discoloration [3]. The unsaturated bonds are oxidised before colour is produced, if sufficient oxygen, UV radiation and a high enough temperature are present [3]. The discoloration of the backsheets of the module samples without a colour change of EVA encapsulant can be excluded as a reason. Experiments showed that this type

of TPT exhibited no significant discoloration after up to 180 kWh m^{-2} (2000 h) of Xe exposure, whether on the light facing side or on the back side, see Figure 5.2. Artificial weathering with irradiation (Xe ageing) resulted in significant yellowing for all module samples. The differences between module and film samples were caused by different microclimates. As the module samples are encapsulated by a glass cover and a backsheet the temperature of the polymeric film can be higher compared to the single films. Also atmospheric gases, like oxygen and water vapour are prevented from coming easily into contact with the EVA due to the covering layers. The ingress of these gases is much slower because a diffusion process has to proceed starting at the sample edges [27–29].

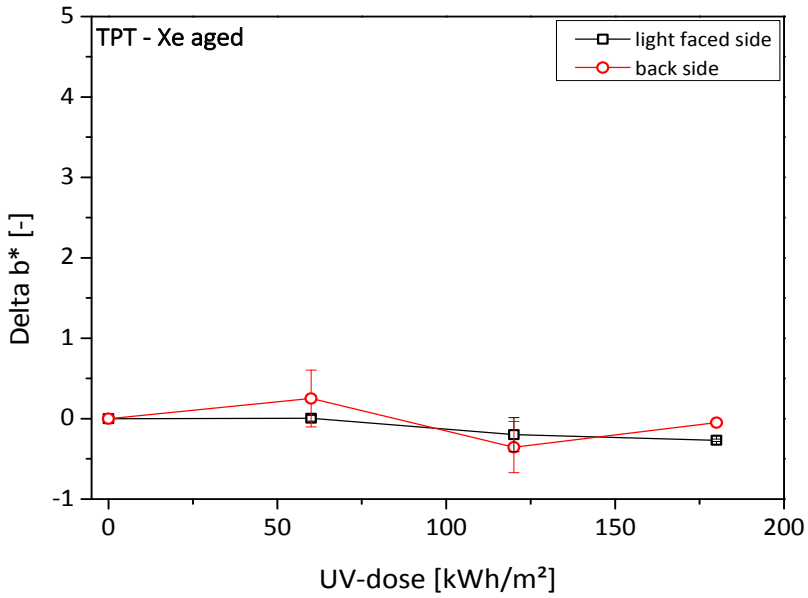

Figure 5.2. Colour change (delta b) of Xe aged TPT film samples.*

The colour trends for EVA could be also observed for the TPO samples in an alleviated way – the b* value settled at around 2.0 after 2000 h of ageing, independent of DH or xenon exposure for the module samples. The film samples exhibited no significant changes in the colour value b*. However the spectra of TPO film samples showed changes in the UV area (250 – 380 nm). As presented in Figure 5.3, spectra of Xe aged samples showed an increase of transmittance. Additionally the UV cut off shifted to lower wavelengths after 2000 h of Xe ageing. This may be attributed to formed chromophoric species during ageing, but also to a partial consumption of a UV absorber [9, 12, 19, 30, 31]. A greater amount of UV light is transmitted and the UV cut off is shifted to lower wavelengths, if the UV absorbers lose their ability to absorb UV light [19, 31]. The peak at 325 nm

may be related to the keto-enol tautomerism of the hydroxyl benzophenone group in the UV absorber [19].

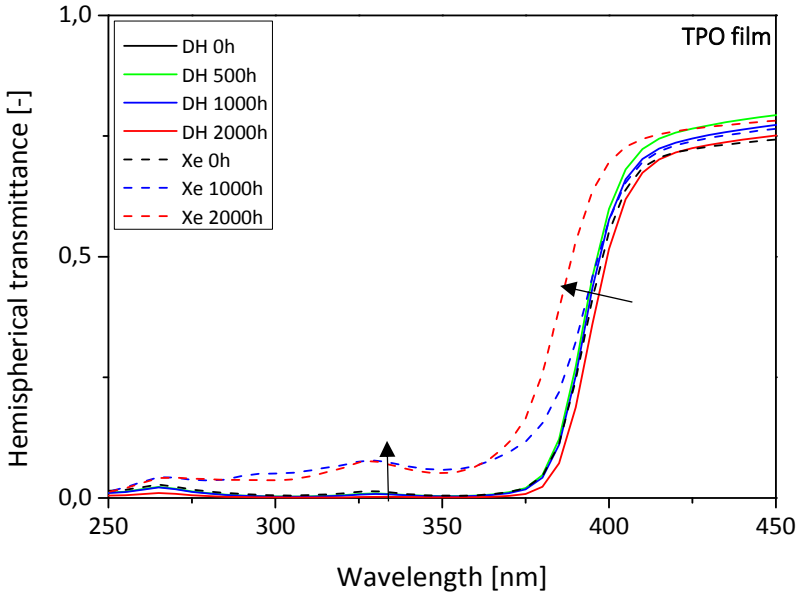

Figure 5.3. UV/Vis spectra of TPO film samples.

The characterisation of the chemical structure via IR spectroscopy revealed characteristic bands for the unaged EVA material, see Figure 5.4. Typical peaks for EVA at 2916, 2848, 1463, 1370 and 730 cm^{-1} caused by the symmetric, asymmetric and deformation vibrations of the CH_2 and CH_3 groups. These bands are mainly caused by the ethylene segments. The bands at 1740, 1238 and 1020 cm^{-1} can be related to carbonyl and ether groups (C=O, C-O), respectively. These absorbance bands can be assigned to the ester group of the VAc segments [12].

Accelerated ageing of module samples caused no significant differences in the IR spectra for any materials, neither after DH nor Xe ageing, respectively. One reason is the fact that the measurements were conducted from the back side of the module samples and therefore the front side of the Xe aged samples could not been characterised. For DH aged module samples this fact should not be relevant, as there was no irradiation during ageing. Also DH ageing of film samples caused no significant changes in the IR spectra for all materials.

Significant functional group changes were evident for Xe aged film samples. Exemplarily the IR spectra of Xe aged EVA 1 film samples are shown in Figure 5.4. Qualitative changes were analysed, as it is not plainly possible to relate quantitative results via ATR-IR measurements. For this purpose measurements in transmission mode would have been necessary. But obtaining a fine powder of

the sample in order to blend it with potassium bromide (KBr) and press it to a disk is often difficult [32]. This process may influence the sample too much when analysing ageing effects.

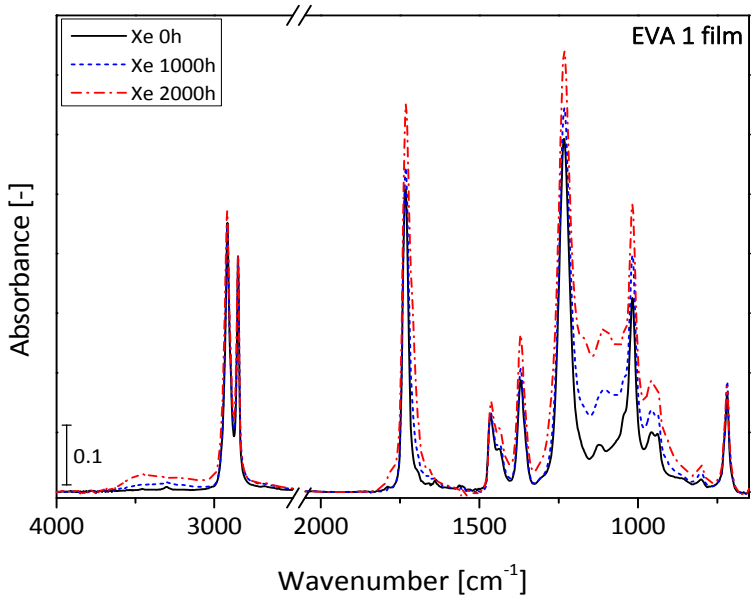

Figure 5.4. IR absorbance spectra of Xe aged EVA 1 film samples.

Significant changes in the regions of around 3700 to 3100 cm^{-1}, 1735 cm^{-1} and 1160 cm^{-1} due to photo-oxidation could be seen. The differences in these wavenumber regions correspond to the absorbance bands of hydroxyl-, ketone- and aliphatic ester groups, respectively, which can be caused by the typical degradation products of EVA (lactone, ketone, acetaldehyde and acid groups) [1, 12, 19]. In detail the absorbance spectra showed a broadening of the carbonyl stretching peak between 1800-1650 cm^{-1}, see Figure 5.5. This can be attributed to the formation of lactone, ketone, anhydride and acid groups [12, 33]. The main volatile degradation product is acetic acid for EVA [34]. The shoulder formed at lower wavenumbers (1660-1720 cm^{-1}) might be caused by the C=O stretching of formed ketone structures (1714 cm^{-1}) and the shoulder between 1750 and 1800 cm^{-1} could be caused due to lactone formation (1773 cm^{-1}) in the polymer chain. Not only the broadening of the peak but also an increase in intensity, possibly due to an increase in ester or aldehyde groups, could be observed [1, 35]. It may be associated with a back-biting process in the vinyl acetate moieties by forming methane [12]. The peak around 1120 cm^{-1} caused by C-O-C stretch vibration confirm this assignment [2, 13]. This can be either caused by evolution of acetaldehyde or alternatively by hydro-peroxides which broke down to ketone groups and water [12]. As support hydroxyl formation was evident in the region 3700-3100 cm^{-1}, see Figure 5.4. The increasing absorbance at about 995 cm^{-1} correlates to the =CH terminal double bond groups,

implicating chemical degradation [15, 36]. The formation of conjugated double bonds is negligible as no significant change of the absorbance around 1600 cm^{-1} was observed [15, 37]. Based on the literature the proposed reactions would appear to be the most likely ones, although other reaction sequences may be involved [12, 33].

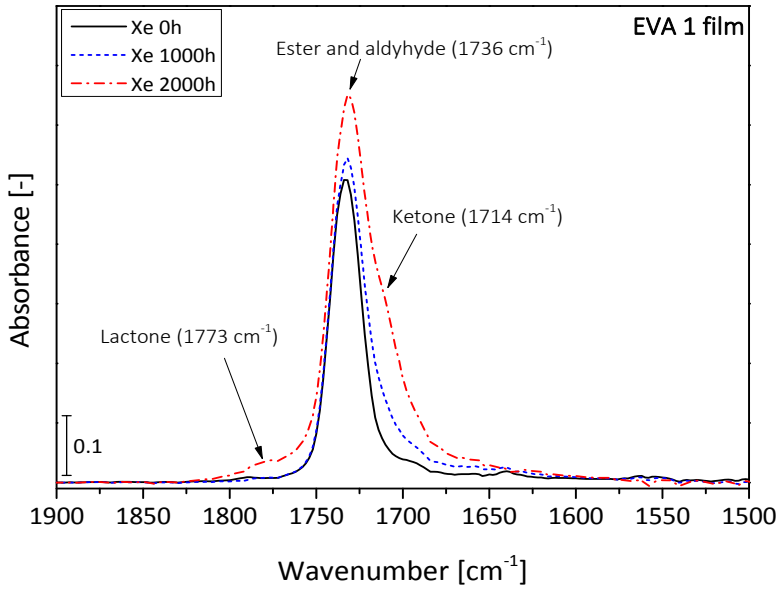

Figure 5.5. Detail of the IR absorbance spectra of Xe aged EVA 1 film samples.

Figure 5.6 shows the IR spectra of TPO film samples. Significant absorbance bands for polyolefins were observed at 3000 to 2800, 1462, 718 cm^{-1} caused by CH_2 and CH_3 groups, respectively. The carbonyl area with around 0.667 was higher for unaged TPO compared to less than 0.1 for linear low density polyethylene (LLDPE), low density polyethylene (LDPE) or high density polyethylene (HDPE) due to the absorbance of the ester (acetate) carbonyl of the EVA parts [35]. Module samples of TPO showed no significant changes, independent of the ageing type (DH or Xe). Only for Xe aged film samples were differences visible. Several additional peaks can be identified: a broad band between 3500 and 3000 cm^{-1} can be assigned to hydroxyl groups of alcohols, peroxides and hydro-peroxides. Between 1800 and 1450 cm^{-1} (C=O vibration) the absorbance increased, which indicated oxidation processes during ageing. The shoulders at 1638 and 1706 cm^{-1} can be attributed to the formation of saturated and unsaturated acid groups, at 1736 cm^{-1} to aliphatic esters and at 1778 cm^{-1} to lactones. The broad peak around 1130 cm^{-1} corresponds to the carbonyl stretch vibration of ketone and C-O-C stretch vibration of aliphatic ester. The shoulder which appeared at 1641 cm^{-1} (C=C stretch) and at 960 cm^{-1} (trans vinylidene groups) and the peak at about 3008 cm^{-1} (=CH stretch) are related to the formation of double bonds. The continuous

increase of these absorbance peaks with ageing time indicates the successive progress of photo-degradation in the film samples.

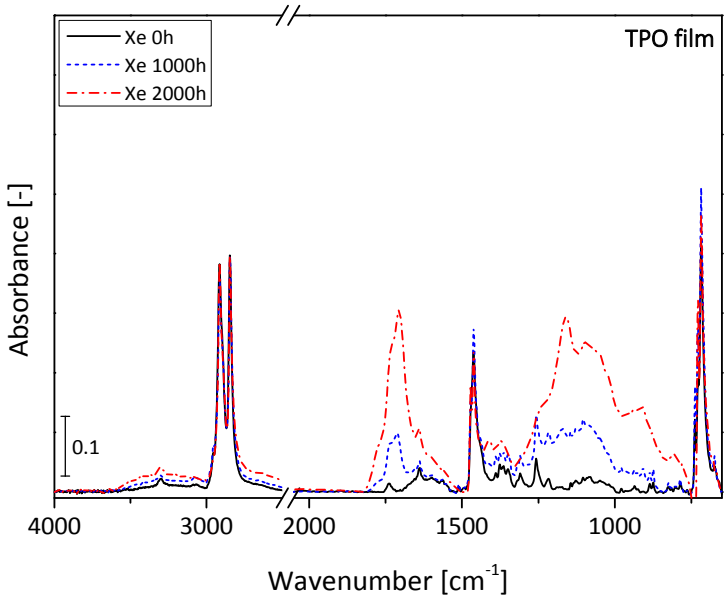

Figure 5.6. IR spectra of TPO film samples.

In order to compare the degradation of the different samples absorbance ratios were used. As Jin et al. already confirmed VAc groups are more vulnerable to stress factors, like temperature, oxygen and UV light compared to the non-polar ethylene chain segments [1]. Therefore the area of the absorbance of the ether (C-O-C) groups in relation to the overall CH was used as numerator for all EVA materials. For the TPO material the carbonyl region was evaluated, which can be also affected by oxidation of ethylene units. Therefore the spectra were integrated from 1150 to 1060 cm^{-1} and 1780 to 1700 cm^{-1} for EVA and TPO, respectively [4]. The methylene C-H symmetric stretching at 2850 cm^{-1} was used as an internal standard, due to the fact, that it is narrower and less likely to be overloaded compared to the one at 2921 cm^{-1} [4]. The oxidation indices (OI) were given as

$$\mathrm{OI}_{EVA} = \left(\frac{\int_{1150}^{1060} \text{Absorbance}}{\int_{2875}^{2760} \text{Absorbance}}\right) \qquad \mathrm{OI}_{TPO} = \left(\frac{\int_{1780}^{1700} \text{Absorbance}}{\int_{2875}^{2760} \text{Absorbance}}\right)$$

The OI indices were calculated for all spectra, which were measured by a variable angle ATR unit. By changing the angle of incidence the depth of the infrared radiation in the sample can be varied. Important parameters are the refractive indices of the crystal and the sample and the wavelength of radiation [35]. With this method it was possible to determine a depth profile for the OI indices.

As the accelerated ageing of all EVA module samples caused no significant changes in the IR spectra, no differences in the OI index could be observed. This was caused by the fact, that the module samples could only be measured from the back side (side away from the light). Also the DH aged film samples exhibited no changes. However, Xe aged film samples showed interesting results: with increasing ageing time the OI index increased. This effect is stronger on the surface, which affirms a photo-oxidative induced degradation, see Figure 5.7. Obviously, DH ageing was not causing the same ageing effects as Xe ageing.

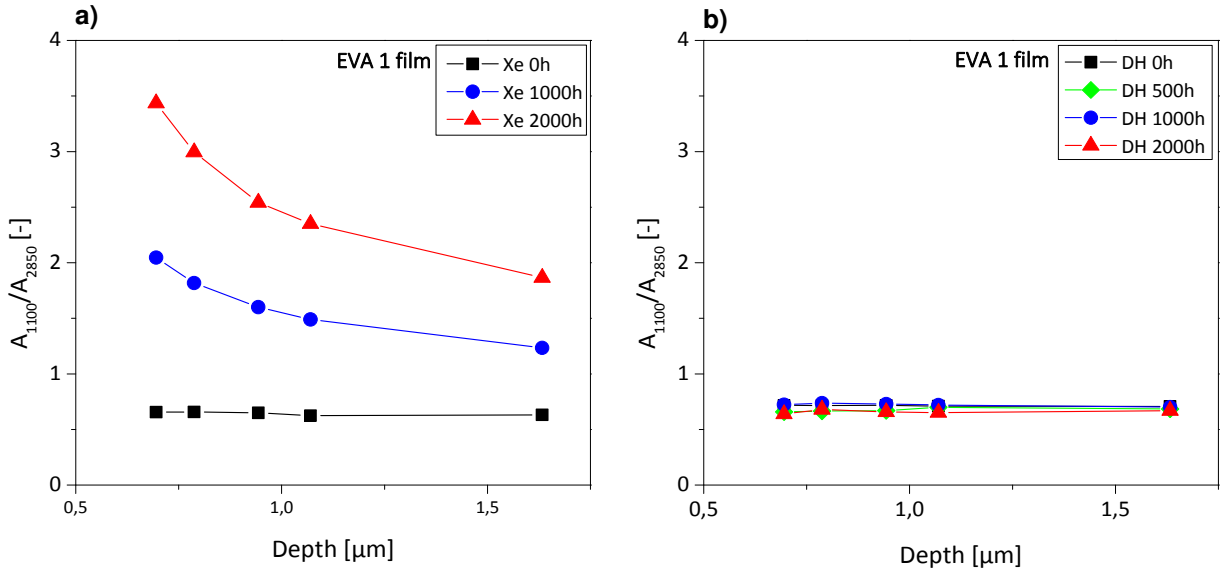

Figure 5.7. Ageing index of EVA 1 film samples aged under a) Xe and b) DH conditions.

Artificial ageing of all TPO module samples caused no significant changes in the OI index, or of the DH aged film samples. The OI values for Xe aged TPO film samples are shown in Figure 5.8. A similar trend could be observed for the EVA samples. With increasing ageing time the OI index increased. The effect is also slightly stronger on the surface. This affirms that the different ageing types had a different impact on the degradation behaviour of polymeric encapsulant – in contrast to DH ageing, the radiation of Xe ageing caused significant increase in oxidation products in the film samples.

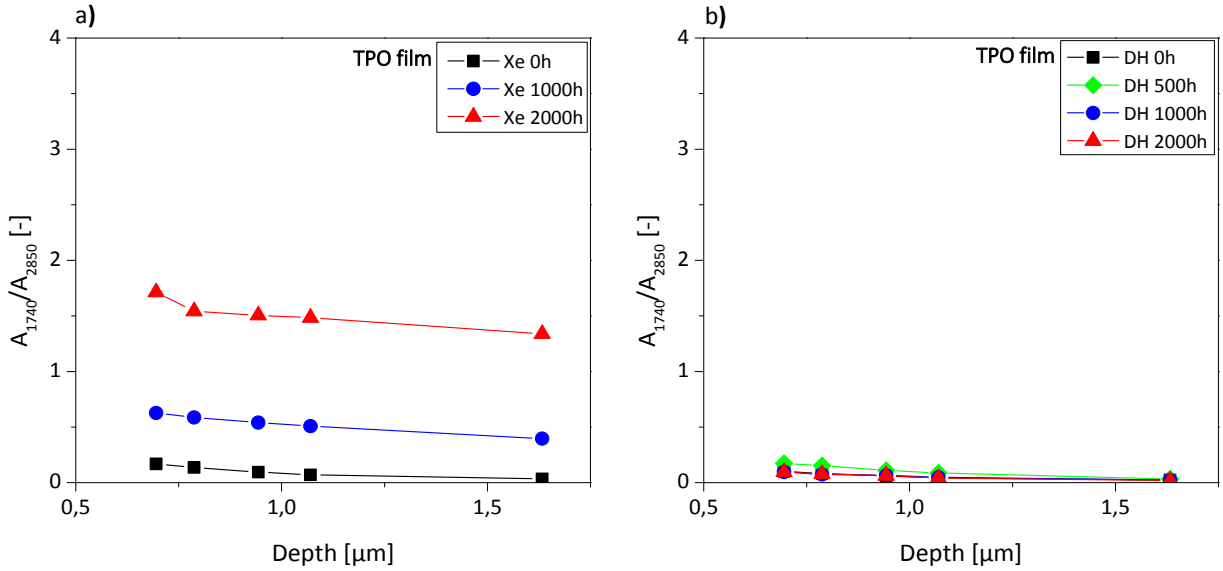

Figure 5.8. Ageing index of TPO film samples aged under a) Xe and b) DH conditions.

As Peike et al. already stated observing the Raman raw spectra is a quick way to analyse EVA degradation [38]. The reason is the investigation of the fluorescence background. The Raman spectroscopic measurements showed typical peaks for EVA in the region between 3000 and 2830 (CH_2 and CH_3 stretching vibrations), 1740 (C=O stretching vibration), 1440 (CH deformation vibration), 1298 (CH deformation vibration), 1130 (CC stretching vibration) and 1064 cm^{-1} (CC stretching vibration), see Figure 5.9 [39]. Significant changes were observable for Xe aged module samples for all EVA materials. A decrease in peak intensities in combination with an increase in the baseline due to fluorescence suggests chemical degradation for this type of samples [28, 38, 40, 41]. This is due to the fact that the fluorescence intensity can be correlated to the amount of chromophores formed during degradation [28]. This corresponds well to the UV/Vis/NIR results, where the Xe aged module samples exhibited the highest discoloration, suggesting that the same groups were responsible for the discoloration and for the increase of fluorescence, respectively. The spectra at the outer edges of the module sample showed less fluorescence than at the centre. This suggests diffusion induced bleaching reactions [40]. The ageing effect was not visible for DH aged module samples. Also Xe aged film samples showed no significant increase in fluorescence. The already described photo-bleaching effect (UV light in combination with oxygen) could be the reason, which corresponds well to the previously stated results [3, 4]. No significant differences in the Raman spectra of the TPO samples were observed.

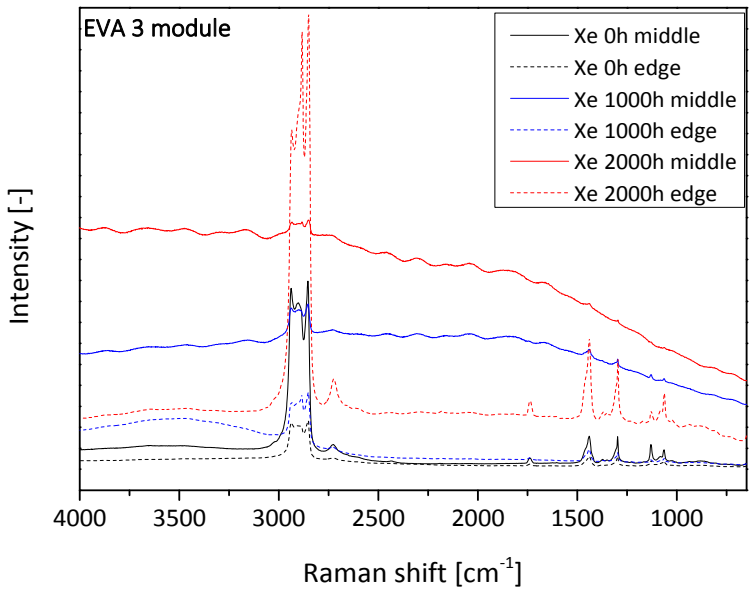

Figure 5.9. Raman spectra of EVA 3 module samples.

Figure 5.10 exemplarily illustrates the thermograms of unaged EVA 3 film and module samples. In general the DSC measurements showed no significant differences between samples located on the edges or in the centre of the module samples for all materials. The unaged film samples exhibited a major melting peak at around 41°C and a medium peak at around 60°C which overlap each other. This is due to the randomly introduced VAc units in the ethylene chain segments, which cause a different ability to crystallise. Lower VAc unit content leads to longer crystallisable ethylene chain segments, which have a positive impact on the spherulite growth and crystal perfection [1, 42].

These two peaks were the consequence of two populations of crystalline perfection – the lower temperature peak can be the result of imperfect, smaller crystallites, while the higher temperature endotherm can be described as the result of melting of larger, more regularly formed crystallites [42, 43]. Only the ultra-fast cure EVA 2 exhibited a higher medium peak temperature at around 68°C which may be due to a lower amount of VAc and/or a lower degree of crosslinking than for EVA 1 or 3, respectively [44]. The slightly higher degree of crystallinity of EVA 2 compared to EVA 1 and 3 supported the assumption of fewer VAc units, see Table 5.3 [42]. For the module samples the major melting peak was around 44°C. This difference of 4°C compared to the film samples was possibly caused by the lamination set-up during the lamination process, which was for the film samples a separator sheet, EVA and a separator sheet and for the module samples a glass layer, EVA and the TPT backsheet. Due to this different prevailing temperatures in the polymeric

films were possible during the lamination process. EVA 2 exhibited a slightly higher medium peak temperature around 64°C compared to 60°C for EVA 1 and EVA 3.

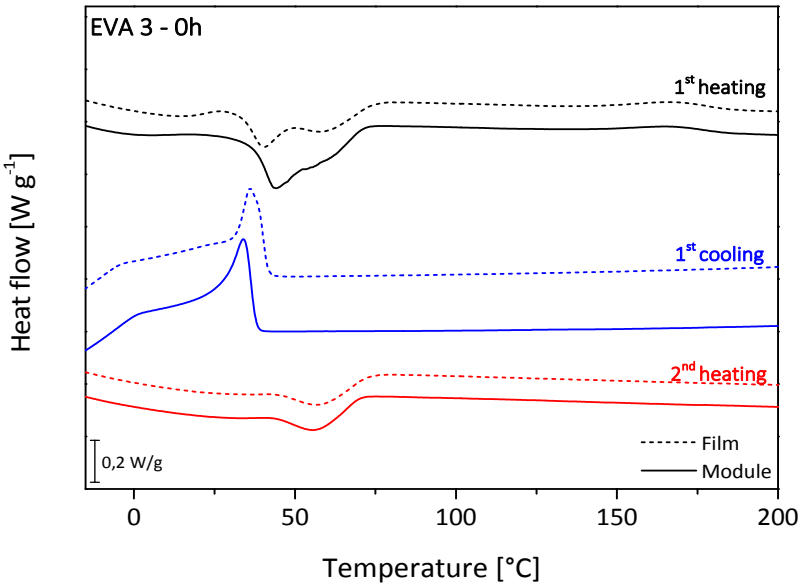

Figure 5.10. DSC thermograms of unaged EVA 3 film and module samples.

In general the module samples exhibited a higher degree of crystallinity versus the film samples, see Table 5.3. This can be caused by the fact that the cool down of the module samples was slower than of the film samples, due to the sample set-up. A small exothermal peak was visible in the first heating between 150 and 170°C for the unaged material, independent of film or module sample. This can be attributed to the heat release of a crosslinking reaction of EVA [26]. The higher value of the degree of curing for all module samples compared to the film samples was also a result of the slower cool down of the module samples, see Table 5.3. Even though EVA 2 was an ultra-fast-cure type it showed not a significantly higher degree of curing than EVA 1 or EVA 3. The degree of curing for all EVA materials is in good comparison with values from the literature measured by DSC [26]. The exothermic peak diminished after ageing, suggesting a fully cured system.

Table 5.3. Degree of crystallinity and curing for unaged EVA film and module samples.

Material	Degree of crystallinity		Degree of curing	
	Film	Module	Film	Module
EVA 1	8.5 ± 0.1%	10.4 ± 0.2%	82.7 ± 1.1%	83.0 ± 1.2%
EVA 2	12.4 ± 0.2%	16.6 ± 0.4%	79.0 ± 3.3%	85.8 ± 3.3%
EVA 3	8.6 ± 0.0%	10.9 ± 0.5%	75.3 ± 8.4%	79.3 ± 3.7%

Small differences in the crystallisation peak temperature were visible between film and module samples (34°C and 36°C). The second heating was conducted in order to remove the thermal history of the sample. The thermal behaviour during the second heating showed no significant difference between film and module samples – a single peak at 57°C was observable and the degree of crystallinity was 4.7 ± 0.1%. Compared to the first heating run, it showed in the second run the influence of a different microclimate due to the set-up of the samples during the lamination process.

The major melting peak of the first heating run of the film samples (40°C) was not influenced by ageing, see Figure 5.11 a. During ageing the primary crystalline region in polymers is very stable but amorphous, and secondary crystallisation regions can be affected and to rearrange themselves [1, 44]. After 2000 h of DH ageing the medium peak temperature increased by 5°C for EVA 3. This effect was also visible for EVA 1. This behaviour could not been seen for EVA 2. Xe ageing caused no significant differences in the thermal behaviour of any of the EVA film samples. Module samples exhibited also only minor changes in the melting behaviour, see Figure 5.11 b).

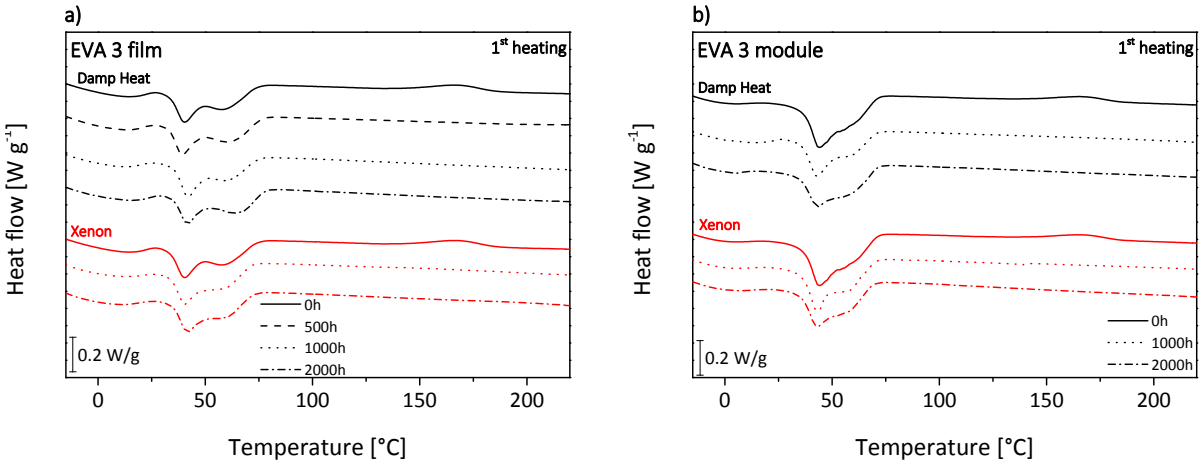

Figure 5.11. DSC heating graphs of EVA 3 a) film and b) module samples.

The crystallisation temperature, which is an indicator for the molecular mass, significantly changed only for the DH aged film samples, Figure 5.12. The crystallisation temperature is affected by molar weight and therefore by chemical changes in the polymer [45]. The reason is that shorter chains, previously formed by chain scission, exhibited a higher fluidity. This led to a higher mobility of the shorter chains and with it a better ability to form crystallites [45]. Additionally, all terminal groups acted as nucleating agents and smaller crystallites with higher crystallisation temperatures were formed [24, 45, 46]. The DH aged film samples showed an increase from 36°C to 41°C after 2000 h. This behaviour was found for all EVA types. It may be caused by the scission of acetic acid from the

molecular chain. This behaviour may be similar to the hydrolysis process known for polyesters, as Knausz et al. described [47]. Samples aged with irradiation (Xe aged) showed no significant changes in this parameter. As Valadez-Gonzalez et al. stated, there are two competing reactions (chain scission and curing reaction) in polyolefins during photo-degradation [18]. Presumably due to the split of acetic acid the curing reaction was more pronounced, so that the possible decrease of molecular mass was compensated. The second heating run showed no changes due to ageing for any EVA materials, which showed that there were reversible structural changes in the material during ageing, depending on the microclimate.

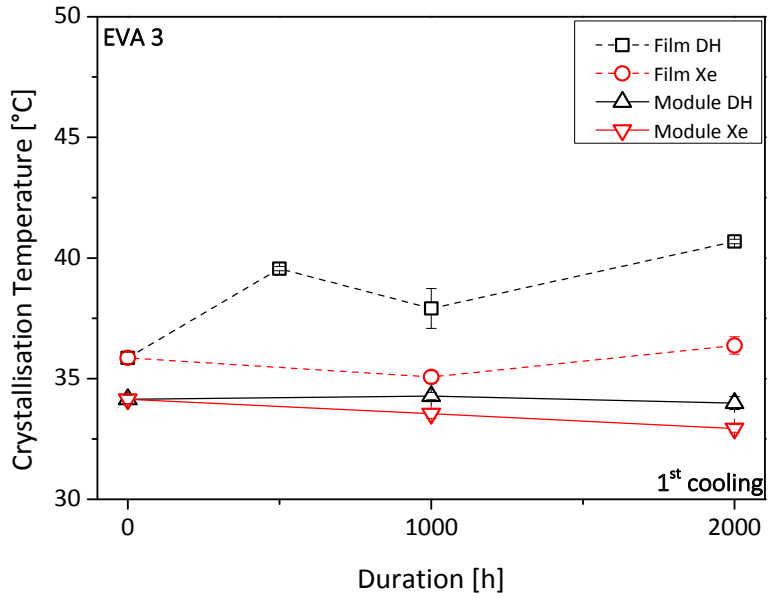

Figure 5.12. Crystallisation temperature of EVA 3 film and module samples.

DSC thermograms of the unaged TPO film and module samples are shown in Figure 5.13. Similar behaviour can be seen compared to EVA – two overlapping melting peaks at 50°C and 96°C for the film samples. The TPO module samples exhibited different peak temperatures with 47°C and 92°C, respectively. These differences were caused by different microclimates due to the different sample set-ups during the lamination process. The degree of crystallinity is slightly higher for module samples. The crystallisation run and the second heating run showed similar results for film and module samples.

Figure 5.14 shows the first heating run of all aged TPO film and module samples, respectively. Independent of the type of sample, the curve progression changed after the first 500 h of DH ageing similarly – a secondary melting area between 30°C and 80°C and a narrow peak around 96°C were visible. This secondary melting area can be attributed to smaller crystallites, which were formed

during ageing at elevated temperatures (post-crystallisation). Furthermore it was not detected in the second heating run, which confirms the reversible and ageing-induced character. The degree of crystallinity and the crystallisation temperature did not change after DH ageing. This is probably due to the fact, that no acetic acid is formed and split. This supports the previous assumption that scission of acetic acid is the reason for the increase of the crystallisation temperature of all EVAs, like the hydrolysis process for polyesters. Further DH exposure for 1000 h and 2000 h did not result in further changes.

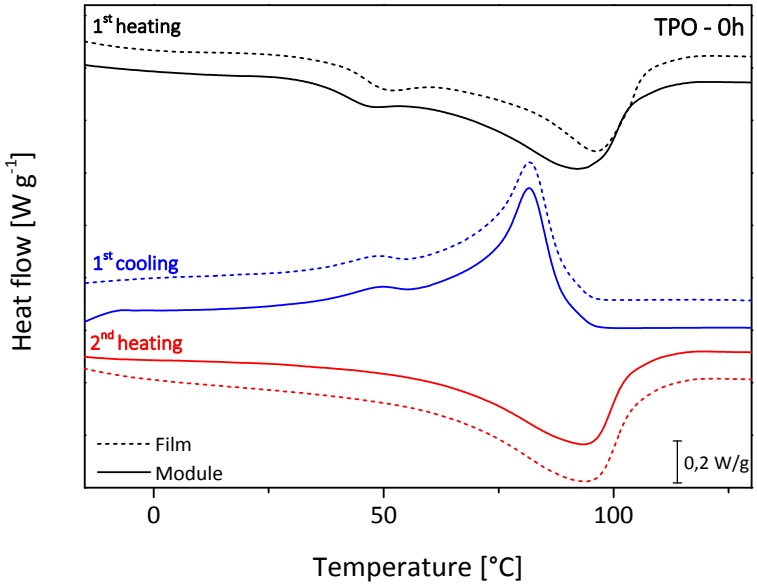

Figure 5.13. Thermograms of unaged TPO film and module samples.

Compared to that, 1000 h of Xe ageing caused a secondary melting area and two melting peaks at 86°C and 100°C for film samples, respectively. This could be caused by different types of crystallinity. After 2000 h the secondary melting area and a single peak could be detected (103°C). Changes in the degree of crystallinity were not visible for the film samples.

Xe aged module samples exhibited a reversible secondary melting area, like the film samples, but at a higher temperature range between 40°C and 90°C. Additionally a major peak at 98°C and a smaller at 113°C appeared after 1000 h of Xe ageing. These peaks shifted to lower temperatures (96°C and 108°C, respectively) after 2000 h. No changes in the crystallisation temperature could be observed. The DSC results confirmed differences due to the influence of the microclimate and in addition ageing, caused by a different sample set-up.

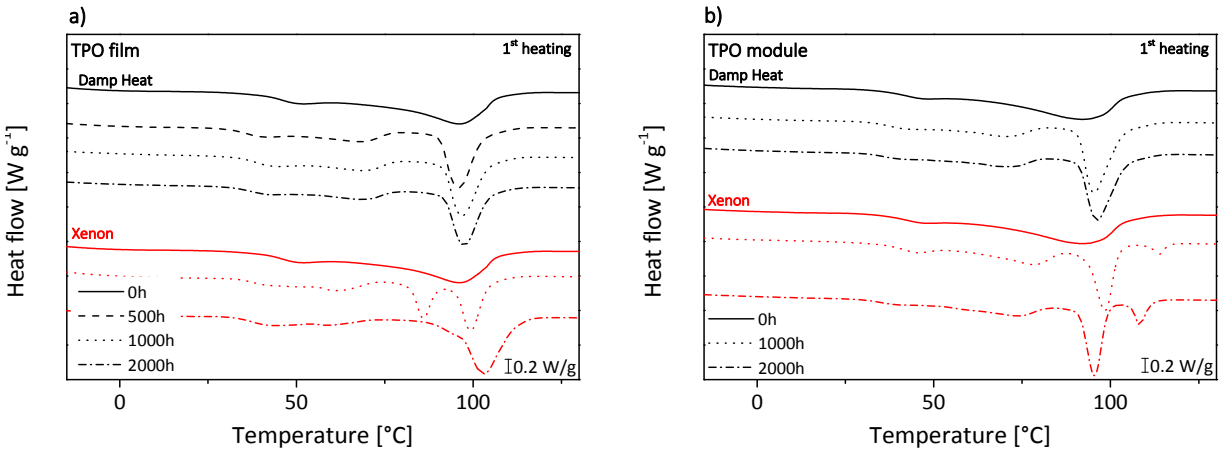

Figure 5.14. DSC heating graphs of TPO a) film and b) module samples.

5.4. Summary and conclusion

The purpose of this work was the investigation of the influence of the microclimate on the ageing behaviour of polymeric encapsulants for photovoltaic (PV) modules. Four different types of encapsulation films were investigated (curable and non-curable materials). Single film and laminated samples (glass/encapsulant/backsheet) were produced and artificially aged under different conditions (with and without irradiation).

The optical characterisation showed discoloration only for the module samples aged under irradiation. Presumably a photo-bleaching effect prevented the discoloration of film samples. Significant influences of the microclimate could be detected due to sample set-up and ageing type. In contrast to that the chemical structure revealed that only film samples aged with radiation showed an increase in the absorbance bands caused by oxidation products. This supports the photo-bleaching effect assumption. With a variable angle IR device the photo-degradation starting at the surface of the film samples could be verified. The results were confirmed by Raman measurements. Thermograms showed that the different sample set-ups had an influence on the unaged material state, by the different results in the first heating runs. Ageing with irradiation caused no significant differences in the morphology of the film samples. In contrast ageing without irradiation caused an increase in the crystallisation temperature for all curable films, which could be explained by the forming and scission of acetic acid. Post-crystallisation effects were determined for the non-curing encapsulant by differences in the first heating runs after ageing with and without irradiation.

The results showed that there is a strong influence of the microclimate on the ageing behaviour of polymeric encapsulant materials. Differences were even detectable in the unaged state between film and module samples after the production process. Not only did the sample set-up (film or laminated module sample) highly influence the degradation of the encapsulants, but also the type of ageing (dark ageing or ageing with irradiation).

5.5. References

[1] Jin, J., Chen, S., and Zhang, J. 2010. UV aging behaviour of ethylene-vinyl acetate copolymers (EVA) with different vinyl acetate contents. *Polymer Degradation and Stability* 95, 5, 725–732.

[2] Oreski, G. and Wallner, G. M. 2009. Evaluation of the aging behavior of ethylene copolymer films for solar applications under accelerated weathering conditions. *Solar Energy* 83, 7, 1040–1047.

[3] Czanderna, A. W. and Pern, F. J. 1996. Encapsulation of PV modules using ethylene vinyl acetate copolymer as a pottant: A critical review. *Solar Energy Materials and Solar Cells* 43, 2, 101–181.

[4] Klemchuk, P., Ezrin, E., Lavigne, G., Holley, W., Galica, J., and Agro, S. 1997. Investigation of the degradation and stabilization of EVA-based encapsulant in field-aged solar energy modules. *Polymer Degradation and Stability,* 55, 347–365.

[5] Ayutthaya, S. I. N. and Wootthikanokkhan, J. 2008. Investigation of the photodegradation behaviors of an ethylene/vinyl acetate copolymer solar cell encapsulant and effects of antioxidants on the photostability of the material. *J. Appl. Polym. Sci.* 107, 6, 3853–3863.

[6] Steiner, A.-J., Krumlacher, W., Muckenhuber, H., Plank, M., Sundl, K., and Ziegler, E. New Thermoplastic, Non-Curing Encapsulation Material for PV Module Applications. In *28th European Photovoltaic Solar Energy Conference and Exhibition, Paris, France, 2013*.

[7] López-Escalante, M., Caballero, L. J., Martín, F., Gabás, M., Cuevas, A., and Ramos-Barrado, J. 2016. Polyolefin as PID-resistant encapsulant material in 5PV6 modules. *Solar Energy Materials and Solar Cells* 144, 691–699.

[8] Stollwerck, G., Schoeppel, W., Graichen, A., and Jaeger, C. Polyolefin Backsheet and New Encapsulant Supress Cell Degradation in the Module. In *28th European Photovoltaic Solar Energy Conference and Exhibition, Paris, France, 2013*.

[9] Rodríguez-Vázquez, M., Liauw, C. M., Allen, N. S., Edge, M., and Fontan, E. 2006. Degradation and stabilisation of poly(ethylene-stat-vinyl acetate): 1 – Spectroscopic and rheological

examination of thermal and thermo-oxidative degradation mechanisms. *Polymer Degradation and Stability* 91, 1, 154–164.

[10] Kempe, M. D., Jorgensen, G. J., Terwilliger, K. M., McMahon, T. J., Kennedy, C. E., and Borek, T. T. 2007. Acetic acid production and glass transition concerns with ethylene-vinyl acetate used in photovoltaic devices. *Solar Energy Materials and Solar Cells* 91, 4, 315–329.

[11] Oreski, G. and Wallner, G. M. 2005. Aging mechanisms of polymeric films for PV encapsulation. *Solar Energy* 79, 6, 612–617.

[12] Allen, N. S., Edge, M., Rodriguez, M., Liauw, C. M., and Fontan, E. 2000. Aspects of the thermal oxidation of ethylene vinyl acetate copolymer. *Polymer Degradation and Stability,* 68, 363–371.

[13] Allen, N. S., Edge, M., Rodriguez, M., Liauw, C. M., and Fontan, E. 2001. Aspects of the thermal oxidation, yellowing and stabilisation of ethylene vinyl acetate copolymer. *Polymer Degradation and Stability,* 71, 1–14.

[14] Rodríguez-Vázquez, M., Liauw, C. M., Allen, N. S., Edge, M., and Fontan, E. 2006. Degradation and stabilisation of poly(ethylene-stat-vinyl acetate): 1 – Spectroscopic and rheological examination of thermal and thermo-oxidative degradation mechanisms. *Polymer Degradation and Stability* 91, 1, 154–164.

[15] La Mantia, F. P., Malatesta, V., Ceraulo, M., Mistretta, M. C., and Koci, P. 2016. Photooxidation and photostabilization of EVA and cross-linked EVA. *Polymer Testing* 51, 6–12.

[16] Jentsch, A., Eichhorn, K.-J., and Voit, B. 2015. Influence of typical stabilizers on the aging behavior of EVA foils for photovoltaic applications during artificial UV-weathering. *Polymer Testing* 44, 242–247.

[17] Griffini, G. and Turri, S. 2016. Polymeric materials for long-term durability of photovoltaic systems. *Journal of Applied Polymer Science* 133, 11, n/a-n/a.

[18] Valadez-Gonzalez, A., Cervantes-U, J., and Veleva, L. 1999. Mineral fller influence on the photo-oxidation of high density polyethylene: I. Accelerated UV chamber exposure test. *Polymer Degradation and Stability,* 63, 253–260.

[19] Oreski, G., Wallner, G. M., and Lang, R. W. 2009. Ageing characterization of commercial ethylene copolymer greenhouse films by analytical and mechanical methods. *Biosystems Engineering* 103, 4, 489–496.

[20] Oreski, G. and Wallner, G. M. 2005. Delamination behaviour of multi-layer films for PV encapsulation. *Solar Energy Materials and Solar Cells* 89, 2-3, 139–151.

[21] Reid, C. G., Bokria, J. G., and Woods, J. T. UV Aging and Outdoor Exposure Correlation for EVA PV Encapsulants. In *Proceddings of SPIE*, 1–11.

[22] Reid, C., Ferrigan, S. A., Martinez, J. I., and Woods, J. T. Contribution of PV Encapsulant Composition to Reduction of Potential Induced Degradation (PID) of Crystalline Silicon PV Cells. In *28th European Photovoltaic Solar Energy Conference and Exhibition, Paris, France, 2013*.

[23] Phillips, N. H. and Scott, K. P. 2014. Quantifying PV module microclimates and translation into accelerated weathering protocols. In *SPIE Solar Energy + Technology*. SPIE Proceedings. SPIE, 91790L. DOI=10.1117/12.2063122.

[24] Ehrenstein, G. W., Riedel, G., and Trawiel, P. 2004. *Thermal analysis of plastics*. *Theory and practice*. Carl Hanser Verlag, Munich.

[25] International Organisation for Standardisation, ISO 11357-3. 1999. *Plastics - Differential scanning calorimetry (DSC) Part 3: Determination of temperature and enthalpy of melting and crystallization,* 11357-3.

[26] Hirschl, C., Biebl–Rydlo, M., DeBiasio, M., Mühleisen, W., Neumaier, L., Scherf, W., Oreski, G., Eder, G., Chernev, B., Schwab, W., and Kraft, M. 2013. Determining the degree of crosslinking of ethylene vinyl acetate photovoltaic module encapsulants—A comparative study. *Solar Energy Materials and Solar Cells* 116, 0, 203–218.

[27] Hülsmann, P., Weiß, K.-A., and Köhl, M. 2014. Temperature-dependent water vapour and oxygen permeation through different polymeric materials used in photovoltaic-modules. *Prog. Photovolt: Res. Appl.* 22, 4, 415–421.

[28] Peike, C., Hülsmann, P., Blüml, M., Schmid, P., Weiß, K.-A., and Köhl, M. 2012. Impact of Permeation Properties and Backsheet-Encapsulant Interactions on the Reliability of PV Modules. *ISRN Renewable Energy* 2012, 1–4, 1–5.

[29] Hülsmann, P., Jäger, M., Weiss, K. A., and Köhl, M. Measuring and simulation of water vapour permeation into PV-modules under different climatic conditions. In *SPIE 7773; Reliability of Photovoltaic Cells, Modules, Components and Systems III, Bellingham, USA, 2010*.

[30] Oreski, G. Accelerated indoor durability testing of polymeric photovoltaic encapsulation materials. In *SPIE Solar Energy + Technology, San Diego, USA, 2010. DOI*=10.1117/12.860390.

[31] Beinert, A., Peike, C., Dürr, I., Kempe, M., and Weiß, K.-A. The Influence of the Additive Composition on the Photochemical Degradation of EVA. In *29th European Photovoltaic Solar Energy Conference and Exhibition, Amsterdam, Netherlands, 2014*.

[32] Gulmine, J. V., Janissek, P. R., Heise, H. M., and Akcelrud, L. 2002. Polyethylene characterization by FTIR. *Polymer Testing,* 21, 557–563.

[33] McNeill, I. C., Shafique, A., and Memetea, L. 1995. Thermal degradation of vinyl acetatemethacrylic acid copolymer and homopolymers. I. An FTIR spectroscopic investigation

of structural changes in the degrading material. *Polymer Degradation and Stability,* 47, 423–433.

[34] Sultan, B.-A. and Soervik, E. 1991. Thermal degradation of EVA and EBA. A comparison. I. Volatile decomposition products. *Journal of Applied Polymer Science* 43, 9, 1737–1745.

[35] Gulmine, J. V., Janissek, P., Heise, H., and Akcelrud, L. 2003. Degradation profile of polyethylene after artificial accelerated weathering. *Polymer Degradation and Stability,* 79, 385–397.

[36] Günzler, H. and Heise, M. H. 1996. *IR-Spektroskopie*. *Eine Einführung*.

[37] Günzler, H. and Gremlich, H.-U. 2003. *IR-Spektroskopie*. Wiley-VCH Verlag GmbH & Co. KGaA, Weinheim, Germany.

[38] Peike, C., Kaltenbach, T., Weiß, K.-A., and Koehl, M. 2011. Non-destructive degradation analysis of encapsulants in PV modules by Raman Spectroscopy. *Solar Energy Materials and Solar Cells* 95, 7, 1686–1693.

[39] Shimoyama, M., Maeda, H., Matsukawa, K., Inoue, H., and Ninomiya, T. 1997. Discrimination of ethylene/vinyl acetate copolymers with different composition and prediction of the vinyl acetate content in the copolymers using Fourier-transform Raman spectroscopy and multivariate data analysis. *Vibrational Spectroscopy,* 14, 253–259.

[40] Peike, C., Hoffmann, S., Dürr, I., Weiß, K.-A., and Koehl, M. 2013. The Influence of Laminate Design on Cell Degradation. *Energy Procedia* 38, 516–522.

[41] Morlier, A. *Einfluss des Laminationsprozesses auf das Alterungsverhalten von PV Modulen*.

[42] Brogly, M., Nardin, M., and Schultz, J. 1997. Effect of Vinylacetate Content on Crystallinity and Second-Order Transitions in Ethylene–Vinylacetate Copolymers. *J. Appl. Polym. Sci.* 64, 10, 1903–1912.

[43] Agroui, K. and Collins, G. 2014. Determination of thermal properties of crosslinked EVA encapsulant material in outdoor exposure by TSC and DSC methods. *Renewable Energy* 63, 741–746.

[44] Oreski, G. and Wallner, G. M. Damp Heat induced physical ageing of PV encapsulation materials. In *12th Intersociety Conference on Thermal and Thermomechanical Phenomena in Electronic Systems, Las Vegas, USA, 2010*.

[45] Frick, A. and Stern, C. 2006. *DSC-Prüfung in der Anwendung*. Carl Hanser Verlag, Munich.

[46] Badia, J., Strömberg, E., Karlsson, S., and Ribes-Greus, A. 2012. The role of crystalline, mobile amorphous and rigid amorphous fractions in the performance of recycled poly (ethylene terephthalate) (PET). *Polymer Degradation and Stability* 97, 1, 98–107.

[47] Knausz, M., Oreski, G., Eder, G. C., Voronko, Y., Duscher, B., Koch, T., Pinter, G., and Berger, K. A. 2015. Degradation of photovoltaic backsheets: Comparison of the aging induced changes on module and component level. *J. Appl. Polym. Sci.* 132, 42093, 1–8.

6. Summary

The results and findings in this thesis deal with the effect of ageing methods and the influence of the microclimate on the properties of polymeric materials. The results enhance the knowledge in the field of polymer degradation and give an overview of suitable characterisation methods useful to identify different ageing processes and the correlated changes in properties of polymeric films.

It is shown that all polymeric materials exhibit deteriorations and changes in its physical and/or chemical properties after natural and artificial weathering. These changes are dependent on the intensities of the stress levels and the microclimate. A significant correlation of the crystallisation temperature gained by thermal analysis and molar mass characterised by gel permeation chromatography can be found for polyethylene terephthalate films. Even though some changes in infrared spectra are observable, differences dependent on ageing temperatures or humidity levels are hard to distinguish. Therefore, infrared spectroscopy in attenuated total reflection mode is not a suitable method to characterise chemical degradation via hydrolysis.

The ageing behaviour of polymeric multilayer backsheets after natural and artificial weathering is analysed. Natural and artificial weathering of polymeric backsheets show different effects on the properties of the materials. Obviously it is not feasible to conduct artificial weathering tests for accelerated lifetime predictions, unless the parameters and the test design are adapted. The right test design for artificial ageing tests is highly important, as well as the consideration of the degradation mechanisms when trying to simulate natural ageing conditions.

A feasibility study of the correlation of accelerated damp heat (85°C, 2000 hours) and ultra-accelerated pressure cooker ageing of polyester-based backsheets is conducted. The results of mechanical and thermal analysis using unaged and aged samples reveal similar changes in properties independent of the ageing method. Thus, the pressure cooker test (120°C, 96 hours) can be used for fast quality testing to support rapid material development in case of polyester-based backsheets instead of damp heat testing. The use of the pressure cooker test leads to an acceleration of the speed of testing by a factor of 21. Therefore, pressure cooker testing is proposed to significantly reduce the testing time to four days for material quality and infant failures.

Film and laminated module samples have been aged in order to study the effect of microclimates on the ageing behaviour of polyolefin-based films. The results show a strong influence of the microclimate on the respective polymeric ageing behaviour. Differences are even detectable in the unaged state between film and module samples after the production process.